Supporting Information

Control of Electronic and Exchange Coupling by Bridge Substituents in Donor Acceptor Triads with Triptycene Bridges

Christoph Lambert,[a,d]* Chantal Roger,[a] Alexander Schmiedel,[a] Marco Holzapfel,[a] Nikita Lukzen,[b] and Ulrich E. Steiner[c]*

[a]Institut für Organische Chemie, Universität Würzburg, Am Hubland, D-97074 Würzburg, Germany.

[b]International Tomography Center, Russia and Novosibirsk State Universit; Institutskaya 3a, Novosibirsk, Novosibirsk 630090, Russia

[c]Department of Chemistry, University of Konstanz, Universitätsstraße 10; 78464 Konstanz, Germany

[d]Center for Nanosystems Chemistry, Universität Würzburg, Theodor-Boveri-Weg, D-97074 Würzburg, Germany

Contents

1. Synthesis

1.1. General

Commercially available compounds and standard solvents were purchased from either Acros, Chempur, Fluka, Honeywell, Merck or TCI and used without further purification. DCM, ethyl acetate and hexane were distilled prior to usage. All moisture and oxygen sensitive reactions were performed under a nitrogen atmosphere (dried with Sicapent® from Merck and deoxygenated by a copper oxide catalyst R3-11 from BASF) using dry solvents obtained by a solvent purification system from Inert and degassed in a gentle stream of nitrogen for at least 10 min. Thin layer chromatography (TLC) was performed on pre-coated TLC sheets ALUGRAMR Xtra SIL G/UV254 from Macherey Nagel.

1.2. Nuclear Magnetic Resonance Spectroscopy

The measurements of all NMR spectra were done using either a Bruker Avance III HD 400 FT-Spectrometer (^{1}H: 400.13 MHz, ^{13}C: 100.61 MHz), with a Bruker Ultrashield Magnet, a Bruker Avance III HD 400 FT-Spectrometer (^{1}H: 400.03 MHz, ^{13}C: 100.59 MHz), with a Bruker Ascend Magnet, or a Bruker Avance III HD 600 FT-Spectrometer (1H: 600.13 MHz, 13C: 150.90 MHz) equipped with a cryoprobe unit. Chemical shifts are referenced to the residual proton signal of the respective deuterated solvents (^{1}H) or to the signal of the present ^{13}C isotope and are given in ppm (δ-scale). The proton signals and their coupling patterns are given as follows: s (singlet), d (doublet), dd (doublet of doublets), m (multiplet), AA' / BB' (chemically but not magnetically equivalent protons), m´ (overlapping signals of chemically non-equivalent protons that could not be assigned to first-order couplings). The carbon signals are given as: Cq (quaternary), CH (tertiary), CH_3 (primary).

1.3. Mass Spectrometry

A Bruker Daltonic microTOF focus (ESI, APCI) or a Bruker Daltonics UltrafleXtreme (MALDI) were used to record the mass spectra. For MALDI spectra DCTB (trans-2-[3-(4-*tert*-butylphenyl)-2-methyl-2- propenylidene]malononitrile) was used as a matrix. The software Bruker Daltonics Isotope Pattern was used to calculate the respective theoretical masses. The given measured mass refers to the 100 % peak calculated by the software.

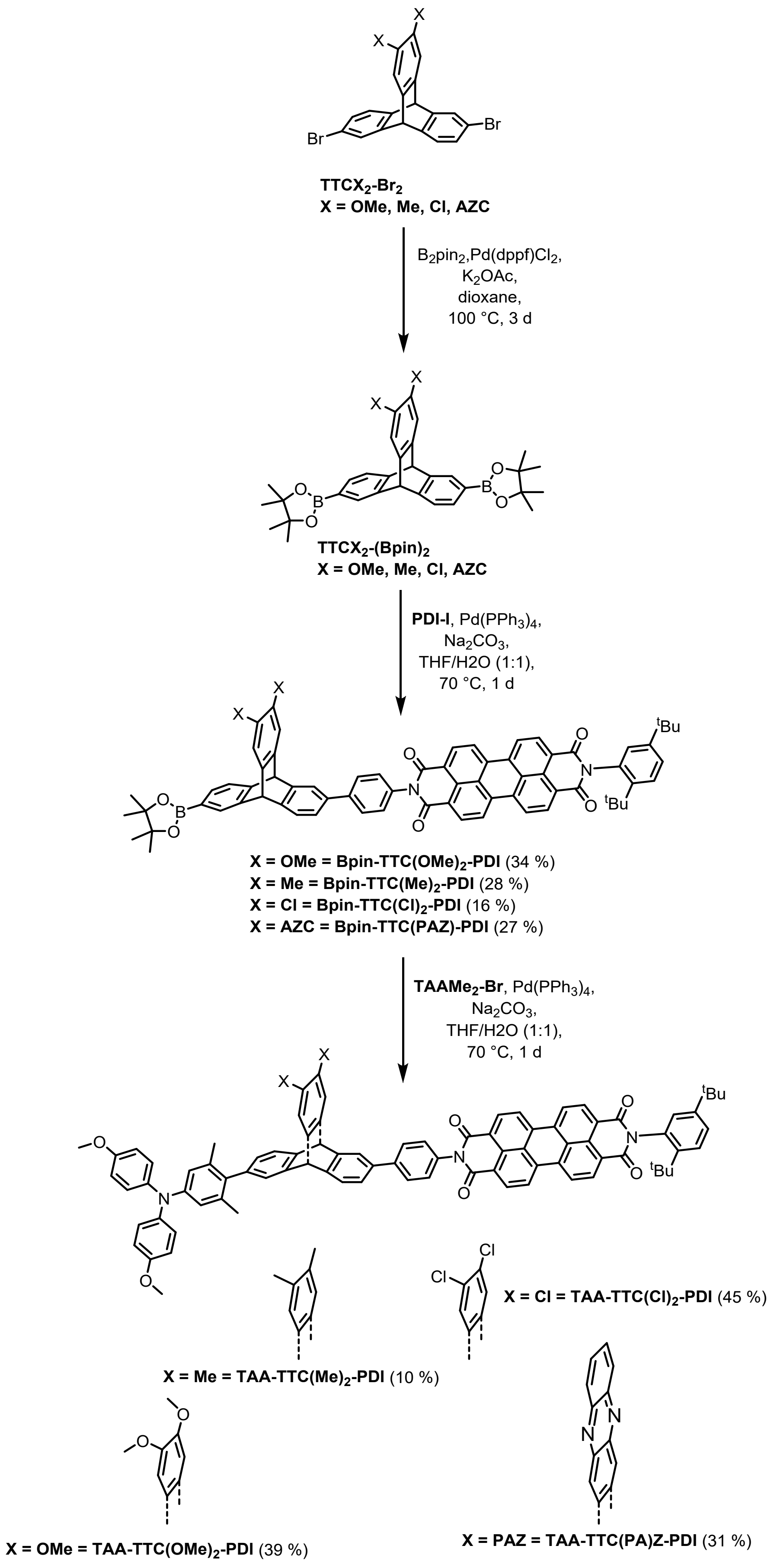

Scheme S1: Synthetic route for the triads.

1.4. Synthetic procedures

The synthesis of the TAA donor, the PDI acceptor and of the unsubstituted triad is described in reference.[1]

General procedure for the synthesis of the triptycene bridging units (GP I)

2,6-Dibromoanthracene (1 eq.) was dissolved in dioxane and heated to 120 °C. The appropriate anthranilic acid derivative (2-4 eq.) was dissolved in dioxane / THF (v:v; 1:1) and added to the anthracene solution via syringe pump over 6 h. Isoamyl nitrite (20 eq.) was added dropwise simultaneously to the reaction mixture. After complete addition, the mixture was stirred at 120 °C for another 30 min and afterwards cooled to rt. The solvent was removed under reduced pressure and the product was separated from the reactant by washing the solid with hexanes/DCM (v:v 20:1 – 10:1). The crude product was purified by column chromatography on silica gel.[2-3]

General procedure for the *Suzuki-Miaura* borylation (GP II)

The appropriate triptycene derivative (1 eq.), bis(pinacalto)diboron (2.5 eq.), Pd(dppf)Cl_2 (5 mol%) and potassium acetate (4 eq.) were dissolved in dioxane under inert gas atmosphere. After heating the reaction mixture to 100 °C for 3 d the solvent was removed under reduced pressure and the residue was dissolved in DCM. The organic phase was washed with water and dried over Na_2SO_4. The solvent was removed under reduced pressure and the crude product was purified by column chromatography on silica gel.[4]

General procedure for the *Suzuki*-Coupling reaction (GP III)

The appropriate borylated species (1 eq), the halogenated species (variating eq.) and sodium carbonate (4 eq) were dissolved in a mixture of THF and degassed water (v:v 4:1) under an inert gas atmosphere. Afterwards $Pd(PPh_3)_4$ (5 mol%) was added and the reaction mixture was heated to 70 °C for 12 h. The solvent was removed under reduced pressure, the residue dissolved in DCM and the organic layer washed with water. The aqueous phases were extracted with DCM and the combined organic phases were dried over Na_2SO_4. The solvent was removed under reduced pressure and the crude product was purified by column chromatography on silica gel.

2,6-Dibromo-14,15-dimethoxytriptycene (TTC(OMe$_2$)-Br$_2$)

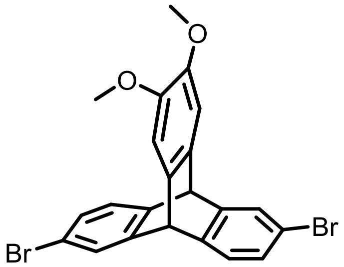

CA: [-]

Synthesis according to **GP I**. [2-3]

2,6-Dibromoanthracene (1.00 g, 2.98 mmol) in dry dioxane (70 ml). 4,5-Dimethoxyanthranilic acid (2.35 g, 11.9 mmol) in dry THF (20 ml) and dry dioxane (20 ml). Isoamyl nitrite (7.00 ml, 52.0 mmol). Column chromatography (silica gel, eluent: hexanes/DCM 1:1, hexanes/EA 5:1).

Yield: 323 mg (684 µmol, 23 %) of a colourless solid.

$C_{22}H_{16}Br_2O_2$ [472.17 g/mol]

^{1}H-NMR (400.1 MHz, CDCl$_3$):

δ [ppm] = 7.51 (d, $^4J_{H,H}$ = 1.9 Hz, 2H), 7.22 (d, $^3J_{H,H}$ = 7.8 Hz, 2H), 7.12 (dd, $^3J_{H,H}$ = 7.8 Hz, $^4J_{H,H}$ = 1.9 Hz, 2H), 7.00 (s, 2H), 5.27 (s, 2H), 3.84 (s, 6H).

^{13}C-NMR (100.6 MHz, CDCl$_3$):

δ [ppm] = 147.7 (C$_q$); 146.5 (C$_q$), 144.3 (C$_q$), 136.8 (C$_q$), 128.1 (CH), 126.6 (CH), 125.0 (CH), 118.8 (C$_q$), 108.7 (CH), 56.3 (CH$_3$), 52.9 (CH).

APCI-MS: m / z: calc. [M+H]$^{\bullet+}$ 472.95707; found [M+H]$^{\bullet+}$ 472.95608, Δ = 2.09 ppm.

TTC(OMe)$_2$-(Bpin)$_2$

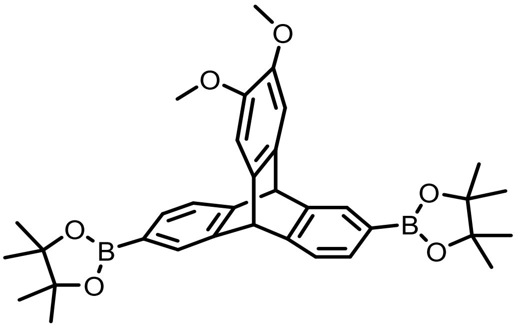

CA: [-]

Synthesis according to **GP II**.[4]

TTC(OMe)$_2$-Br$_2$ (1.16 g, 2.46 mmol), bis(pinacalto)diboron (1.56 g, 6.14 mmol), Pd(dppf)Cl$_2$ (100 mg, 137 µmol), potassium acetate (964 mg, 9.83 mmol) in dry dioxane (30 ml) 3 d, 80 °C Column chromatography (silica gel, eluent: EA/hexanes 1:4).

Yield: 902 mg (1.59 mmol, 65 %) of a colourless solid.

$C_{34}H_{40}B_2O_6$ [566.30 g/mol].

^{1}H-NMR (400.1 MHz, $CDCl_3$):

δ [ppm] = 7.81 (s, 2H), 7.47 (dd, $^3J_{H,H}$ = 7.3 Hz, $^4J_{H,H}$ = 1.1 Hz, 2H), 7.35 (d, $^3J_{H,H}$ = 7.3 Hz, 2H), 6.97 (s, 2H), 5.37 (s, 2H), 3.81 (s, 6H), 1.29 (s, 24H).

^{13}C-NMR (100.6 MHz, $CDCl_3$):

δ [ppm] = 149.0 (C_q), 146.1 (C_q), 144.7 (C_q), 137.6 (C_q), 132.4 (CH), 129.3 (CH), 123.0 (CH), 108.6 (CH), 83.8 (C_q), 56.3 (CH_3), 53.9 (CH), 24.9 (CH_3).[1]

APCI-MS: m / z: calc. $[M+H]^{\bullet+}$ 567.3095; found $[M+H]^{\bullet+}$ 567.3099.

---

[1] The C atom next to the Bpin group is not visible.

2,6-Dibromo-14,15-dimethyltriptycene (TTCMe$_2$-Br$_2$)

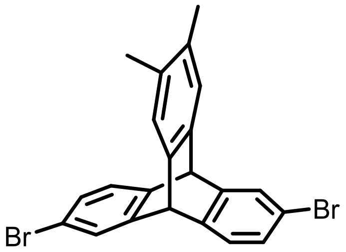

CA: [-]

Synthesis according to **GP I**.[2-3]

2,6-Dibromoanthracene (1.00 g, 2.98 mmol) in dry dioxane (20 ml). 4,5-Dimethylanthranilic acid (1.48 g, 8.96 mmol) in dry THF (20 ml) and dry dioxane (30 ml). Isoamyl nitrite (9.21 ml, 68.4 mmol). Column chromatography (silica gel, eluent: DCM, hexanes/toluene 100:6).

Yield: 420 mg (954 µmol, 32 %) of a colourless solid.

$C_{22}H_{16}Br_2$ [440.17 g/mol]

^{1}H-NMR (400.1 MHz, $CDCl_3$):

δ [ppm] = 7.50 (d, $^4J_{H,H}$ = 2.0 Hz, 2H), 7.22 (d, $^3J_{H,H}$ = 7.9 Hz, 2H), 7.18 (s, 2H), 7.12 (dd, $^3J_{H,H}$ = 7.9 Hz, $^4J_{H,H}$ = 2.0 Hz, 2H), 5.28 (s, 2H), 2.17 (s, 6H).

^{13}C-NMR (100.6 MHz, $CDCl_3$):

δ [ppm] = 147.5 (C_q), 144.1 (C_q), 141.8 (C_q), 133.8 (C_q), 128.2 (CH), 126.9 (CH), 125.4 (CH), 125.2 (CH), 118.9 (C_q), 52.8 (CH), 19.7 (CH_3).

APCI-HRMS: m / z: calc. $[M+H]^{\bullet+}$ 440.96723; found $[M+H]^{\bullet+}$ 440.96804, Δ = 1.84 ppm.

TTCMe$_2$-(Bpin)$_2$

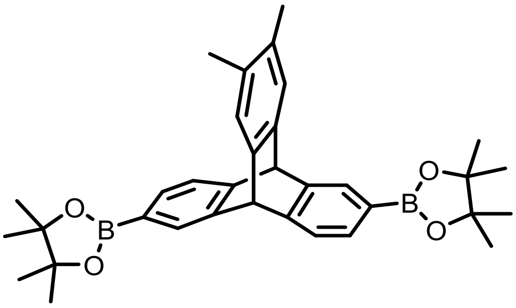

CA: [-]

Synthesis according to **GP II**.[4]

TTCMe$_2$-Br$_2$ (900 mg, 2.04 mmol), bis(pinacalto)diboron (1.25 g, 4.92 mmol), Pd(dppf)Cl$_2$ (83.5 mg, 114 µmol), potassium acetate (803 mg, 8.18 mmol) in dry dioxane (50 ml) 3 d, 80 °C Column chromatography (silica gel, eluent: DCM/hexanes 9:1).

Yield: 484 mg (906 µmol, 44 %) of a colourless solid.

$C_{34}H_{40}B_2O_4$ [534.30 g/mol].

^{1}H-NMR (400.1 MHz, $CDCl_3$):

δ [ppm] = 7.78 (s, 2H), 7.44 (dd, $^3J_{H,H}$ = 7.2 Hz, $^4J_{H,H}$ = 1.1 Hz, 2H), 7.33 (d, $^3J_{H,H}$ = 7.2 Hz, 2H), 7.12 (s, 2H), 5.36 (s, 2H), 2.12 (s, 6H), 1.28 (s, 24H).

^{13}C-NMR (100.6 MHz, $CDCl_3$):

δ [ppm] =148.9 (C_q), 144.6 (C_q), 142.5 (C_q), 133.1 (C_q), 132.4 (CH), 129.5 (CH), 125.3 (CH), 123.1 (CH), 83.7 (C_q), 53.8 (CH), 24.95 (CH_3), 24.90 (CH_3), 19.6 (CH_3).[2]

APCI-MS: m / z: calc. $[M+H]^{\bullet+}$ 535.3197; found $[M+H]^{\bullet+}$ 535.3197.

---

[2] The C atom next to the Bpin group is not visible.

2,6-Dibromo-14,15-dichlorotriptycene (TTCCl$_2$-Br$_2$))

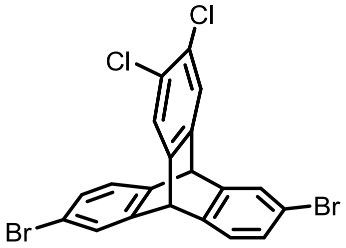

CA: [-]

Synthesis according to **GP I**.[2-3]

2,6-Dibromoanthracene (1.00 g, 2.98 mmol) in dry dioxane (70 ml). 4,5-Dichloroanthranilic acid (1.23 g, 5.97 mmol) in dry THF (20 ml) and dry dioxane (20 ml), Isoamyl nitrite (6.00 ml, 44.6 mmol). Column chromatography (silica gel, hexanes/DCM 1:1, hexanes/tol 100:3).

Yield: 516 mg (1.07 mmol, 36 %) of a colourless solid.

$C_{20}H_{10}Br_2Cl_2$ [481.01 g/mol]

^{1}H-NMR (400.1 MHz, $CDCl_3$):

δ [ppm] = 7.51 (d, $^4J_{H,H}$ = 1.9 Hz, 2H), 7.43 (s, 2H), 7.23 (d, $^3J_{H,H}$ = 7.9 Hz, 2H), 7.17 (dd, $^3J_{H,H}$ = 7.8 Hz, $^4J_{H,H}$ = 1.9 Hz, 2H), 5.28 (s, 2H).

^{13}C-NMR (100.6 MHz, $CDCl_3$):

δ [ppm] = 146.6 (C_q), 144.2 (C_q) 142.7 (C_q) 129.2 (C_q), 128.8 (CH), 127.3 (CH), 125.9 (CH), 125.3 (CH), 119.4 (C_q), 52.5 (CH).

APCI-MS: m / z: calc. $[M]^{\bullet +}$ 479.8499; found $[M]^{\bullet +}$ 479.8507.

TTCCl$_2$-(Bpin)$_2$

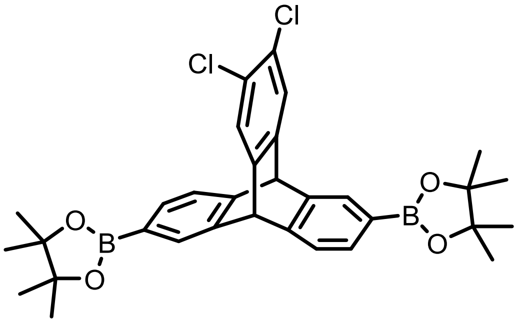

CA: [-]

Synthesis according to **GP II**. [4]

TTCCl$_2$-Br$_2$ (300 mg, 624 µmol), bis(pinacalto)diboron (348 mg, 1.37 mmol), Pd(dppf)Cl$_2$ (22.8 mg, 31.2 µmol), potassium acetate (245 mg, 2.50 mmol) in dry dioxane (15 ml), 1 d, 80 °C. Column chromatography (silica gel, eluent: DCM/hexanes 3:2 – DCM).

Yield: 129 mg (224 µmol, 36 %) of a colourless solid.

$C_{32}H_{34}B_2Cl_2O_4$ [575.14 g/mol].

^{1}H-NMR (400.1 MHz, $CDCl_3$):

δ [ppm] = 7.82 (s, 2H), 7.50 (dd, $^3J_{H,H}$ = 7.3 Hz, $^4J_{H,H}$ = 1.1 Hz, 2H) 7.41 (s, 2H), 7.36 (d, $^3J_{H,H}$ = 7.3 Hz, 2H), 5.39 (s, 2H), 1.30 (s, 24H).

^{13}C-NMR (100.6 MHz, $CDCl_3$):

δ [ppm] = 147.4 (C_q), 145.0 (C_q), 143.3 (C_q), 132.9 (CH), 129.9 (CH), 128.7 (C_q), 125.8 (CH), 123.5 (CH), 83.9 (C_q), 53.4 (CH), 25.0 (CH_3), 24.9 (CH_3).

APCI-MS: m / z: calc. $[M]^{\bullet+}$ 574.2027; found $[M]^{\bullet+}$ 574.2034.

$TTCO_2$-Br_2

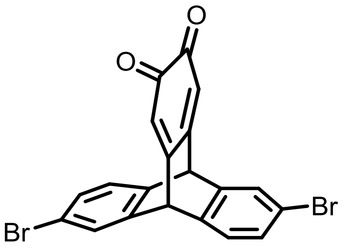

Synthesis according to literature.[5]

CA: [-]

$TTC(OMe)_2$-Br_2 (2.07 g, 4.38 mmol) was dissolved in DCM (100 ml) and acetic acid (100 ml) was added. Concentrated nitric acid (21 ml) was added dropwise until a colour change to dark red appeared. The reaction mixture was poured on ice water immediately. The product was extracted with DCM, the organic phases were combined and washed with sodium bicarbonate solution (10 %, 70 ml). The organic phase was dried over Na_2CO_3 and the solvent removed under reduced pressure. The crude product was purified by column chromatography (silica gel, eluent: DCM).

Yield: 1.03 g (2.33 mmol, 53 %) of a red solid.

$C_{20}H_{10}Br_2O_2$ [442.10 g/mol].

^{1}H-NMR (400.1 MHz, $CDCl_3$):

δ [ppm] =. 7.59 (d, $^4J_{H,H}$ = 1.9 Hz, 2H), 7.42 (dd, $^3J_{H,H}$ = 8.0 Hz, $^4J_{H,H}$ = 1.9 Hz, 2H), 7.30 (d, $^3J_{H,H}$ = 8.0 Hz, 2H), 6.36 (s, 2H), 5.08 (s, 2H).

^{13}C-NMR (100.6 MHz, $CDCl_3$):

δ [ppm] = .179.5 (C_q), 151.7 (C_q), 140.6 (C_q), 137.3 (C_q), 131.3 (CH), 127.9 (CH), 126.2 (CH), 122.3 (CH), 122.2 (C_q), 51.3 (CH).

APCI-HRMS: m / z: calc. $[M+H]^{\bullet+}$ 442.91010; found $[M+H]^{\bullet+}$ 442.91084, Δ = 1.67 ppm.

TTC(PAZ)-Br$_2$

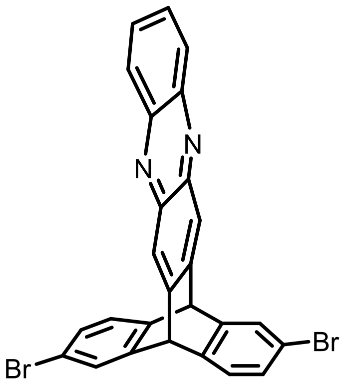

Synthesis according to literature.[5]

CA: [-]

TTCO$_2$-Br$_2$ (500 mg, 1.13 mmol) and benzene-1,2-diamine (245 mg, 2.27 mmol) were dissolved in chloroform (80 ml) and acetic acid (80 ml) was added. The reaction mixture was stirred for 1 d at 110 °C and then poured on ice water (100 ml). The aqueous phase was neutralised with sodium carbonate solution (10 %) and the product was extracted with DCM (200 ml). The organic phases were combined, washed with sodium carbonate solution (10 %, 100 ml) and dried over Na_2CO_3. The solvent was removed under reduced pressure. The crude product was purified by column chromatography (silica gel, eluent: DCM).

Yield: 456 mg (887 µmol, 78 %) of a yellow solid.

$C_{26}H_{14}Br_2N_2$ [514.21 g/mol].

^{1}H-NMR (400.1 MHz, $CDCl_3$):

δ [ppm] = 8.18 (m, 2H), 8.08 (s, 2H), 7.77 (m, 2H), 7.64 (d, $^4J_{H,H}$ = 1.8 Hz, 2H), 7.34 (d, $^3J_{H,H}$ = 7.9 Hz, 2H), 7.24 (dd, $^3J_{H,H}$ = 7.9 Hz, $^4J_{H,H}$ = 1.8 Hz, 2H), 5.59 (s, 2H).

^{13}C-NMR (100.6 MHz, $CDCl_3$):

δ [ppm] = 145.1 (C_q), 145.0 (C_q), 143.3 (C_q), 142.8 (C_q), 141.8 (C_q), 130.2 (CH), 129.6 (CH), 129.4 (CH), 127.6 (CH), 125.9 (CH), 123.1 (CH), 120.0 (C_q), 52.6 (CH).

APCI-HRMS: m / z: calc. $[M+H]^{\bullet+}$ 514.95778; found $[M+H]^{\bullet+}$ 514.95746, Δ = 0.62 ppm.

TTC(PAZ)-(Bpin)$_2$

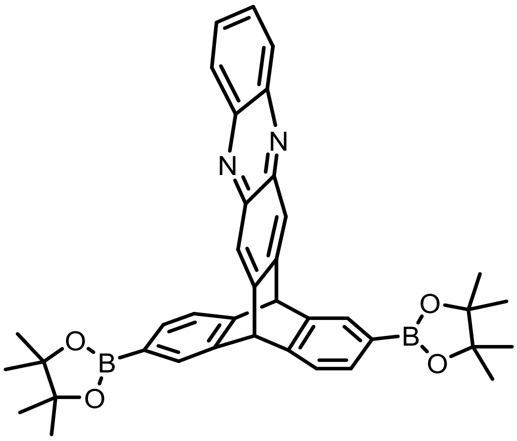

CA: [-]

Synthesis according to **GP II**.[4]

TTC(PAZ)-Br$_2$ (440 mg, 856 µmol), bis(pinacalto)diboron (543 mg, 2.14 mmol), Pd(dppf)Cl$_2$ (34.9 mg, 47.7 µmol), potassium acetate (336 mg, 3.42 mmol) in dry dioxane (10 ml) 3 d, 80 °C. Column chromatography (silica gel, eluent: DCM – DCM/EA 500:25).

Yield: 198 mg (325 µmol, 38 %) of a yellow solid.

$C_{38}H_{38}B_2N_2O_4$ [608.34 g/mol].

^{1}H-NMR (400.1 MHz, CDCl$_3$):

δ [ppm] = 8.17 (m, 2H), 8.05 (s, 2H), 7.94 (s, 2H), 7.76 (m, 2H), 7.57 (dd, $^3J_{H,H}$ = 7.3 Hz, $^4J_{H,H}$ = 1.1 Hz, 2H), 7.49 (d, $^3J_{H,H}$ = 7.3 Hz, 2H), 5.68 (s 2H), 1.30 (s, 24H).

^{13}C-NMR (100.6 MHz, CDCl$_3$):

δ [ppm] = 146.5 (C$_q$), 146.3 (C$_q$), 143.2 (C$_q$), 143.0 (C$_q$), 142.3 (C$_q$), 133.4 (CH), 130.3 (CH), 129.9 (CH), 129.6 (CH), 123.8 (CH), 122.7 (CH), 84.0 (C$_q$), 53.8 (CH), 25.0 (CH$_3$), 24.9 (CH$_3$).[3]

APCI-MS: m / z: calc. $[M+H]^{\bullet+}$ 609.3103; found $[M+H]^{\bullet+}$ 609.3096.

---

[3] The C$_q$ next to the Bpin group is not visible.

Bpin-TTC(OMe)$_2$-PDI

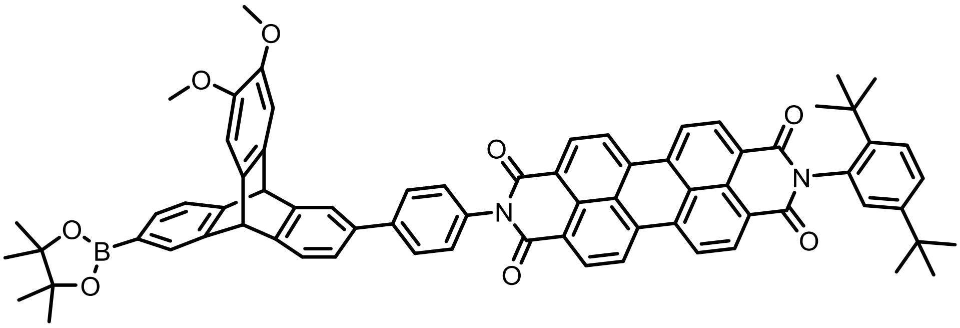

CA: [-]

Synthesis according to **GP III**.[4]

TTC(OMe)$_2$-(Bpin)$_2$ (300 mg, 530 µmol), **PDI-I** (103 mg, 132 µmol), sodium carbonate (225 mg, 2.12 mmol) in THF (6 ml) and water (1.5 ml). Pd(PPh$_3$)$_4$ (30.6 mg, 26.5 µmol). Column chromatography on silica gel (eluent: DCM – DCM/toluene (4:1) – DCM/toluene/EA (400:100:1)).

Yield: 50.0 mg (45.7 µmol, 34 %) of a red solid.

$C_{72}H_{61}BN_2O_8$ [1093.08 g/mol]

^{1}H-NMR (400.1 MHz, CDCl$_3$):

δ [ppm] = 8.75 (m', 8H), 7.86 (s, 1H), 7.68 (AA', 2H), 7.65 (d, $^4J_{H,H}$ = 1.7 Hz, 1H), 7.61 (d $^3J_{H,H}$ = 8.6 Hz, 1H), 7.51 (dd, $^3J_{H,H}$ = 7.3 Hz, $^4J_{H,H}$ = 1.1 Hz, 1H), 7.48 (dd, $^3J_{H,H}$ = 8.6 Hz, $^4J_{H,H}$ = 2.3 Hz, 1H), 7.44 (m', 2H), 7.38 (BB', 2H), 7.25 (m, 1H), 7.05 (m', 3H), 5.44 (s, 1H), 5.43 (s, 1H), 3.85 (s, 3H), 3.84 (s, 3H), 1.33 (s, 9H), 1.31 (s, 12H), 1.30 (s, 9H).

^{13}C-NMR (100.6 MHz, CDCl$_3$):

δ [ppm] = 164.5 (C$_q$), 163.8 (C$_q$), 150.3 (C$_q$), 149.0 (C$_q$), 146.3 (C$_q$), 146.2 (C$_q$), 146.1 (C$_q$), 145.2 (C$_q$), 145.1 (C$_q$), 143.9 (C$_q$), 142.2 (C$_q$), 137.9 (C$_q$), 137.8 (C$_q$), 137.5 (C$_q$), 135.3 (C$_q$), 135.1 (C$_q$), 134.0 (C$_q$),132.7 (C$_q$), 132.5 (CH), 132.1 (CH), 132.08 (CH), 130.0 (C$_q$), 129.98 (C$_q$), 129.3 (CH), 129.0 (CH), 128.9 (CH), 128.5 (CH), 127.8 (CH), 126.94 (C$_q$), 126.87 (C$_q$), 126.6 (CH), 124.5 (CH), 123.9 (C$_q$), 123.8 (CH), 123.6 (C$_q$), 123.54 (CH), 123.46 (CH), 123.1

(CH), 122.9 (CH), 108.8 (CH), 108.6 (CH), 83.8 (C_q), 56.4 (CH_3),56.3 (CH_3), 54.2 (CH), 53.5 (CH), 35.7 (C_q), 34.4 (C_q), 31.9 (CH_3), 31.4 (CH_3), 25.0 (CH_3), 24.9 (CH_3).[4]

MALDI-MS (pos): m/z calc. $[M]^+$ 1092.45270, found $[M]^+$ 1092.44710.

Bpin-TTCMe$_2$-PDI

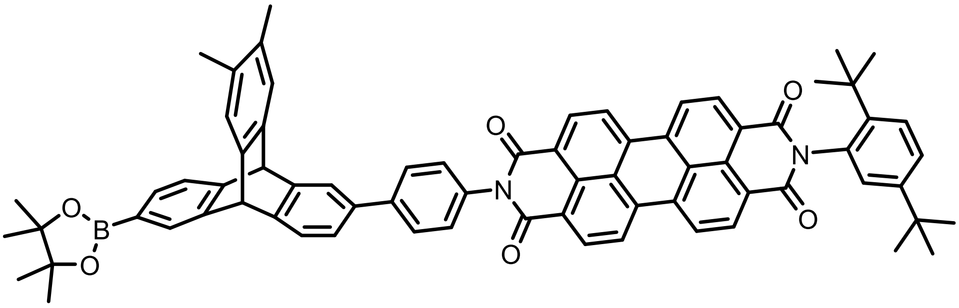

CA: [-]

Synthesis according to **GP III**.[4]

TTCMe$_2$-(Bpin)$_2$ (100 mg, 187 µmol), **PDI-I** (73.1 mg, 93.6 µmol), sodium carbonate (49.6 mg, 468 µmol) in THF (12 ml) and water (3 ml). $Pd(PPh_3)_4$ (5.41 mg, 4.68 µmol). Column chromatography on silica gel (eluent: DCM – DCM/toluene/EA (400:100:10)).

Yield: 28.0 mg (26.4 µmol, 28 %) of a red solid.

$C_{72}H_{61}BN_2O_6$ [1061.08 g/mol]

^{1}H-NMR (400.1 MHz, $CDCl_3$):

δ [ppm] = 8.74 (m’, 8H), 7.85 (s, 1H), 7.66 (AA’, 2H), 7.63 (d, $^4J_{H,H}$ = 1.8 Hz, 1H), 7.61 (d, $^3J_{H,H}$ = 8.6 Hz, 1H), 7.49 (m’, 2H), 7,42 (m’ 2H), 7.37 (BB’, 2H), 7.22 (m’, 3H), 7.04 (d, $^4J_{H,H}$ = 2.2 Hz, 1H), 5.45 (s, 1H), 5.43 (s, 1H), 2.17 (s, 3H), 2.16 (s, 3H), 1.33 (s, 9H), 1.30 (m’, 21H).

^{13}C-NMR (100.6 MHz, $CDCl_3$):

---

[4] C_q next to the Bpin group is not visible.

δ [ppm] = 164.6 (C_q), 163.8 (C_q), 150.3 (C_q), 148.9 (C_q), 146.0 (C_q), 145.1 (C_q), 144.9 (C_q), 143.9 (C_q), 142.8 (C_q), 142.5 (C_q), 142.4 (C_q), 137.8 (C_q), 135.3 (C_q), 135.1 (C_q), 133.9 (C_q), 133.4 (C_q), 133.2 (C_q), 132.7 (C_q), 132.5 (CH), 132.10 (CH), 132.09 (CH), 130.00 (C_q), 129.99 (C_q), 129.5 (CH), 129.0 (2 x CH), 128.5 (CH), 127.8 (CH), 127.0 (C_q), 126.9 (C_q), 126.6 (CH), 125.4 (CH), 125.3 (CH), 124.6 (CH), 123.94 (CH), 123.91 (C_q), 123.6 (C_q), 123.5 (CH), 123.47 (CH), 123.3 (CH), 123.0 (CH), 83.8 (C_q), 54.1 (CH), 53.4 (CH), 35.7 (C_q), 34.4 (C_q), 31.9 (CH_3), 31.4 (CH_3), 25.0 (CH_3), 24.9 (CH_3), 19.68 (CH_3), 19.67 (CH_3).[5]

MALDI-MS (pos): m/z calc. $[M]^+$ 1060.46287, found $[M]^+$ 1060.46272.

Bpin-TTCCl$_2$-PDI

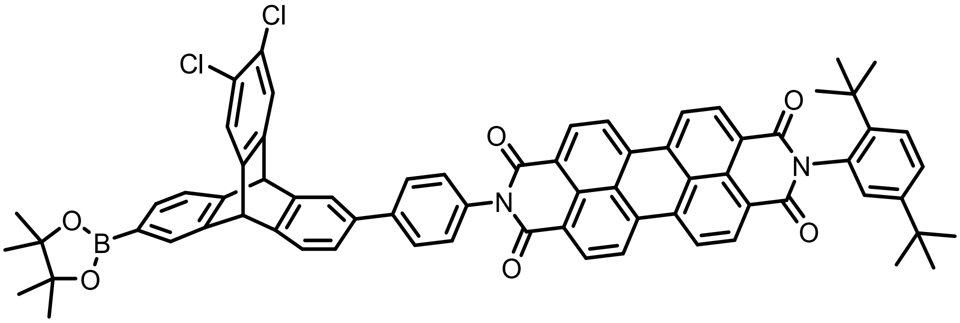

CA: [-]

Synthesis according to **GP III**.[4]

TTCCl$_2$-(Bpin)$_2$ (320 mg, 556 µmol), **PDI-I** (217 mg, 278 µmol) sodium carbonate (118 mg, 1.11 mmol) in THF (24 ml) and water (6 ml). $Pd(PPh_3)_4$ (16.1 mg, 13.9µmol) Column chromatography on silica gel (eluent: DCM – DCM/toluene (5:1) – DCM/toluene/EA (400:100:20)).

Yield: 49.0 mg (44.5 µmol, 16 %) of a red solid.

$C_{70}H_{55}BCl_2N_2O_6$ [1101.91 g/mol]

---

[5] C_q next to the Bpin group is not visible.

^{1}H-NMR (400.1 MHz, $CDCl_3$):

δ [ppm] = 8.74 (m´, 8H), 7.88 (s, 1H), 7.67 (m´, 3H), 7.61 (d, $^3J_{H,H}$ = 8.7 Hz, 1H), 7.55 (dd, $^3J_{H,H}$ = 7.3 Hz, $^4J_{H,H}$ = 1.1 Hz, 1H), 7.48 (m', 5H), 7.39 (AA´, 2H), 7.30 (dd, $^3J_{H,H}$ = 7.6 Hz, $^4J_{H,H}$ = 1.8 Hz, 1H), 7.05 (d, $^4J_{H,H}$ = 2.2 Hz, 1H), 5.48 (s, 1H), 5.45 (s, 1H), 1.33 (s, 9H), 1.32 (s, 12H), 1.30 (s, 9H).

^{13}C-NMR (100.6 MHz, $CDCl_3$):

δ [ppm] = 164.5 (C_q), 163.8 (C_q), 150.4 (C_q), 147.4 (C_q), 145.3 (C_q), 145.0 (C_q), 144.7 (C_q), 143.9 (C_q), 143.7 (C_q), 143.6 (C_q), 141.9 (C_q), 138.4 (C_q), 135.3 (C_q), 135.0 (C_q), 134.2 (C_q), 133.0 (CH), 132.6 (C_q), 132.1 (CH), 132.1 (CH), 130.0 (C_q), 130.0 (C_q), 129.9 (CH), 129.0 (2 x CH), 128.9 (C_q), 128.8 (C_q), 128.5 (CH), 127.9 (CH), 126.92 (C_q), 126.86 (C_q), 126.6 (CH), 126.0 (CH), 125.8 (CH), 125.0 (CH), 124.3 (CH), 124.0 (C_q), 123.6 (CH), 123.54 (CH), 123.53 (C_q), 123.5 (CH), 123.3 (CH), 84.0 (C_q), 53.6 (CH), 52.9 (CH), 35.7 (C_q), 34.4 (C_q), 31.9 (CH_3), 31.3 (CH_3), 25.0 (CH_3), 24.9 (CH_3).[6]

APCI-MS: (pos): m/z calc. $[M+H]^+$ 1101.3614, found $[M+H]^+$ 1101.3489.

Bpin-TTC(PAZ)-PDI

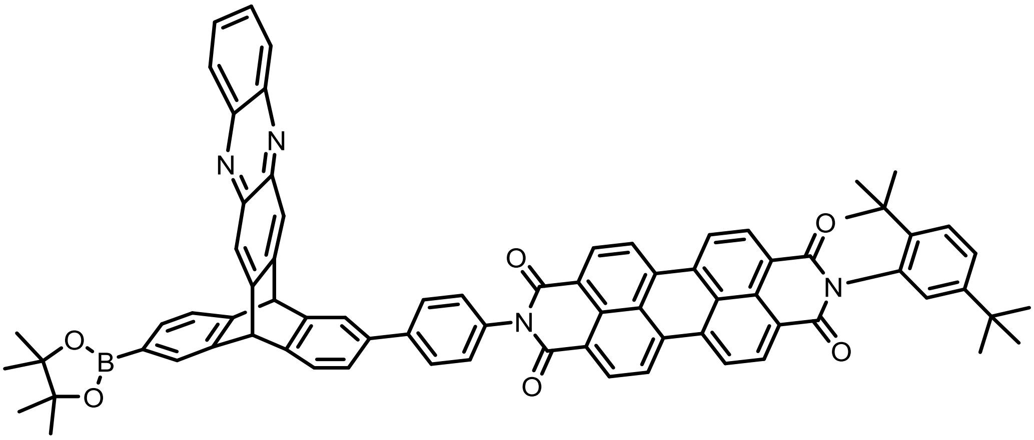

Synthesis according to literature.[4]

CA: [-]

Synthesis according to **GP III**.

---

[6] C_q next to Bpin-group not visible in NMR.

TTC(PAZ)-(Bpin)₂ (150 mg, 247 µmol), **PDI-I** (96.2 mg, 123 µmol), sodium carbonate (52.3 mg, 493 µmol) in THF (6 ml) and water (1.5 ml). $Pd(PPh_3)_4$ (7.12 mg, 6.16 µmol). Column chromatography on silica gel (eluent: DCM/EA (10:1)).

Yield: 38.0 mg (33.5 µmol, 27 %) of a red solid.

$C_{76}H_{59}BN_4O_6$ [1135.12 g/mol]

^{1}H-NMR (400.1 MHz, $CDCl_3$):

δ [ppm] = 8.73 (m’, 8H), 8.18 (m, 2H), 8.14 (s, 1H), 8.10 (s, 1H), 8.00 (s, 1H), 7.78 (m’, 3H), 7.71 (AA’, 2H), 7.61 (m’, 4H), 7.48 (dd, $^3J_{H,H}$ = 8.6 Hz, $^4J_{H,H}$ = 2.3 Hz, 1H), 7.40 (m’, 3H), 7.05 (d, $^4J_{H,H}$ = 2.3 Hz, 1H), 5.78 (s, 1H), 5.75 (s, 1H), 1.33 (s, 9H), 1.32 (s, 12H), 1.30 (s, 9H).

^{13}C-NMR (100.6 MHz, $CDCl_3$):

δ [ppm] = 164.5 (C_q), 163.8 (C_q), 150.3 (C_q), 146.41 (C_q), 146.38 (C_q), 146.2 (C_q), 143.9 (C_q), 143.7 (C_q), 143.20 (C_q), 143.18 (C_q), 143.13 (C_q), 143.06 (C_q), 142.8 (C_q), 142.6 (C_q), 141.8 (C_q), 139.0 (C_q), 135.3 (C_q), 135.0 (C_q), 134.3 (C_q), 133.5 (CH), 132.7 (C_q), 132.09 (CH), 132.07 (CH), 130.3 (CH), 130.00 (C_q, CH), 129.98 (C_q), 129.97 (CH), 129.6 (2 x CH), 129.0 (2 x CH), 128.5 (CH), 127.9 (CH), 126.92 (C_q), 126.86 (C_q), 126.6 (CH), 125.7 (CH), 124.7 (CH), 123.9 (C_q, CH), 123.6 (CH), 123.5 (CH), 123.45 (C_q), 123.4 (CH), 122.9 (CH), 122.7 (CH), 84.0 (C_q), 54.0 (CH), 54.3 (CH), 35.7 (C_q), 34.4 (C_q), 31.9 (CH_3), 31.4 (CH_3), 25.0 (CH_3), 24.9 (CH_3).

MALDI-MS (pos): m/z calc. $[M+H]^+$ 1135.46124 , found $[M]^+$ 1135.46246.

TAA-TTC(OMe)$_2$-PDI

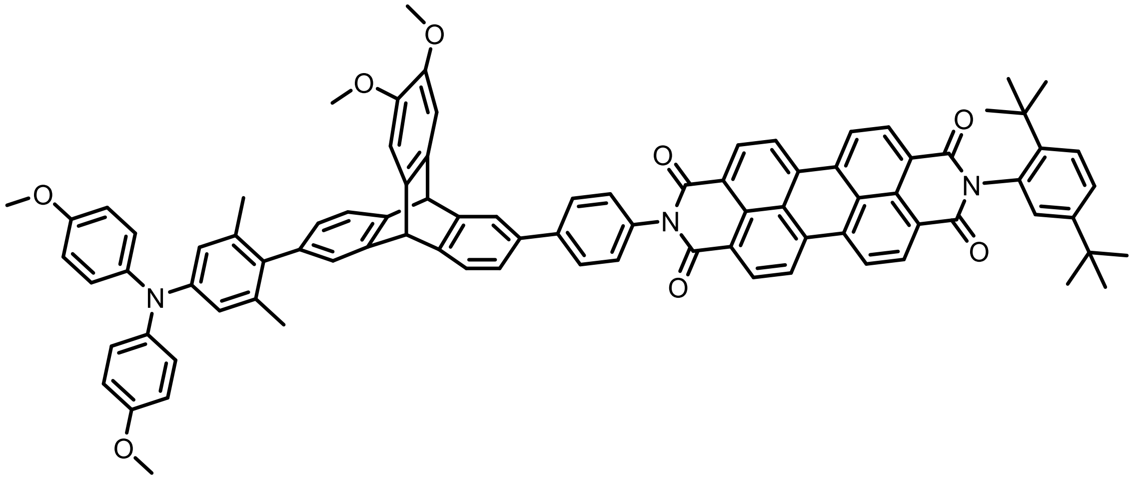

CA: [-]

Synthesis according to **GP III**.[4]

Bpin-TTC(OMe)$_2$-PDI (50.0 mg, 45.7 µmol), **TAAMe$_2$-Br** (37.7 mg, 91.4 µmol), sodium carbonate (19.4 mg, 183 µmol) in THF (6 ml) and water (1.5 ml). Pd(PPh$_3$)$_4$ (2.64 mg, 2.28 µmol). Column chromatography (eluent: DCM – DCM/EA (50:1)). The product was dissolved in DCM and precipitated by addition of hexane.

Yield: 23.0 mg (17.7 µmol, 39 %) of a red solid.

$C_{88}H_{71}N_3O_8$ [1298.52 g/mol]

^{1}H-NMR (600.1 MHz, CD_2Cl_2):

δ [ppm] = 8.74 (m', 8H), 7.75 (m', 3H), 7.62 (d, $^3J_{H,H}$ = 8.6 Hz, 1H), 7.50 (m', 3H), 7.41 (AA', 2H), 7.35 (dd, $^3J_{H,H}$ = 7.6 Hz, $^4J_{H,H}$ = 1.8 Hz, 1H), 7.23 (dd, $^4J_{H,H}$ = 1.5 Hz, 1H), 7.09 (m', 3H), 7.04 (AA', 4H), 6.83 (m', 5H), 6.63 (s, 2H), 5.51 (s, 1H), 5.43 (s, 1H), 3.83 (s, 3H), 3.82 (s, 3H), 3.78 (s, 6H), 1.84 (s, 6H), 1.33 (s, 9H), 1.28 (s, 9H).

^{13}C-NMR (150.9 MHz, CD_2Cl_2):

δ [ppm] = 164.8 (C_q), 164.0 (C_q), 156.1 (C_q), 150.8 (C_q), 147.7 (C_q), 147.3 (C_q), 146.71 (C_q), 146.70 (C_q), 146.1 (C_q), 146.0 (C_q), 144.6 (C_q), 144.0 (C_q), 142.1 (C_q), 141.6 (C_q), 138.44

(C_q),138.41 (C_q), 137.7 (C_q), 137.2 (C_q), 137.1 (C_q), 135.5 (C_q), 135.4 (C_q), 134.9 (C_q), 134.8 (C_q), 133.6 (C_q), 132.1 (CH), 132.0 (CH), 130.2 (C_q), 130.1 (C_q), 129.5 (CH), 129.3 (CH), 128.4 (CH), 128.3 (CH), 127.2 (C_q), 127.1 (C_q), 126.6 (CH), 126.5 (C_q, CH), 125.1 (CH), 124.6 (CH), 124.09 (CH), 124.07 (C_q), 123.9 (CH), 123.88 (CH), 123.87 (C_q), 123.7 (CH), 123.4 (CH), 122.9 (CH), 120.1 (2 x CH), 114.9 (CH), 109.5 (CH), 109.4 (CH), 56.6 (2 x CH_3), 55.8 (CH_3), 54.2 (2 x CH), 50.8 (C_q), 35.8 (C_q), 34.6 (C_q), 31.8 (CH_3), 31.3 (CH_3), 21.31 (CH_3), 21.29 (CH_3).

MALDI-HRMS (pos): m/z calc. $[M]^{\cdot+}$ 1297.52357, found $[M]^{\cdot+}$ 1297.52841, *Δ* = 3.73 ppm.

TAA-TTC(Me)$_2$-PDI

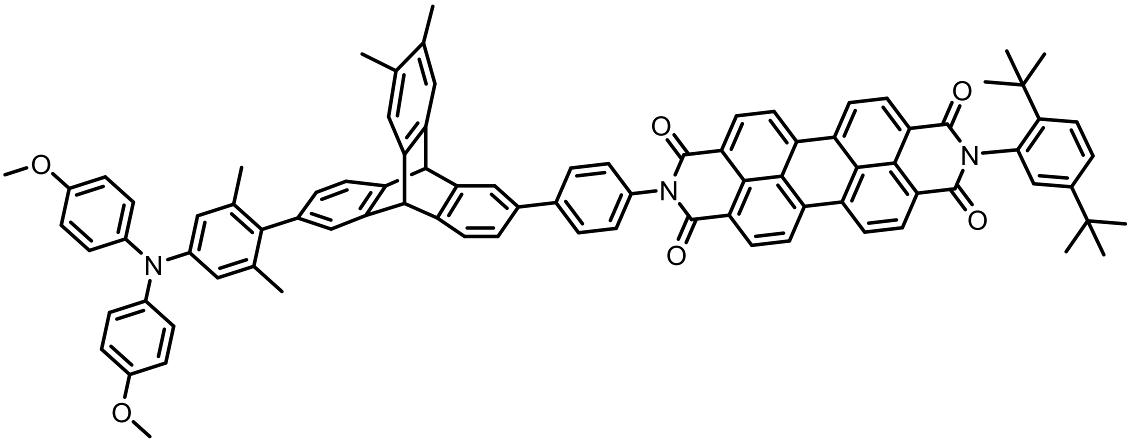

CA: [-]

Synthesis according to **GP III**.[4]

(Bpin)-TTCMe$_2$-PDI (35.0 mg, 33.0 µmol), **TAAMe$_2$-Br** (27.2 mg, 66.0 µmol), sodium carbonate (14.0 mg, 132 µmol) in THF (6 ml) and water (1.5 ml). $Pd(PPh_3)_4$ (1.91 mg, 1.65 µmol). Column chromatography (eluent: DCM – DCM/EA (100:1)). The product was dissolved in DCM and precipitated by addition of hexane.

Yield: 4.00 mg (3.16 µmol, 10 %) of a red solid.

$C_{88}H_{71}N_3O_6$ [1266.53 g/mol]

^{1}H-NMR (600.1 MHz, CD_2Cl_2):

δ [ppm] = 8.74 (m', 8H), 7.74 (m', 3H), 7.63 (d, $^3J_{H,H}$ = 8.7 Hz, 1H), 7.49 (m', 3H), 7.40 (BB', 2H), 7.34 (dd, $^3J_{H,H}$ = 7.6 Hz, $^4J_{H,H}$ = 1.8 Hz, 1H), 7.24 (m', 3H), 7.07 (d, $^4J_{H,H}$ = 2.3 Hz, 1H), 7.04 (AA', 4H), 6.83 (m', 5H), 6.62 (s, 2H), 5.51 (s, 1H), 5.44 (s, 1H), 3.78 (s, 6H), 2.21 (s, 3H), 2.20 (s, 3H), 1.84 (s, 3H), 1.82 (s, 3H), 1.33 (s, 9H), 1.28 (s, 9H).

^{13}C-NMR (150.9 MHz, CD_2Cl_2):

δ [ppm] = 164.9 (C_q), 164.0 (C_q), 156.1 (C_q), 150.8 (C_q), 147.6 (C_q), 147.1 (C_q), 145.9 (C_q), 145.8 (C_q), 144.6 (C_q), 143.8 (C_q), 143.29 (C_q), 143.26 (C_q), 142.2 (C_q), 141.6 (C_q), 138.4 (C_q), 137.8 (C_q), 137.2 (C_q), 137.1 (C_q), 135.5 (C_q), 135.4 (C_q), 134.9 (2 x C_q), 133.60 (C_q), 133.59 (C_q), 133.58 (C_q), 132.1 (CH), 132.0 (CH), 130.23 (C_q), 130.16 (C_q), 129.4 (CH), 129.3 (CH), 128.4 (CH), 128.3 (CH), 127.2 (C_q), 127.1 (C_q), 126.8 (CH), 126.7 (CH), 126.5 (CH), 125.5 (CH), 125.4 (CH), 125.2 (CH), 124.6 (CH), 124.2 (CH), 124.1 (C_q), 123.90 (CH), 123.89 (CH), 123.88 (C_q), 123.81 (CH), 122.9 (CH), 120.11 (CH), 120.09 (CH), 114.9 (CH), 55.8 (CH_3), 54.2 (CH), 54.0 (CH), 35.8 (C_q), 34.6 (C_q), 31.8 (CH_3), 31.3 (CH_3), 21.31 (CH_3), 21.27 (CH_3), 19.6 (2 x CH_3).

MALDI-HRMS (pos): m/z calc. $[M]^{\cdot+}$ 1265.53374, found $[M]^{\cdot+}$ 1265.53127, Δ = 1.95 ppm.

TAA-TTC(Cl)$_2$-PDI

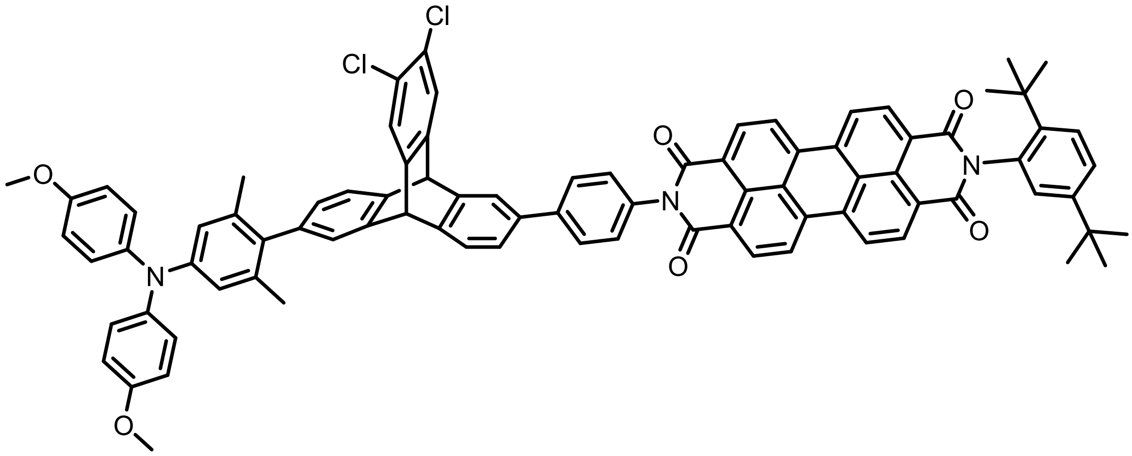

CA: [-]

Synthesis according to **GP III**.[4]

Bpin-TTCCl$_2$-PDI (49.0 mg, 44.5 µmol), **TAAMe$_2$-Br** (36.7 mg, 89.0 µmol), sodium carbonate (18.9 mg, 178 µmol) in THF (6 ml) and water (1.5 ml). $Pd(PPh_3)_4$ (2.57 mg, 2.22 µmol). Column chromatography (eluent: DCM – DCM/toluene (4:1) – DCM/toluene/EA (400:100:3)). The product was dissolved in DCM and precipitated by addition of hexane.

Yield: 26.0 mg (19.9 µmol, 45 %) of a red solid.

$C_{86}H_{65}Cl_2N_3O_6$ [1307.36 g/mol]

^{1}H-NMR (600.1 MHz, CD_2Cl_2):

δ [ppm] = 8.73 (m’, 8H), 7.78 (d, $^4J_{H,H}$ = 1.8 Hz, 1H), 7.75 (AA’, 2H), 7.62 (d, $^3J_{H,H}$ = 8.7 Hz, 1H), 7.55 (m’, 5H), 7.42 (BB’, 2H), 7.39 (dd, $^3J_{H,H}$ = 7.5 Hz, $^4J_{H,H}$ = 1.8 Hz, 1H), 7.25 (d, $^4J_{H,H}$ = 1.5 Hz, 1H), 7.09 (d, $^3J_{H,H}$ = 2.2 Hz, 1H), 7.04 (AA’, 4H), 6.86 (dd, $^3J_{H,H}$ = 7.5 Hz, $^4J_{H,H}$ = 1.7 Hz, 1H), 6.83 (BB’, 4H), 6.62 (s, 2H), 5.57 (s, 1H), 5.49 (s, 1H), 3.78 (s, 6H), 1.83 (s, 3H), 1.81 (s, 3H), 1.33 (s, 9H), 1.27 (s, 9H).

^{13}C-NMR (150.9 MHz, CD_2Cl_2):

δ [ppm] = 164.8 (C_q), 164.0 (C_q), 156.1 (C_q), 150.8 (C_q), 147.8 (C_q), 146.2 (C_q), 146.1 (C_q), 145.7 (C_q), 144.6 (2 x C_q), 144.5 (C_q), 142.5 (C_q), 141.8 (2 x C_q), 141.6 (C_q)¸139.1 (C_q), 137.14 (C_q), 137.06 (C_q), 135.43 (C_q), 135.36 (C_q)¸135.1 (C_q), 134.5 (C_q), 133.6 (C_q), 132.04 (CH), 131.98 (CH), 130.2 (C_q), 130.1 (C_q)¸129.5 (CH), 129.2 (CH), 128.79 (C_q), 128.77 (C_q), 128.4 (CH), 128.3 (CH), 127.4 (CH), 127.13 (C_q), 127.07 (C_q), 126.8 (CH), 126.5 (CH), 126.03 (CH), 126.00 (CH), 125.6 (CH), 125.1 (CH), 124.7 (CH), 124.2 (CH), 124.1 (C_q), 123.89 (CH), 123.87 (CH), 123.84 (C_q), 123.4 (CH), 120.01 (CH), 119.99 (CH), 114.9 (CH), 55.8 (CH_3), 53.4 (CH), 53.2 (CH), 35.8 (C_q), 34.6 (C_q), 31.8 (CH_3), 31.3 (CH_3), 21.3 (CH_3), 21.2 (CH_3).

MALDI-HRMS (pos): m/z calc. $[M]^{\cdot+}$ 1307.42552, found $[M]^{\cdot+}$ 1307.42616, Δ = 0.49 ppm.

TAA-TTC(PAZ)-PDI

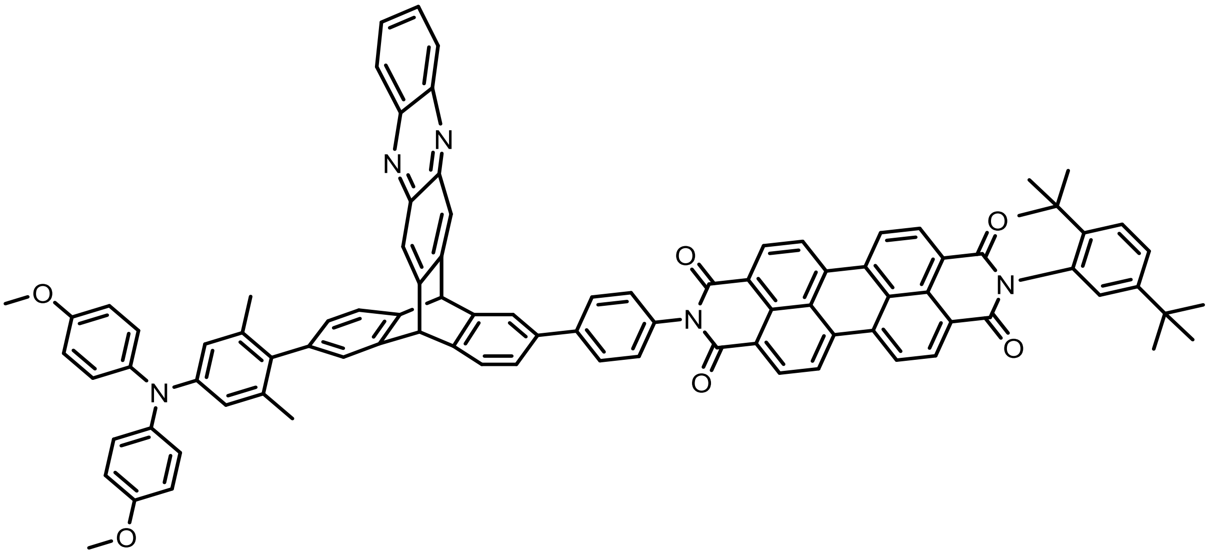

CA: [-]

Synthesis according to **GP III**.[4]

Bpin-TTC(PAZ)-PDI (38.0 mg, 33.5 µmol), **TAAMe$_2$-Br** (27.6 mg, 66.9 µmol) sodium carbonate (14.2 mg, 134 µmol) in THF (6 ml) and water (1.5 ml). Pd(PPh$_3$)$_4$ (1.94 mg, 1.68 µmol) Column chromatography (eluent: DCM/EA (10:1)). The product was dissolved in DCM and precipitated by addition of hexane.

Yield: 14.0 mg (10.4 µmol, 31 %) of a red solid.

$C_{92}H_{69}N_5O_6$ [1340.57 g/mol]

^{1}H-NMR (600.1 MHz, CD_2Cl_2):

δ [ppm] = 8.74 (m', 8H), 8.18 (m, 2H), 8.16 (s, 1H), 8.13 (s, 1H), 7.90 (d, $^4J_{H,H}$ = 1.5 Hz, 1H), 7.78 (m', 4H), 7.67 (d, $^3J_{H,H}$ = 7.9 Hz, 1H), 7.63 (m', 2H), 7.51 (dd, $^3J_{H,H}$ = 8.7 Hz, $^4J_{H,H}$ = 2.2 Hz, 1H), 7.48 (dd, $^3J_{H,H}$ = 7.7 Hz, $^4J_{H,H}$ = 1.7 Hz, 1H), 7.42 (AA', 2H), 7.37 (s, 1H), 7.07 (d, $^4J_{H,H}$ = 2.3 Hz, 1H), 7.04 (AA', 4H), 6.95 (dd, $^3J_{H,H}$ = 7.6 Hz, $^4J_{H,H}$ = 1.5 Hz, 1H), 6.83 (BB', 4H), 6.62 (m, 2H), 5.87 (s, 1H), 5.79 (s, 1H), 3.78 (s, 6H), 1.87 (s, 3H), 1.77 (s, 3H), 1.33 (s, 9H), 1.28 (s, 9H).

^{13}C-NMR (150.9 MHz, CD_2Cl_2):

δ [ppm] = 164.9 (C_q), 164.0 (C_q), 156.1 (C_q), 150.8 (C_q), 147.8 (C_q), 147.0 (C_q), 146.97 (C_q), 144.8 (C_q), 144.6 (C_q), 143.59 (C_q), 143.58 (C_q), 143.53 (C_q), 143.45 (C_q), 143.44 (C_q), 141.8 (C_q), 141.62 (C_q), 141.57 (C_q), 139.7 (C_q), 139.0 (C_q), 137.13 (C_q), 137.05 (C_q), 135.5 (C_q), 135.4 (C_q), 135.1 (C_q), 134.5 (2 x C_q), 133.6 (C_q), 132.1 (CH), 132.0 (CH), 130.23 (C_q), 130.17 (C_q), 130.14 (CH), 130.13 (CH), 129.84 (CH), 129.81 (CH), 129.5 (CH), 129.3 (CH), 128.5 (CH), 128.3 (CH), 128.0 (CH), 127.2 (C_q), 127.1 (C_q), 126.8 (CH), 126.5 (CH), 125.9 (CH), 125.7 (CH), 125.0 (CH), 124.5 (CH), 124.1 (C_q), 123.91 (CH), 123.88 (CH), 123.86 (C_q), 123.7 (CH), 122.91 (CH), 122.88 (CH), 120.02 (CH), 120.01 (CH), 114.9 (CH), 55.8 (CH_3), 53.8 (CH), 53.6 (CH), 35.8 (C_q), 34.6 (C_q), 31.8 (CH_3), 31.3 (CH_3), 21.3 (CH_3), 21.2 (CH_3).

MALDI-HRMS (pos): m/z calc. $[M]^{\cdot+}$ 1339.52424, found $[M]^{\cdot+}$ 139.52399, *Δ* = 0.19 ppm.[7]

TTC-Ph$_2$

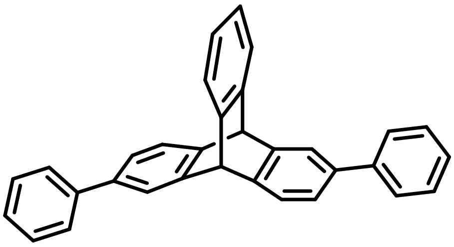

Synthesis according to literature.[4]

CA: [-]

Synthesis according to **GP III**.

TTC-(Bpin)$_2$ (20.0 mg, 39.5 µmol), iodobenzene (20.2 mg, 99.0 µmol), sodium carbonate (16.8 mg, 159 µmol) in THF (6 ml) and water (1.5 ml). Pd(PPh_3)$_4$ (2.28 mg, 1.97 µmol). Column chromatography on silica gel (eluent: DCM/PE (50:5)).

---

[7] Peak refers to the second highest peak.

Yield: 10.0 mg (24.6 µmol, 62 %) of a colourless solid.

$C_{32}H_{22}$ [406.52 g/mol]

^{1}H-NMR (400.1 MHz, $CDCl_3$):

δ [ppm] = 7.64 (d, $^4J_{H,H}$ = 1.8 Hz, 2H), 7.51 (m', 4H), 7.47 (d, $^3J_{H,H}$ = 7.6 Hz, 2H), 7.44 (m, 2H), 7.39 (m, 4H), 7.07 (s, 2H), 7.30 (m', 2H), 7.23 (dd, $^3J_{H,H}$ = 7.6 Hz, $^4J_{H,H}$ = 1.8 Hz, 2H), 5.53 (s, 2H).

^{13}C-NMR (100.6 MHz, $CDCl_3$):

δ [ppm] = 145.9 (C_q), 145.2 (C_q), 144.4 (C_q), 141.4 (C_q), 138.8 (C_q), 128.8 (CH), 127.4 (CH), 127.1 (CH), 125.5 (CH), 124.3 (CH), 124.1 (CH), 123.8 (CH), 122.9 (CH), 55.1 (CH).

APCI-MS (pos): m/z calc. $[M+H]^+$ 407.1794, found $[M]^+$ 407.1800.

TTC(OMe)$_2$-Ph$_2$

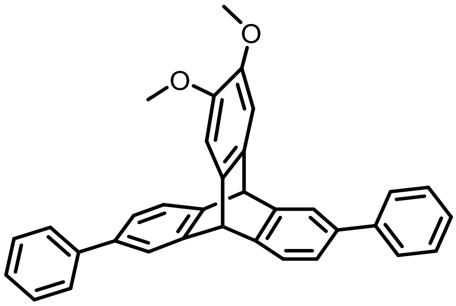

CA: [-]

Synthesis according to **GP III**.[4]

TTC(OMe)$_2$-(Bpin)$_2$ (20.0 mg, 35.3 µmol), iodobenzene (28.8 mg, 141 µmol), sodium carbonate (15.0 mg, 142 µmol) in THF (6 ml) and water (1.5 ml). $Pd(PPh_3)_4$ (2.04 mg, 1.77 µmol). Column chromatography on silica gel (eluent: DCM/PE (5:1)).

Yield: 12.0 mg (25.7 µmol, 73 %) of a colourless solid.

$C_{34}H_{26}O_2$ [466.57 g/mol]

^{1}H-NMR (400.1 MHz, $CDCl_3$):

δ [ppm] = 7.62 (d, $^4J_{H,H}$ = 1.8 Hz, 2H), 7.51 (m', 4H), 7.46 (d, $^3J_{H,H}$ = 7.5 Hz, 2H), 7.39 (m', 4H), 7.30 (m, 2H), 7.22 (dd, $^3J_{H,H}$ = 7.5 Hz, $^4J_{H,H}$ = 1.8 Hz, 2H), 7.07 (s, 2H), 5.45 (s, 2H), 3.85 (s, 6H).

^{13}C-NMR (100.6 MHz, $CDCl_3$):

δ [ppm] = 146.34 (C_q), 146.30 (C_q), 144.8 (C_q), 141.4 (C_q), 138.7 (C_q), 137.9 (C_q), 128.8 (CH), 127.4 (CH), 127.1 (CH), 124.2 (CH), 123.8 (CH), 122.7 (CH), 108.7 (CH), 56.4 (CH_3), 53.7 (CH).

APCI-MS (pos): m/z calc. $[M+H]^+$ 467.2006, found $[M]^+$ 467.2014.

Ph-TTC(OMe)$_2$-PDI

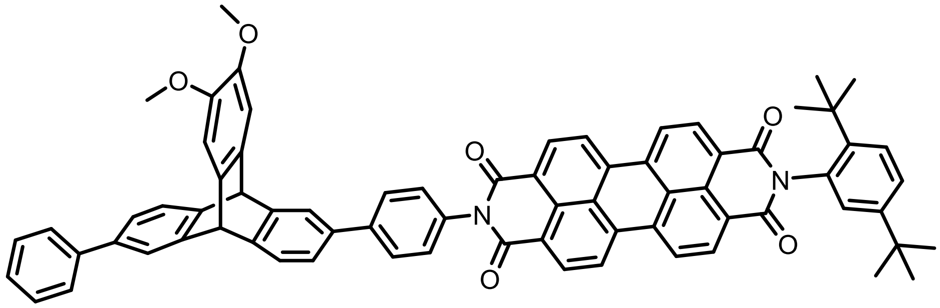

CA: [-]

Synthesis according to **GP III**.[4]

(Bpin)-TTC(OMe)$_2$-PDI (20.0 mg, 18.3 µmol), iodobenzene (7.45 mg, 36.5 µmol), sodium carbonate (7.74 mg, 73.0 µmol) in THF (6 ml) and water (1.5 ml). $Pd(PPh_3)_4$ (1.06 mg, 0.917 µmol). Column chromatography on silica gel (eluent: DCM/EA (10:1), Toluene/EA (7:1)).

Yield: 10.0 mg (9.59 µmol, 52 %) of a red solid.

$C_{72}H_{54}N_2O_6$ [1043.21 g/mol]

^{1}H-NMR (400.1 MHz, $CDCl_3$):

δ [ppm] = 8.73 (m', 8H), 7.70 (m', 3H), 7.65 (d, $^4J_{H,H}$ = 1.7 Hz, 1H), 7.61 (d, $^3J_{H,H}$ = 8.6 Hz, 1H), 7.51 (m', 5H), 7.40 (m', 4H), 7.30 (m', 2H), 7.24 (dd, $^3J_{H,H}$ = 7.6 Hz, $^4J_{H,H}$ = 1.7 Hz, 1H), 7.10 (s, 1H), 7.09 (s, 1H), 7.06 (dd, $^4J_{H,H}$ = 2.2 Hz, 1H), 5.49 (s, 1H), 5.48 (s, 1H), 3.88 (s, 3H), 3.87 (s, 3H), 1.33 (s, 9H), 1.30 (s, 9H).

^{13}C-NMR (100.6 MHz, $CDCl_3$):

δ [ppm] = 164.5 (C_q), 163.8 (C_q), 150.3 (C_q), 146.4 (C_q), 146.35 (C_q), 146.33 (C_q), 146.30 (C_q), 145.2 (C_q), 144.8 (C_q), 143.8 (C_q), 142.2 (C_q), 141.4 (C_q), 138.7 (C_q), 137.94 (C_q), 137.87 (C_q), 137.82 (C_q), 135.3 (C_q), 135.0 (C_q), 134.1 (C_q), 132.7 (C_q), 132.07 (CH), 132.04 (CH), 130.00 (C_q), 129.96 (C_q), 129.0 (CH), 128.9 (CH), 128.8 (CH), 128.5 (CH), 127.9 (CH), 127.4 (CH), 127.3 (CH), 127.2 (CH), 126.91 (C_q), 126.85 (C_q), 126.6 (CH), 124.5 (CH), 124.3 (CH), 123.9 (C_q), 123.87 (CH), 123.84 (CH), 123.545 (C_q), 123.53 (CH), 123.45 (CH), 122.8 (CH), 122.7 (CH), 108.7 (CH), 56.4 (2 x CH), 53.8 (CH_3), 53.7 (CH_3), 35.7 (C_q), 34.4 (C_q), 31.9 (CH_3), 31.4 (CH_3).

MALDI-MS (pos): m/z calc. $[M+H]^+$ 1042.397639.

TTCMe$_2$-Ph$_2$

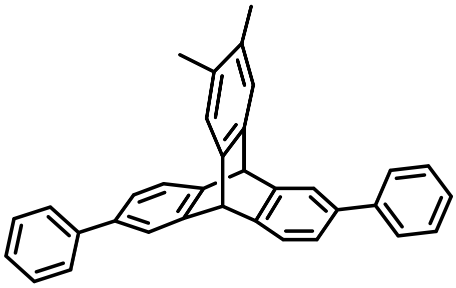

CA: [-]

Synthesis according to **GP III**.[4]

TTCMe$_2$-(Bpin)$_2$ (20.0 mg, 37.4 µmol), iodobenzene (22.9 mg, 112 µmol), sodium carbonate (15.9 mg, 150 µmol) in THF (6 ml) and water (1.5 ml). $Pd(PPh_3)_4$ (2.16 mg, 1.87 µmol). Column chromatography on silica gel (eluent: DCM/PE (1:8)).

Yield: 10.0 mg (23.0 µmol, 61 %) of a colourless solid.

$C_{34}H_{26}$ [434.57 g/mol]

^{1}H-NMR (400.1 MHz, $CDCl_3$):

δ [ppm] = 7.61 (d, $^4J_{H,H}$ = 1.8 Hz, 2H), 7.49 (m', 4H), 7.44 (d, $^3J_{H,H}$ = 7.7 Hz, 2H), 7.38 (m', 4H), 7.29 (m, 2H), 7.24 (s, 2H), 7.20 (dd, $^3J_{H,H}$ = 7.7 Hz, $^4J_{H,H}$ = 1.8 Hz, 2H), 5.46 (s, 2H), 2.18 (s, 6H).

^{13}C-NMR (100.6 MHz, $CDCl_3$):

δ [ppm] = 146.2 (C_q), 144.7 (C_q), 142.8 (C_q), 141.6 (C_q), 138.7 (C_q), 133.4 (C_q), 128.8 (CH), 127.4 (CH), 127.1 (CH), 125.3 (CH), 124.2 (CH), 123.9 (CH), 122.8 (CH), 53.6 (CH), 19.7 (CH_3).

$TTCCl_2$-Ph_2

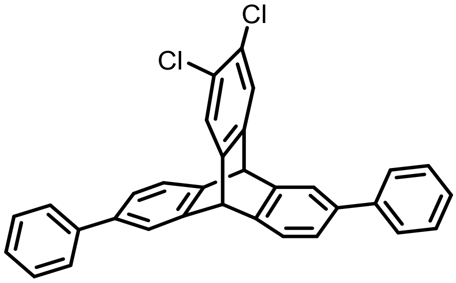

CA: [-]

Synthesis according to **GP III**.[4]

$TTCCl_2$-$(Bpin)_2$ (20.0 mg, 34.8 µmol), iodobenzene (17.7 mg, 86.8 µmol) sodium carbonate (14.7 mg, 139 µmol) in THF (6 ml) and water (1.5 ml). $Pd(PPh_3)_4$ (2.01 mg, 1.74 µmol) Column chromatography on silica gel (eluent: DCM/PE (1:5)).

Yield: 15.0 mg (31.6 µmol, 91 %) of a colourless solid.

$C_{32}H_{20}Cl_2$ [475.41 g/mol]

^{1}H-NMR (400.1 MHz, $CDCl_3$):

δ [ppm] = 7.39 (d, $^4J_{H,H}$ = 1.8 Hz, 2H), 7.26 (m', 5H), 7.23 (d, $^3J_{H,H}$ = 7.6 Hz, 2H), 7.16 (m', 4H), 7.07 (m', 2H), 7.02 (m', 3H), 5.23 (s, 2H).

^{13}C-NMR (100.6 MHz, $CDCl_3$):

δ [ppm] = 145.3 (C_q), 144.9 (C_q), 143.3 (C_q), 141.1 (C_q), 139.3 (C_q), 128.9 (CH), 128.7 (C_q), 127.36 (CH), 127.35 (CH), 125.8 (CH), 124.7 (CH), 124.3 (CH), 123.1 (CH), 53.1 (CH).

APCI-MS (pos): m/z calc. $[M+H]^+$ 475.1015, found $[M+H]^+$ 475.1019.

TTC(PAZ)-Ph$_2$

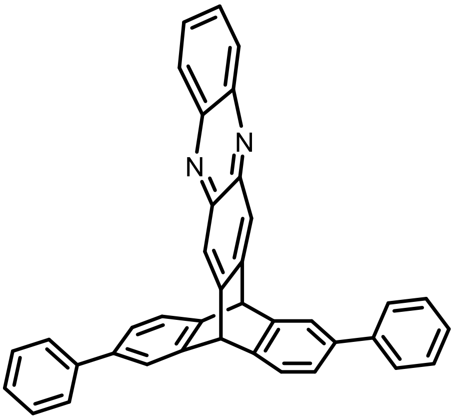

CA: [-]

Synthesis according to **GP III**.[4]

TTC(PAZ)-(Bpin)$_2$ (23.0 mg, 37.8 µmol), iodobenzene (30.9 mg, 151 µmol), sodium carbonate (20.0 mg, 189 µmol) in THF (6 ml) and water (1.5 ml). $Pd(PPh_3)_4$ (2.18 mg, 1.89 µmol). Column chromatography on silica gel (eluent: DCM).

Yield: 14.0 mg (27.5 µmol, 73 %) of a yellow solid.

$C_{38}H_{24}N_2$ [508.61 g/mol]

^{1}H-NMR (400.1 MHz, $CDCl_3$):

δ [ppm] = 8.19 (m, 2H), 8.14 (s, 2H), 7.77 (m', 4H), 7.60 (d, $^3J_{H,H}$ = 7.8 Hz, 2H), 7.53 (m', 4H), 7.41 (m', 4H), 7.33 (m', 4H), 5.78 (s, 2H).

^{13}C-NMR (100.6 MHz, $CDCl_3$):

δ [ppm] = 146.4 (C_q), 143.9 (C_q), 143.2 (C_q), 143.1 (C_q), 142.3 (C_q), 141.1 (C_q), 139.9 (C_q), 130.0 (CH), 129.6 (CH), 128.9 (CH), 127.42 (CH), 127.38 (CH), 125.4 (CH), 124.7 (CH), 123.4 (CH), 122.7 (CH), 53.5 (CH).

APCI-MS (pos): m/z calc. $[M+H]^+$ 509.2012, found $[M+H]^+$ 509.2008.

1.5. NMR spectra of all triads and precursors

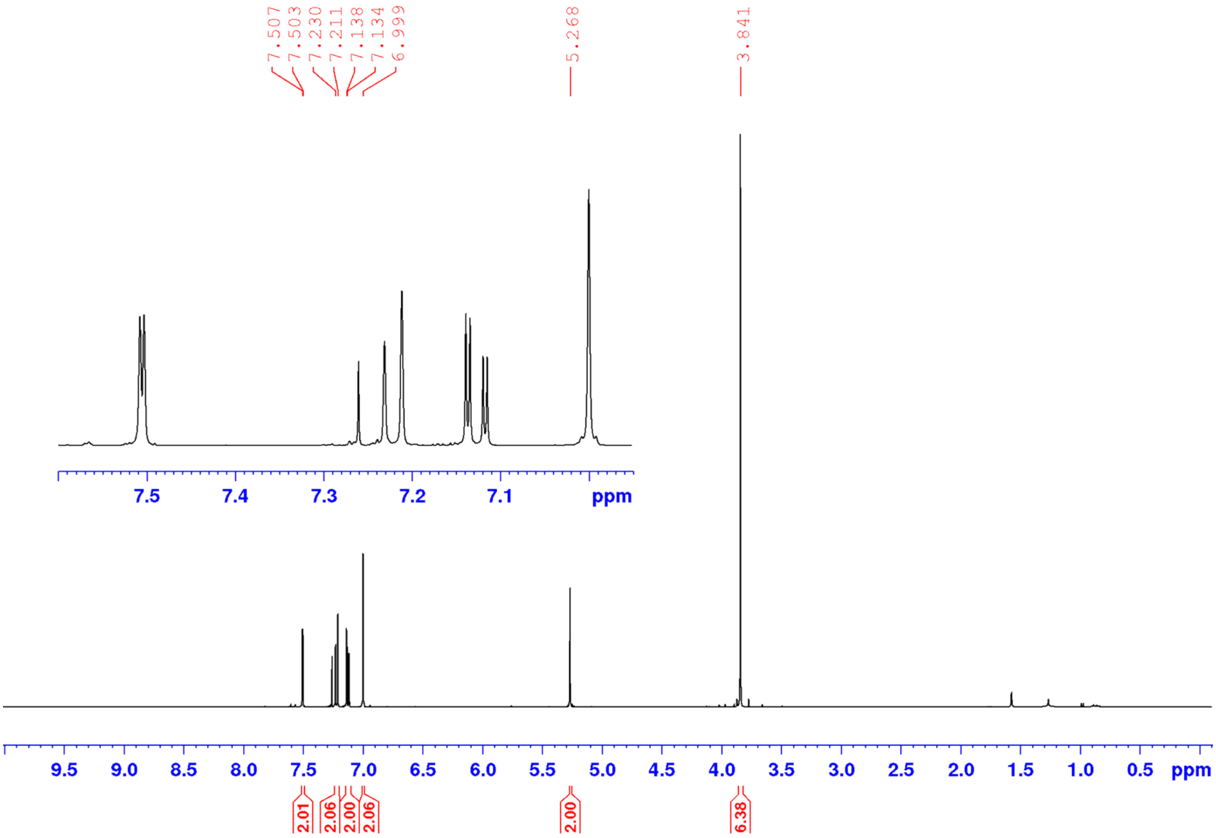

Fig S1: ^{1}H-NMR: TTC(OMe)$_2$-(Br)$_2$ (CDCl$_3$, 400.1 MHz).

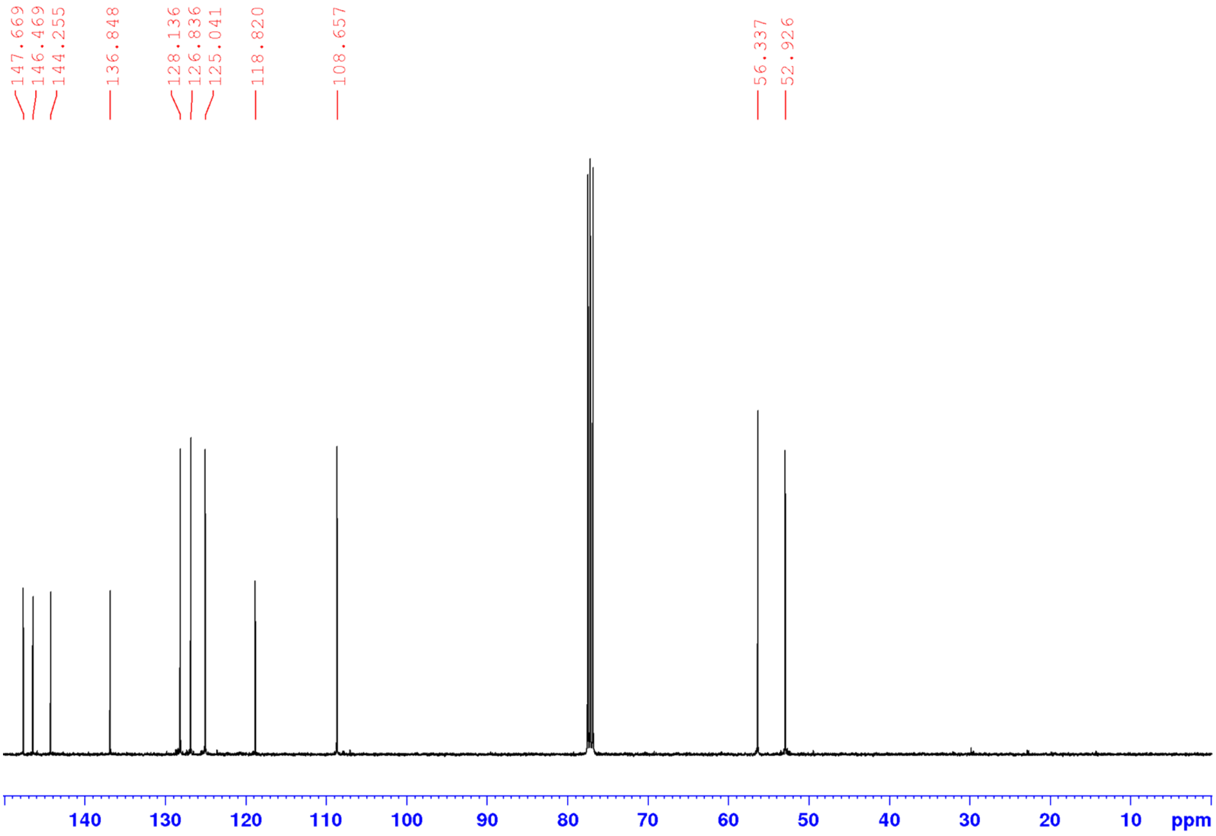

Fig S2: ^{13}C-NMR: TTC(OMe)$_2$-(Br)$_2$ (CDCl$_3$, 100.6 MHz).

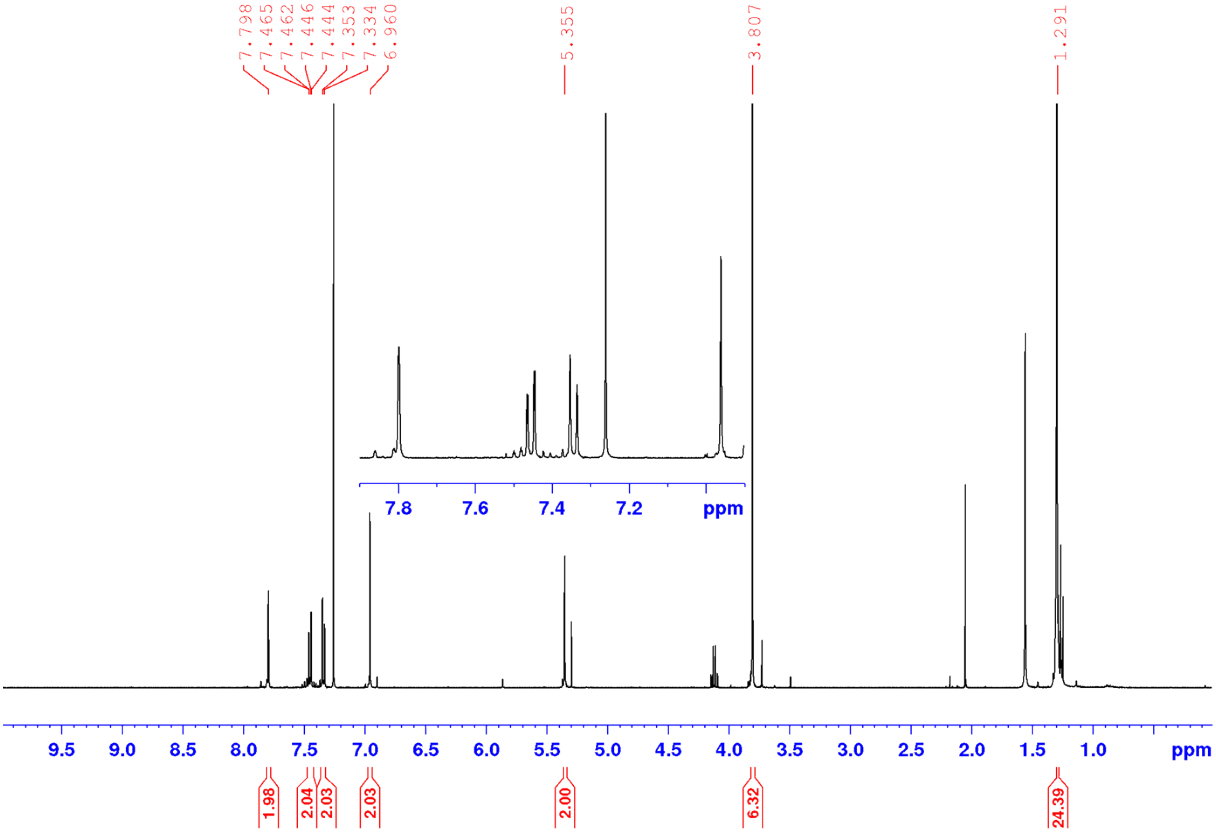

Fig S3: ^{1}H-NMR: TTC(OMe)$_2$-(Bpin)$_2$ (CDCl$_3$, 400.1 MHz). Peaks of ethyl acetate (1.26, 2.06, 4.12).

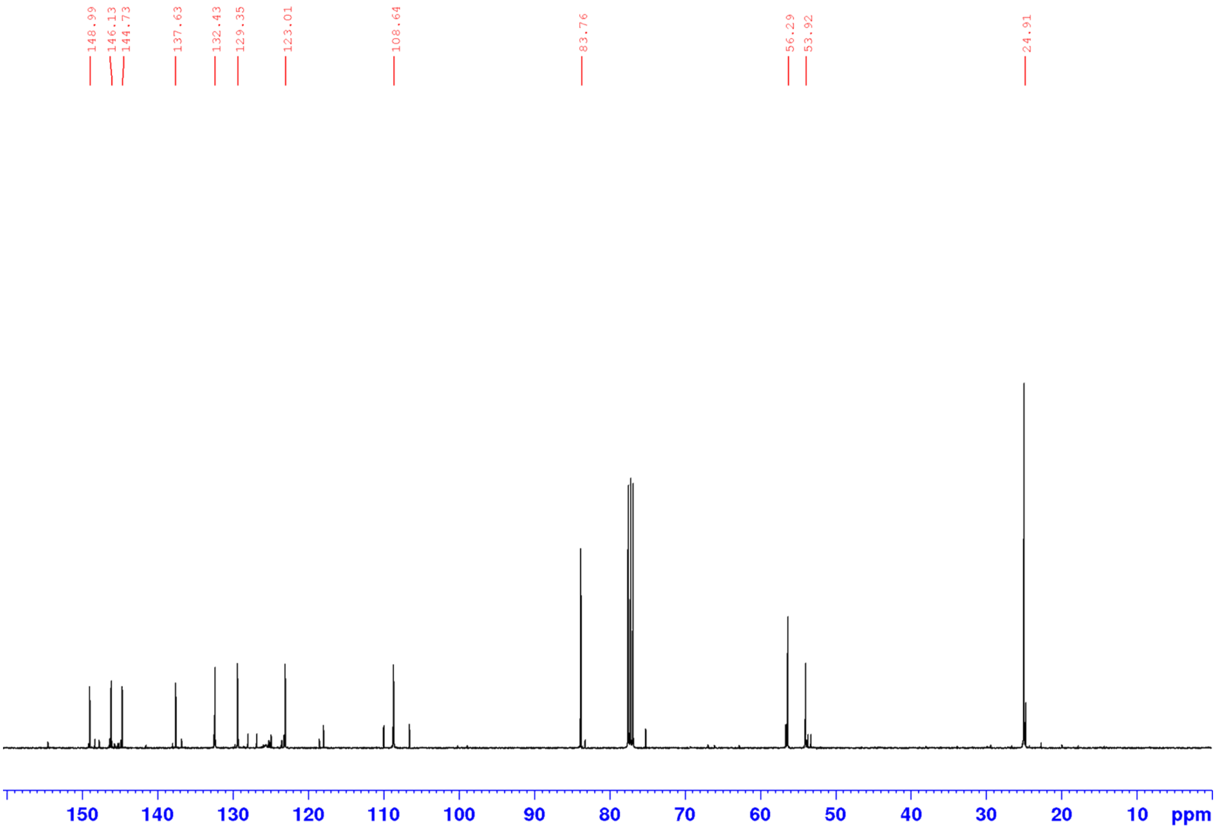

Fig S4: ^{13}C-NMR: TTC(OMe)$_2$-(Bpin)$_2$ (CDCl$_3$, 100.6 MHz).

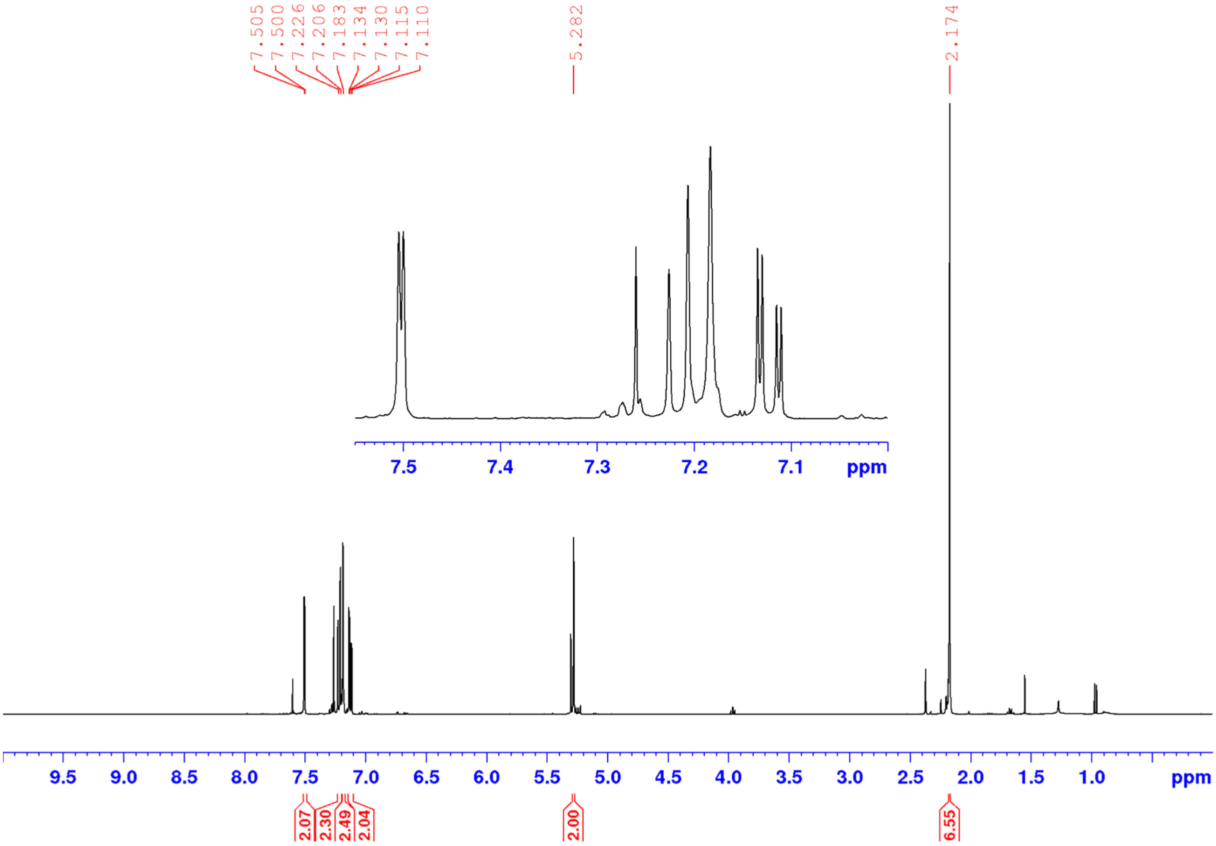

Fig S5: ^{1}H-NMR: TTC(Me)$_2$-(Br)$_2$ (CDCl$_3$, 400.1 MHz).

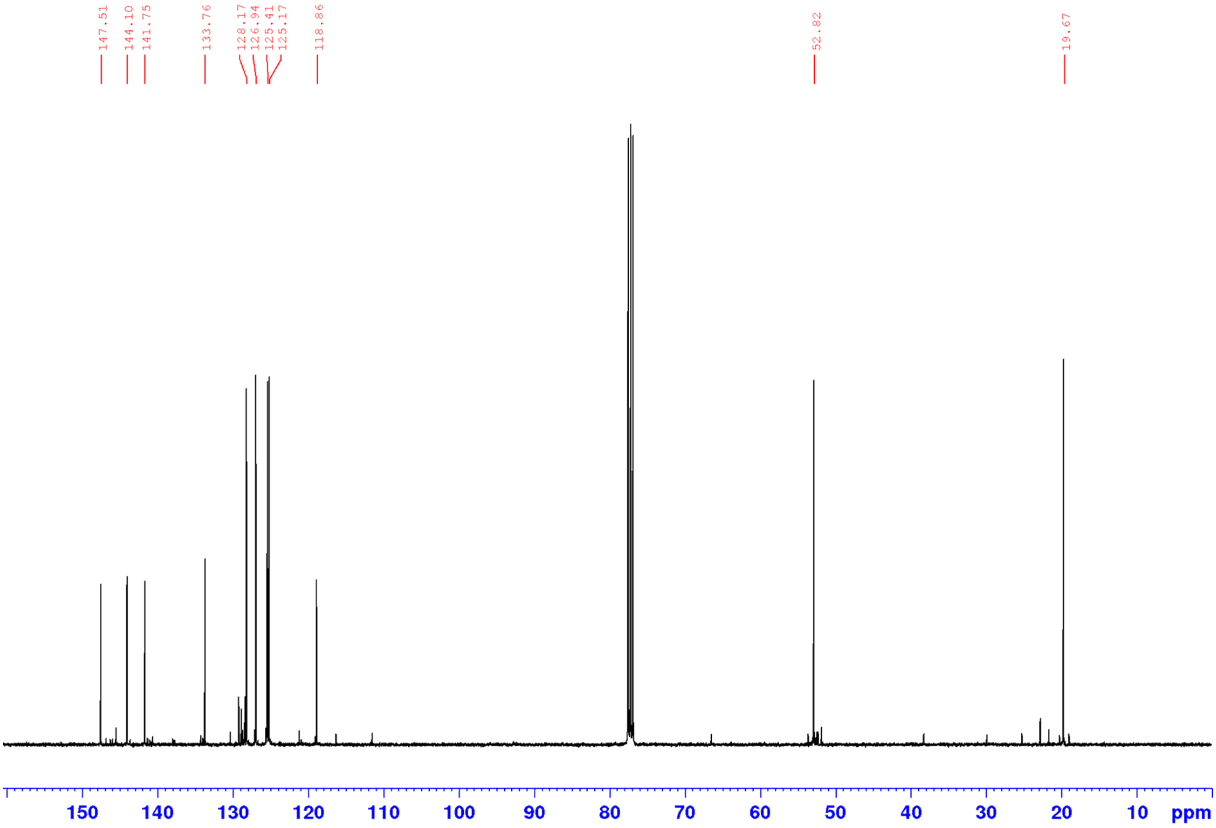

Fig S6: ^{13}C-NMR: TTC(Me)$_2$-(Br)$_2$ (CDCl$_3$, 100.6 MHz).

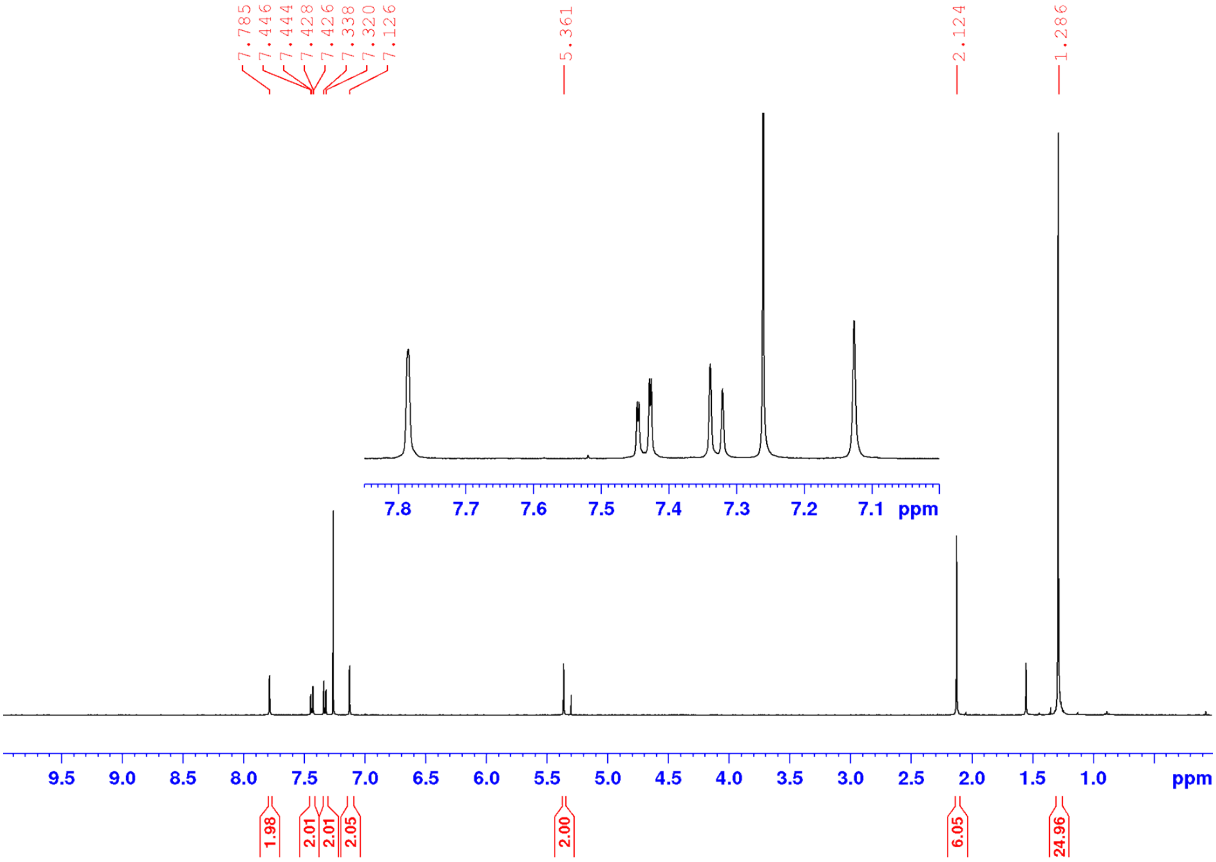

Fig S7: ^{1}H-NMR: TTC(Me)$_2$-(Bpin)$_2$ (CDCl$_3$, 400.1 MHz).

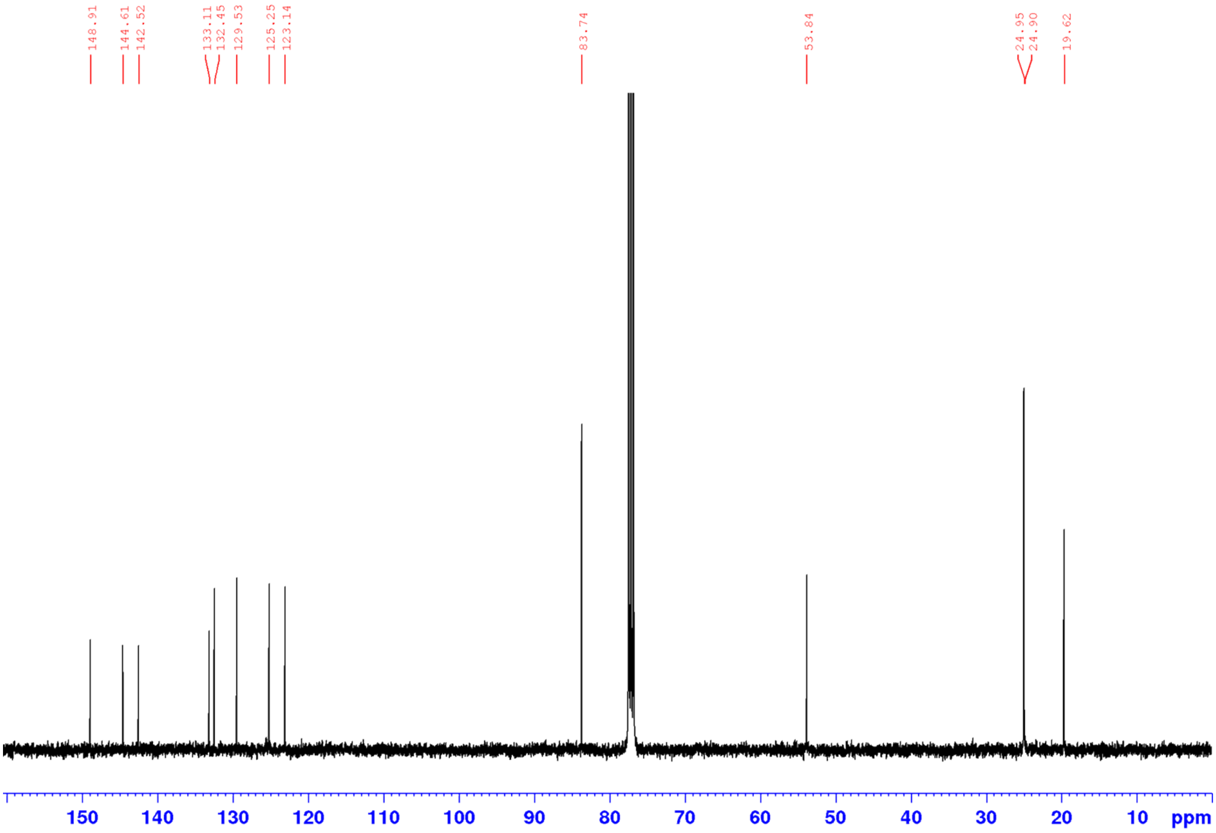

Fig S8: ^{13}C-NMR: TTC(Me)$_2$-(Bpin)$_2$ (CDCl$_3$, 100.6 MHz).

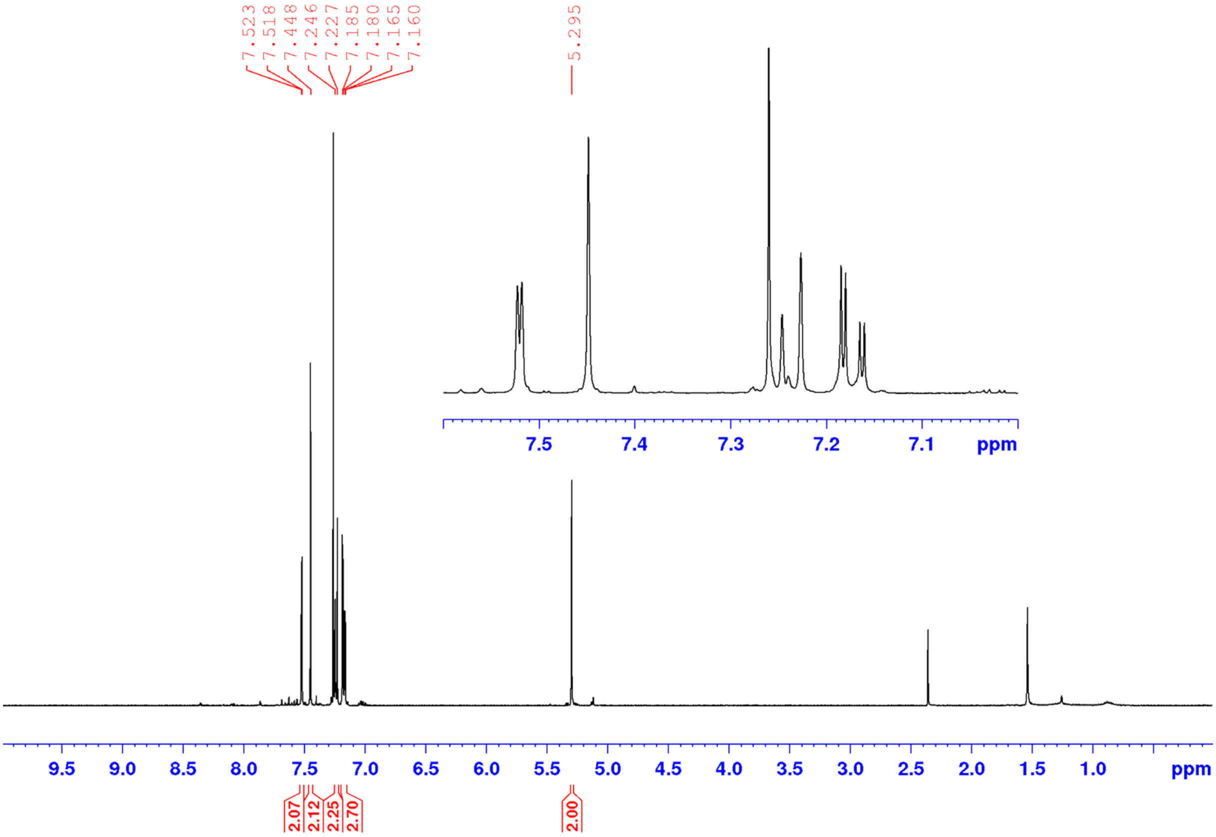

Fig S9: ^{1}**H-NMR:** TTC(Cl)$_2$-(Br)$_2$ (CDCl$_3$, 400.1 MHz).

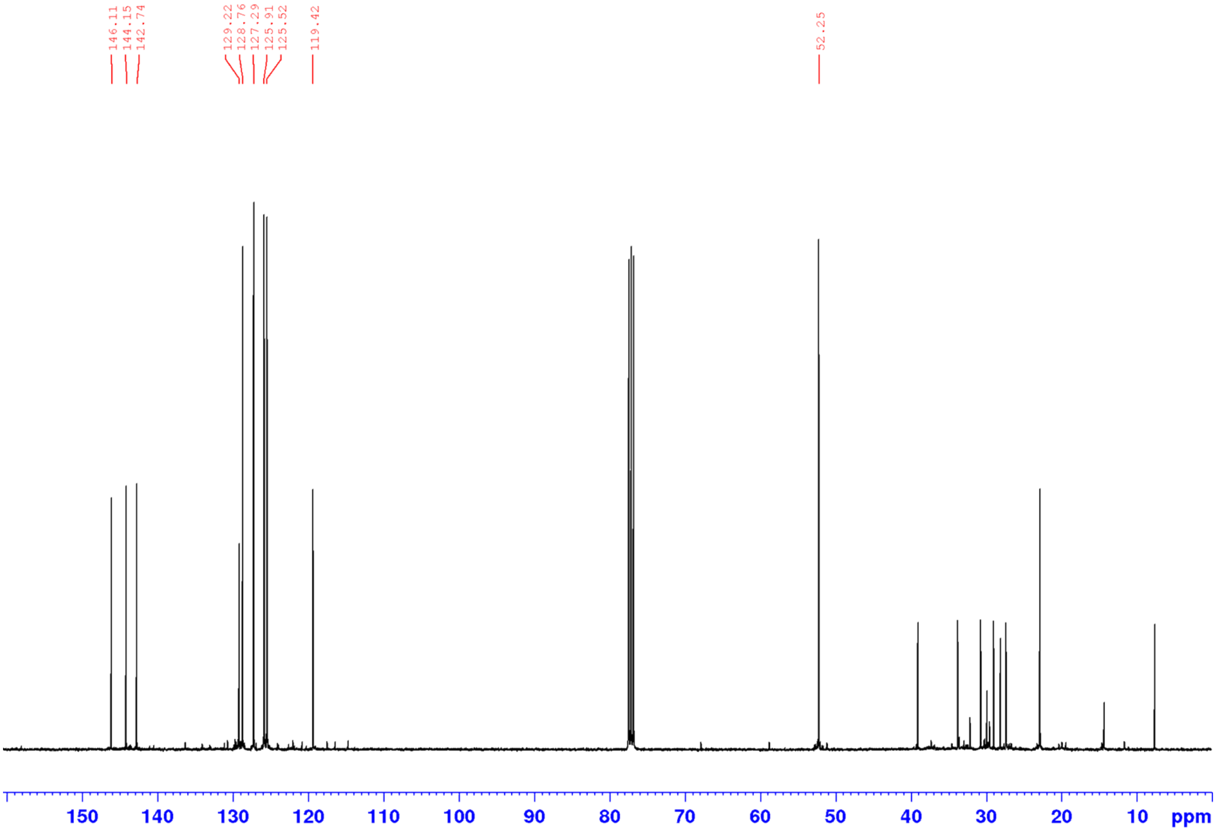

Fig S10: ^{13}**C-NMR:** TTC(Cl)$_2$-(Br)$_2$ (CDCl$_3$, 100.6 MHz). Peaks between 0-40 ppm are from hexanes.

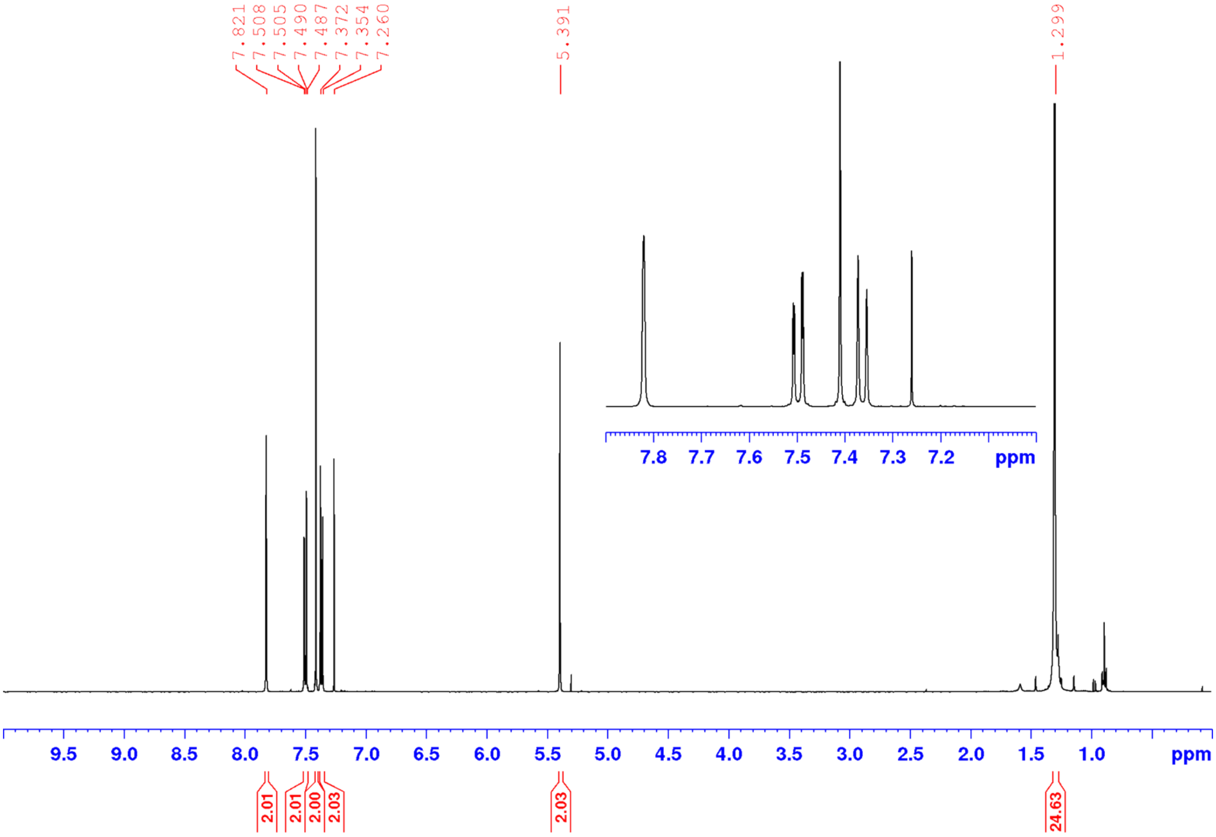

Fig S11: ^{1}**H-NMR:** TTC(Cl)$_2$-(Bpin)$_2$ ($CDCl_3$, 400.1 MHz).

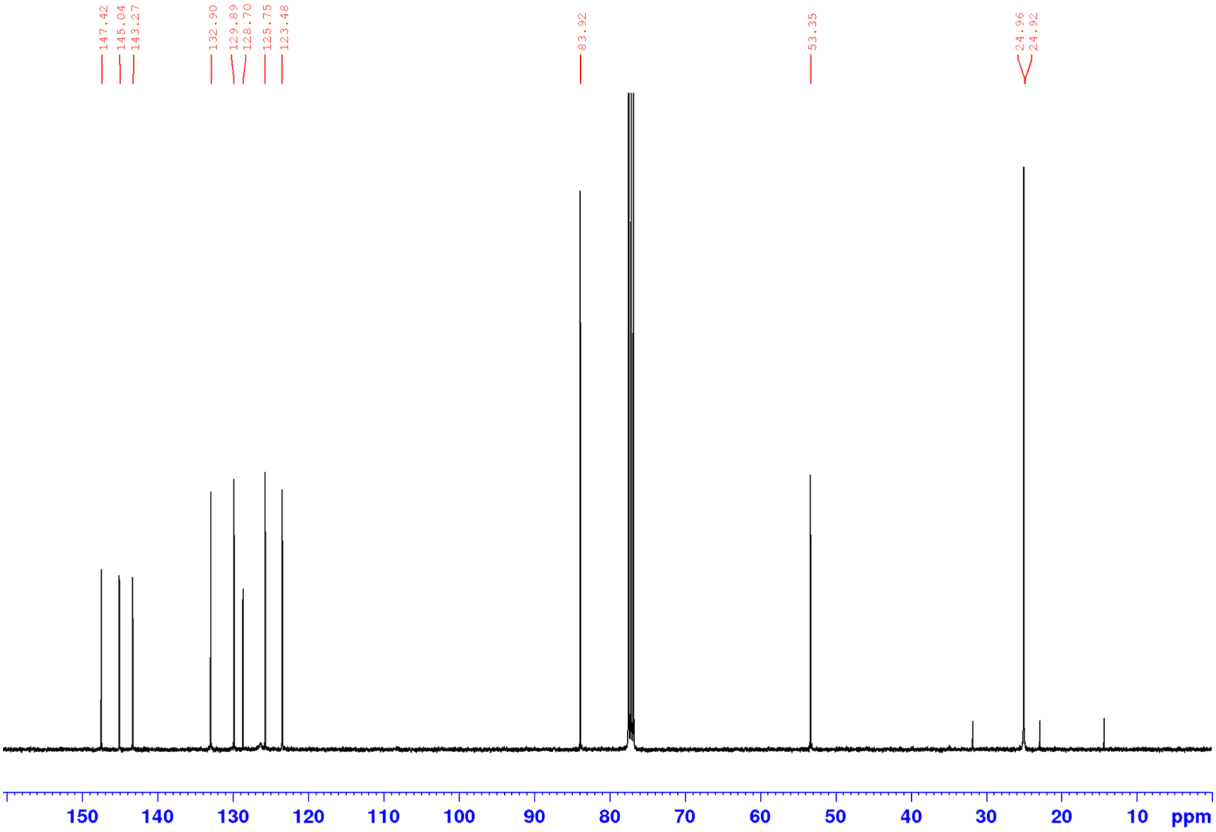

Fig S12: ^{13}**C-NMR:** TTC(Cl)$_2$-(Bpin)$_2$ ($CDCl_3$, 100.6 MHz).

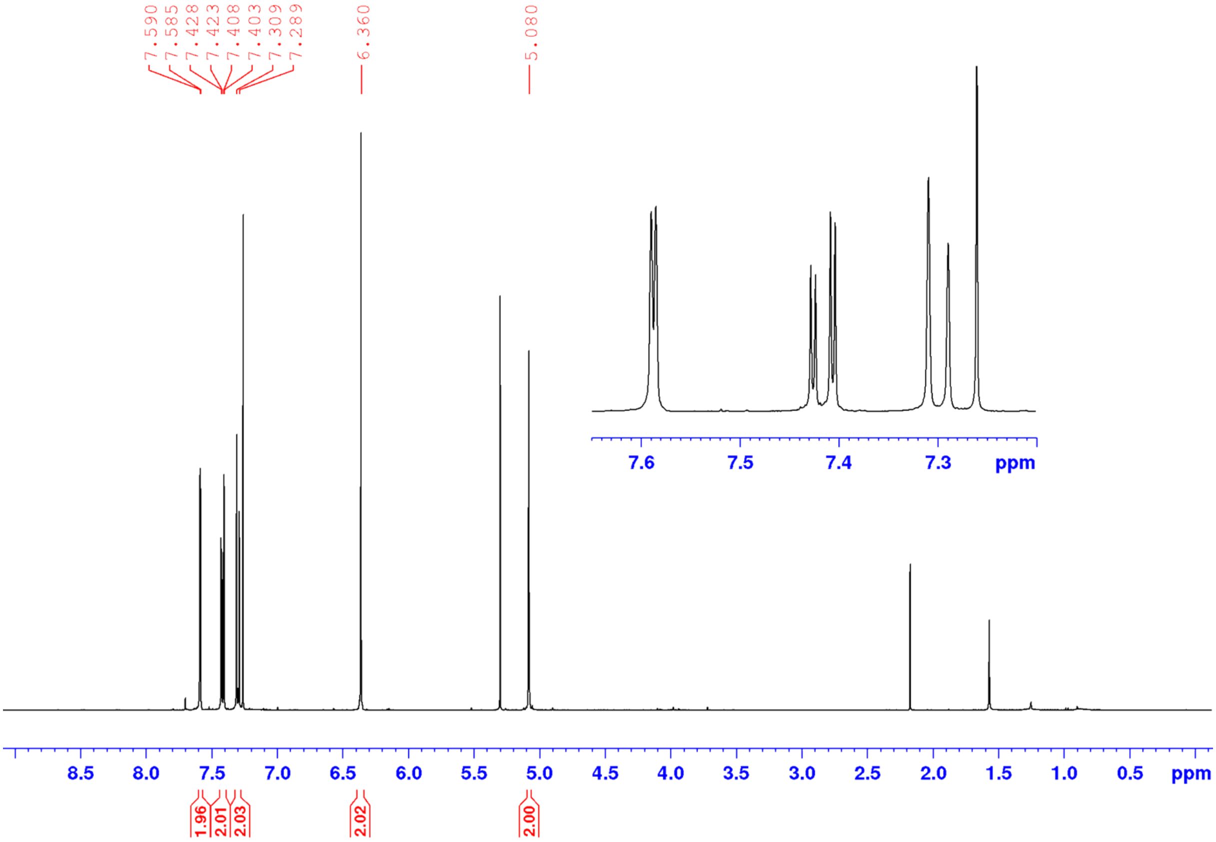

Fig S13: ^{1}**H-NMR:** TTCO$_2$-(Br)$_2$ (CDCl$_3$, 400.1 MHz). Acetone (2.17 ppm).

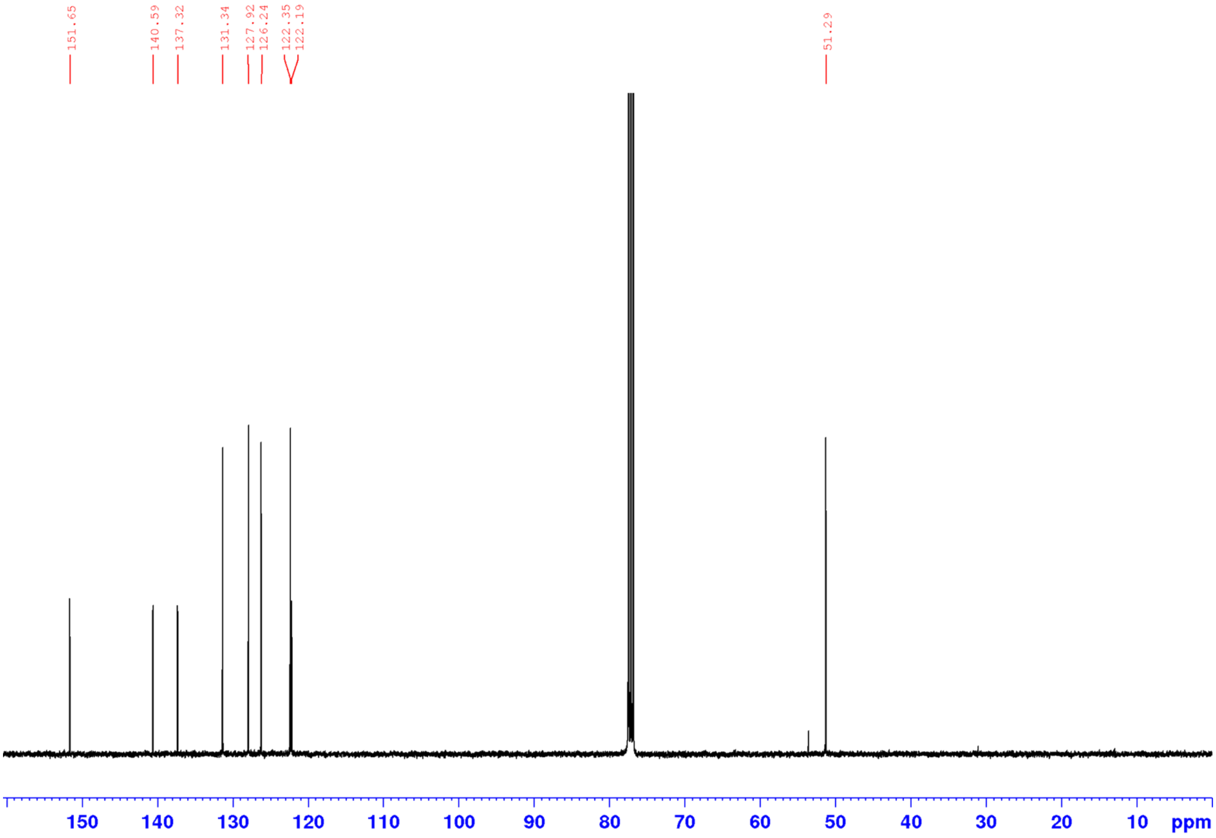

Fig S14: ^{13}**C-NMR:** TTCO$_2$-(Br)$_2$ (CDCl$_3$, 100.6 MHz).

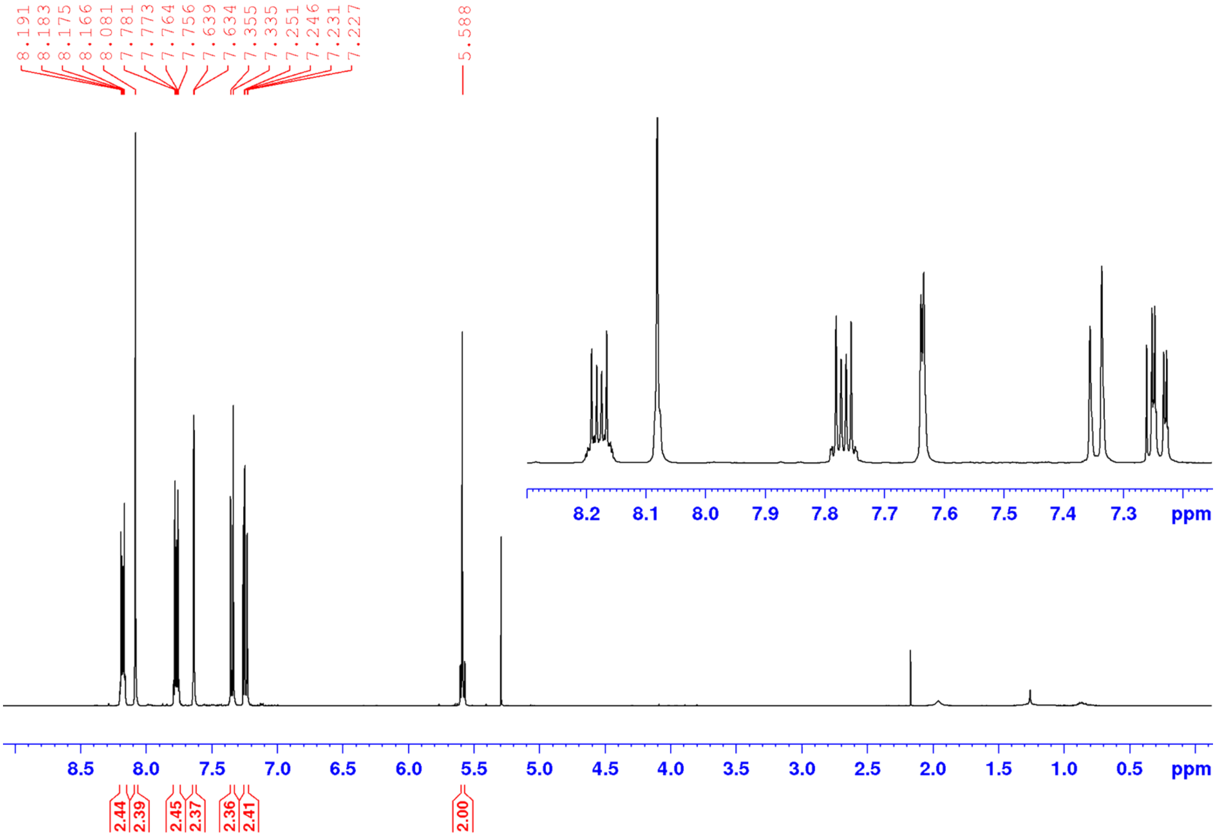

Fig S15: ^{1}**H-NMR:** TTC(PAZ)-(Br)$_2$ (CDCl$_3$, 400.1 MHz).

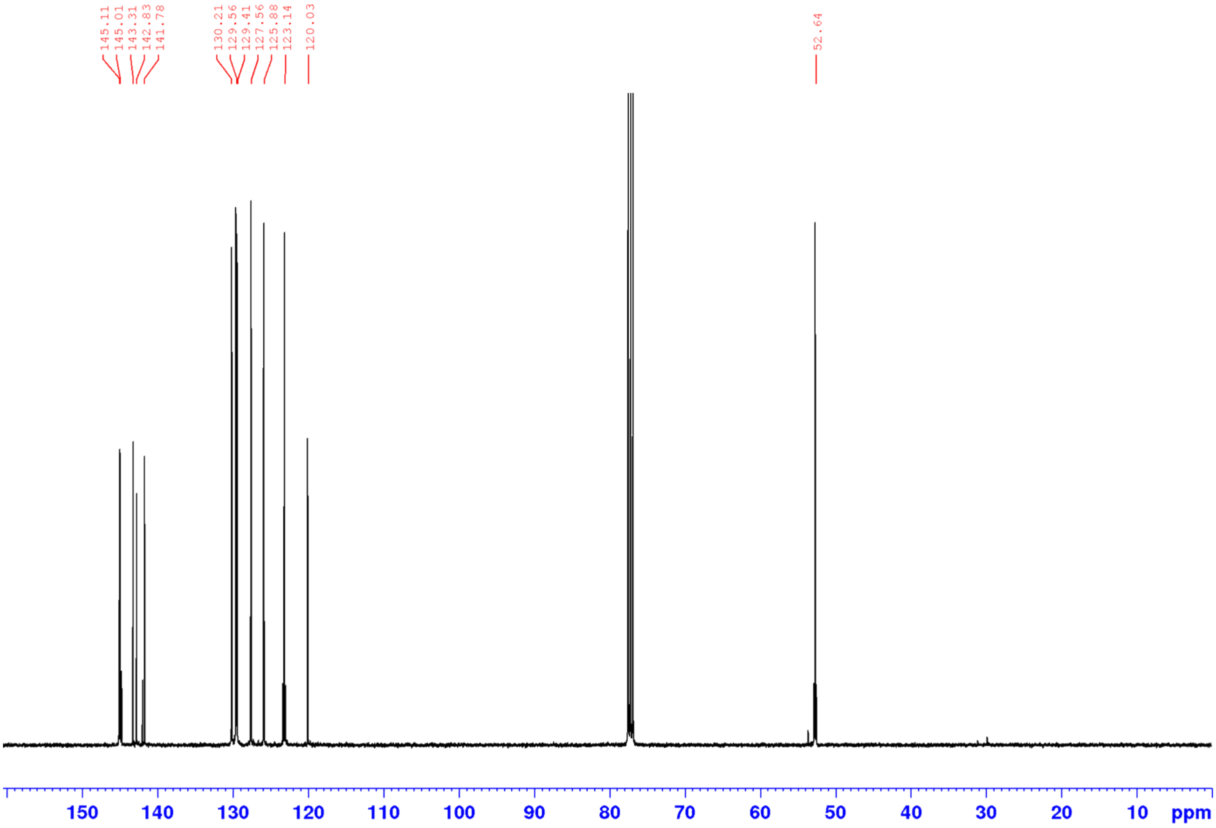

Fig S16: ^{13}**C-NMR:** TTC(PAZ)-(Br)$_2$ (CDCl$_3$, 100.6 MHz).

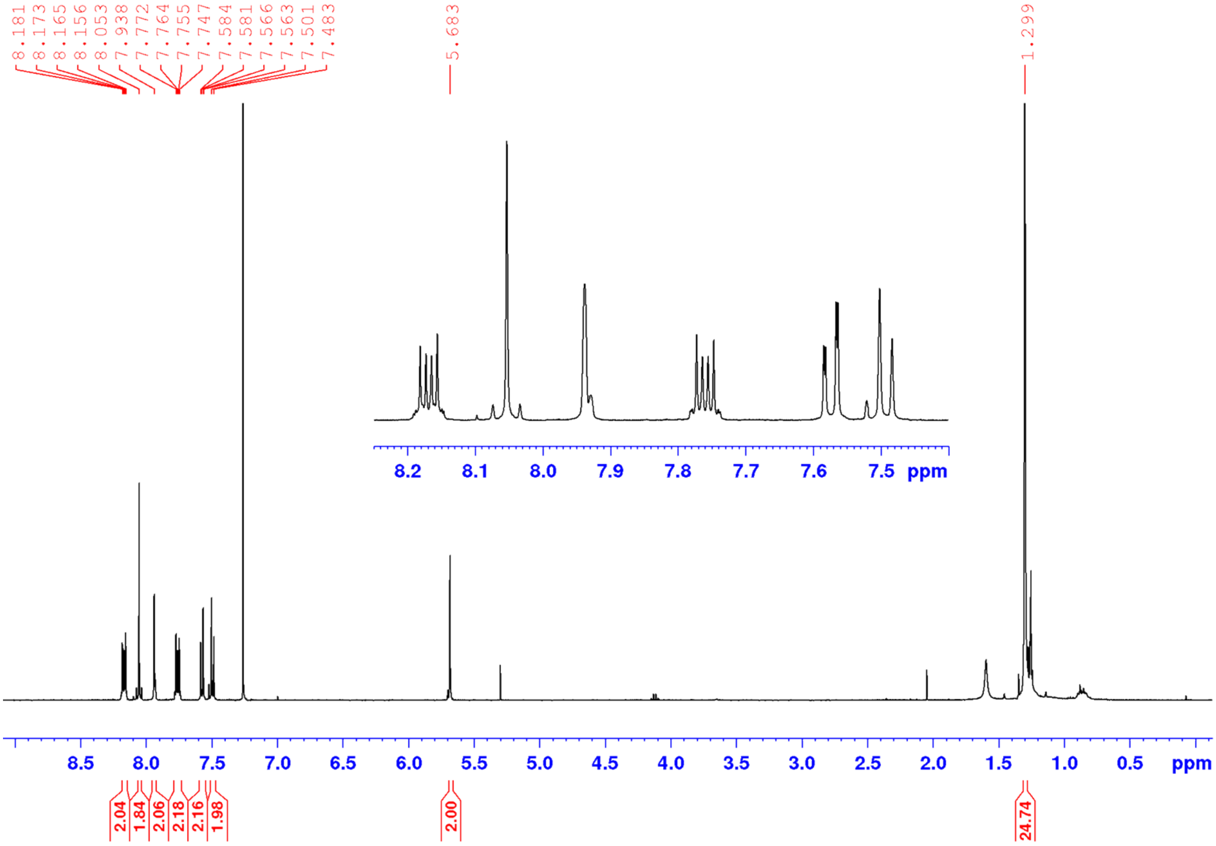

Fig S17: ^{1}H-NMR: TTC(PAZ)-(Bpin)$_2$ (CDCl$_3$, 400.1 MHz).

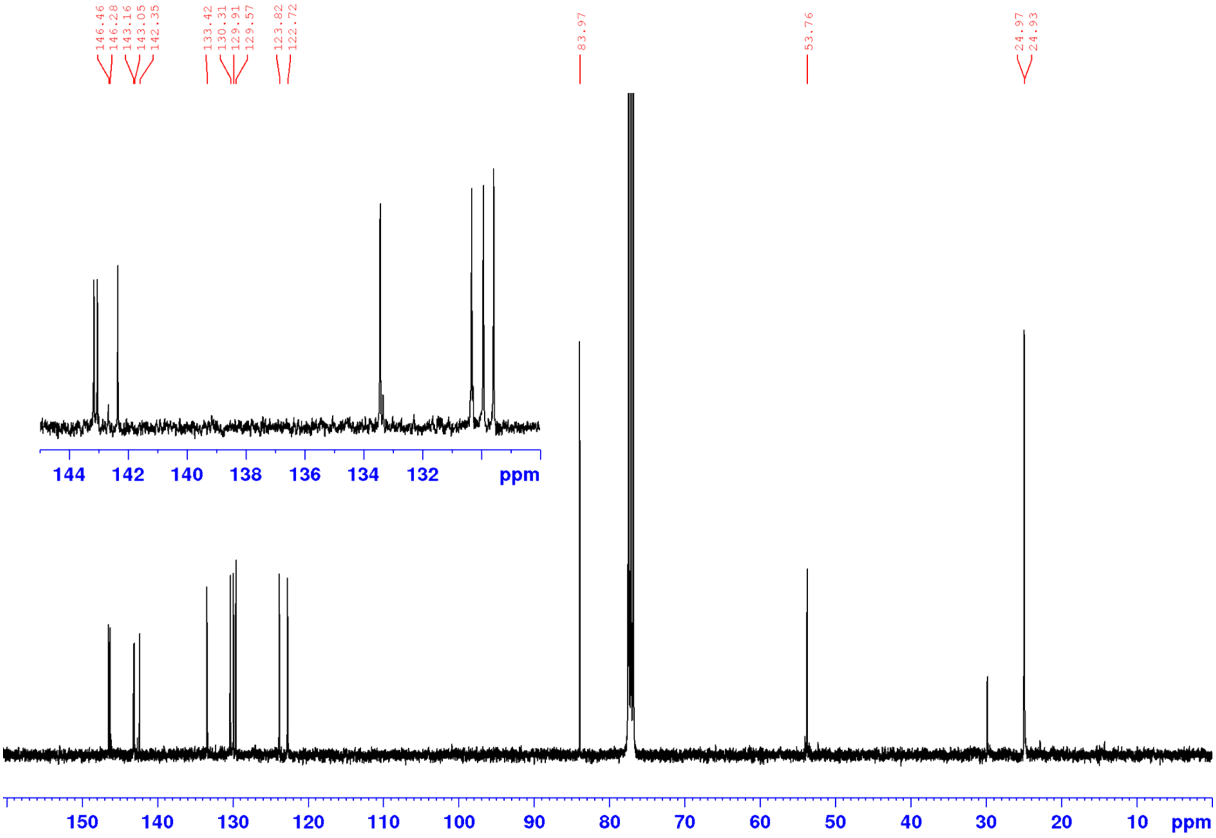

Fig S18: ^{13}C-NMR: TTC(PAZ)-(Bpin)$_2$ (CDCl$_3$, 100.6 MHz).

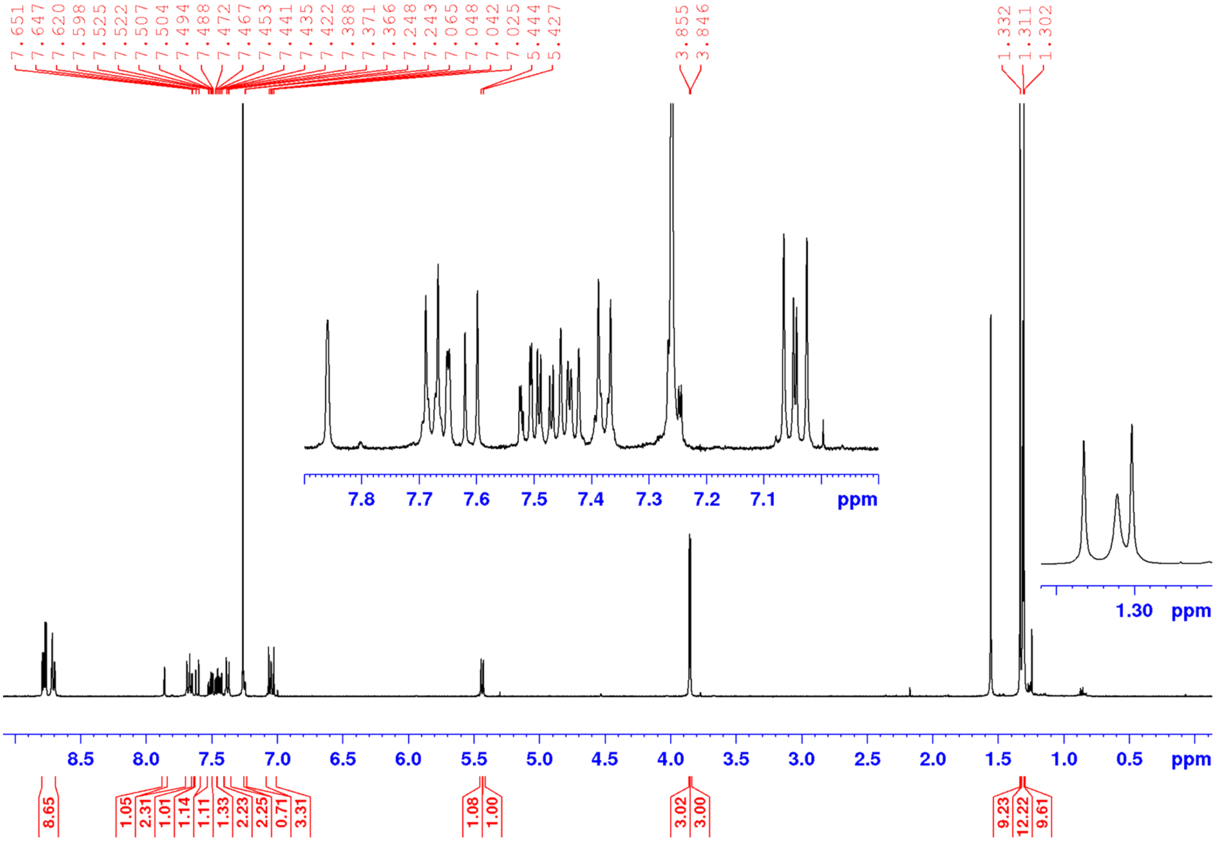

Fig S19: ^{1}H-NMR: Bpin-TTC(OMe)$_2$-PDI (CDCl$_3$, 400.1 MHz).

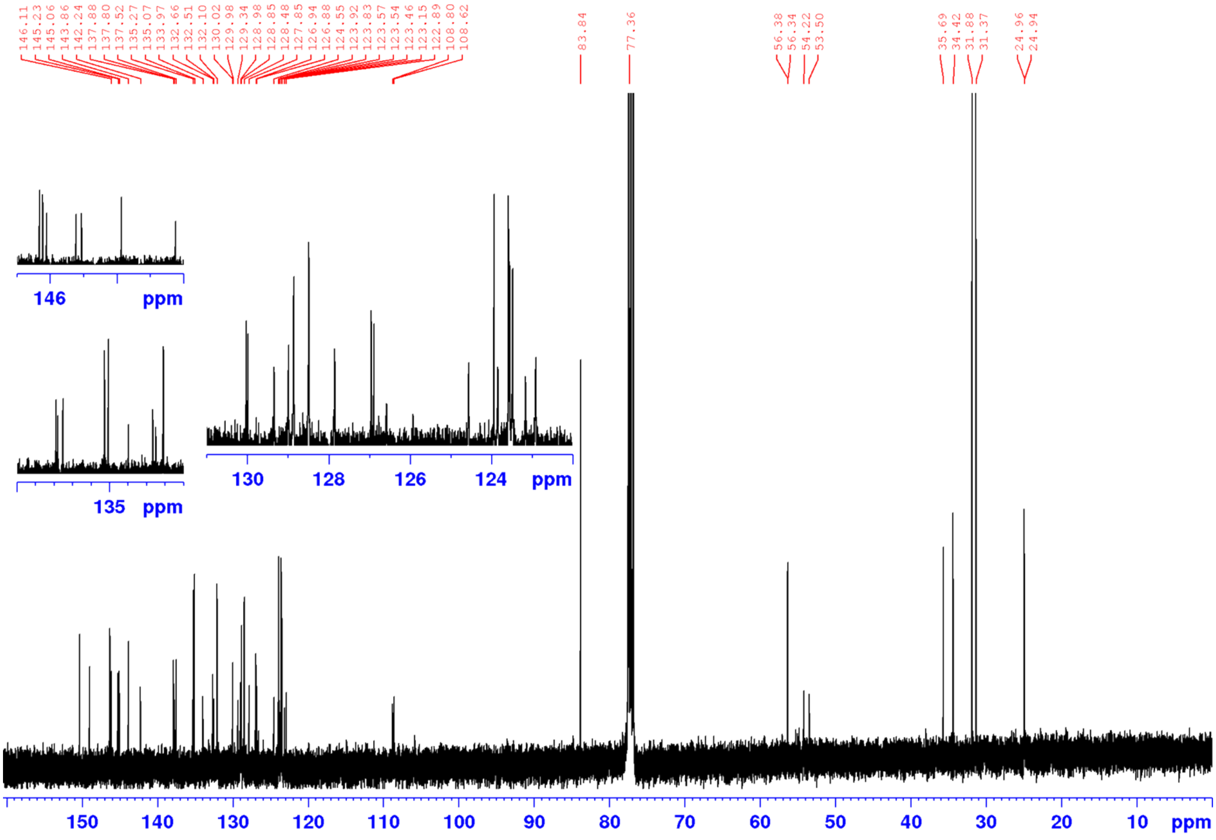

Fig S20: ^{13}C-NMR: Bpin-TTC(OMe)$_2$-PDI (CDCl$_3$, 100.6 MHz).

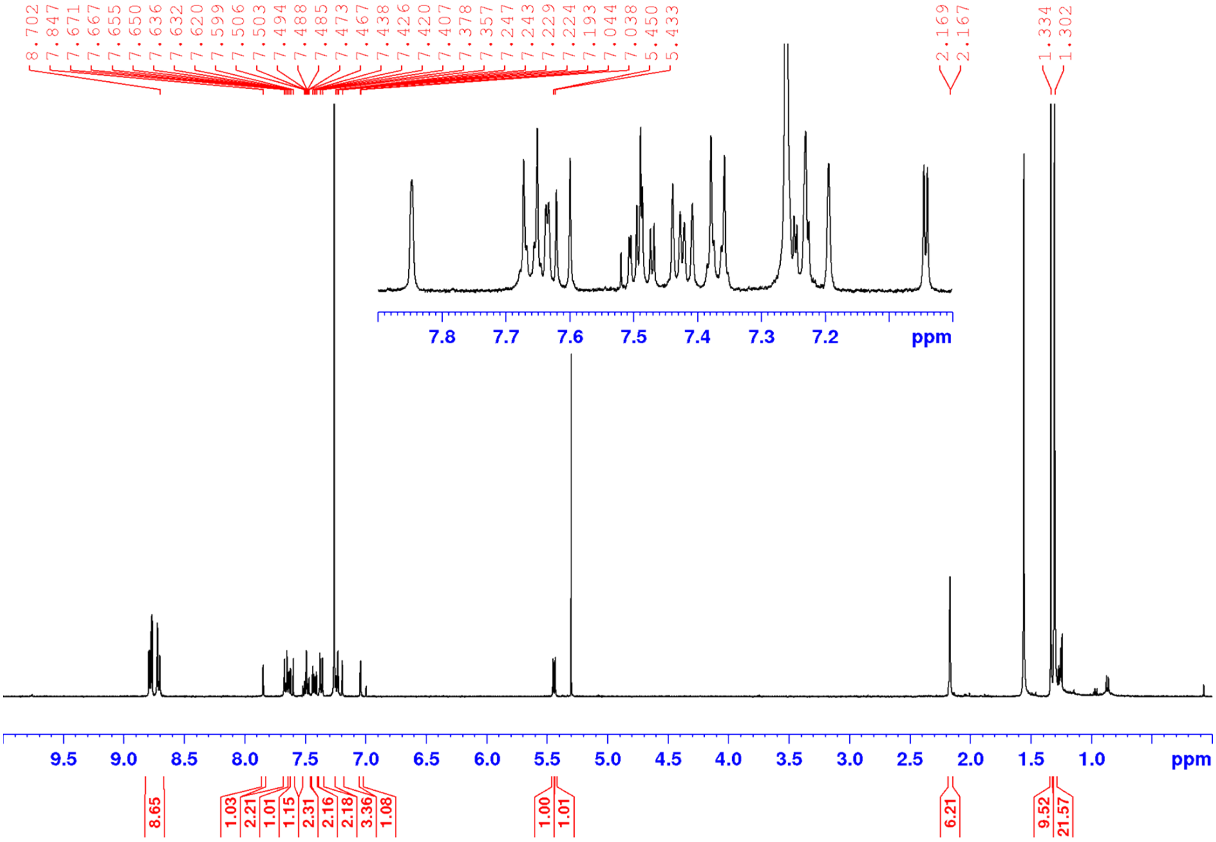

Fig S21: **^{1}H-NMR:** Bpin-TTC(Me)$_2$-PDI (CDCl$_3$, 400.1 MHz).

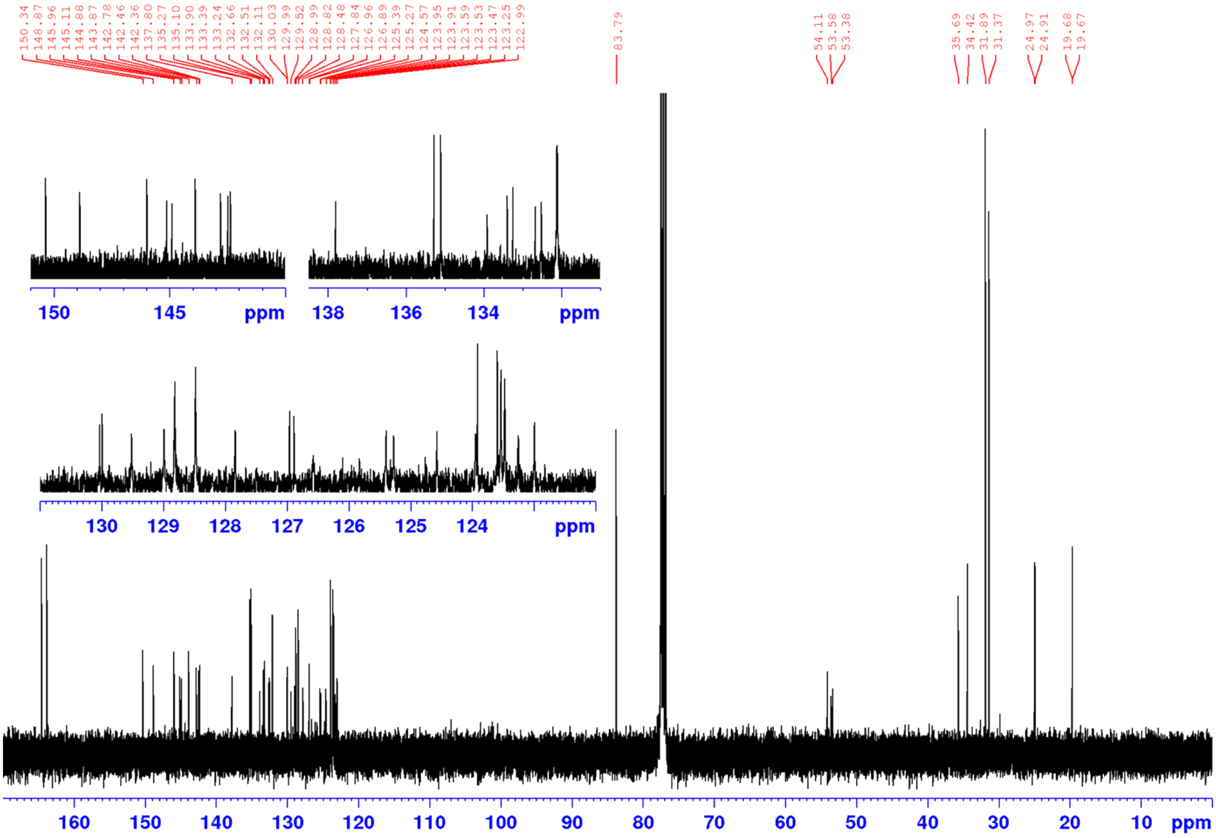

Fig S22: **^{13}C-NMR:** Bpin-TTC(Me)$_2$-PDI (CDCl$_3$, 100.6 MHz).

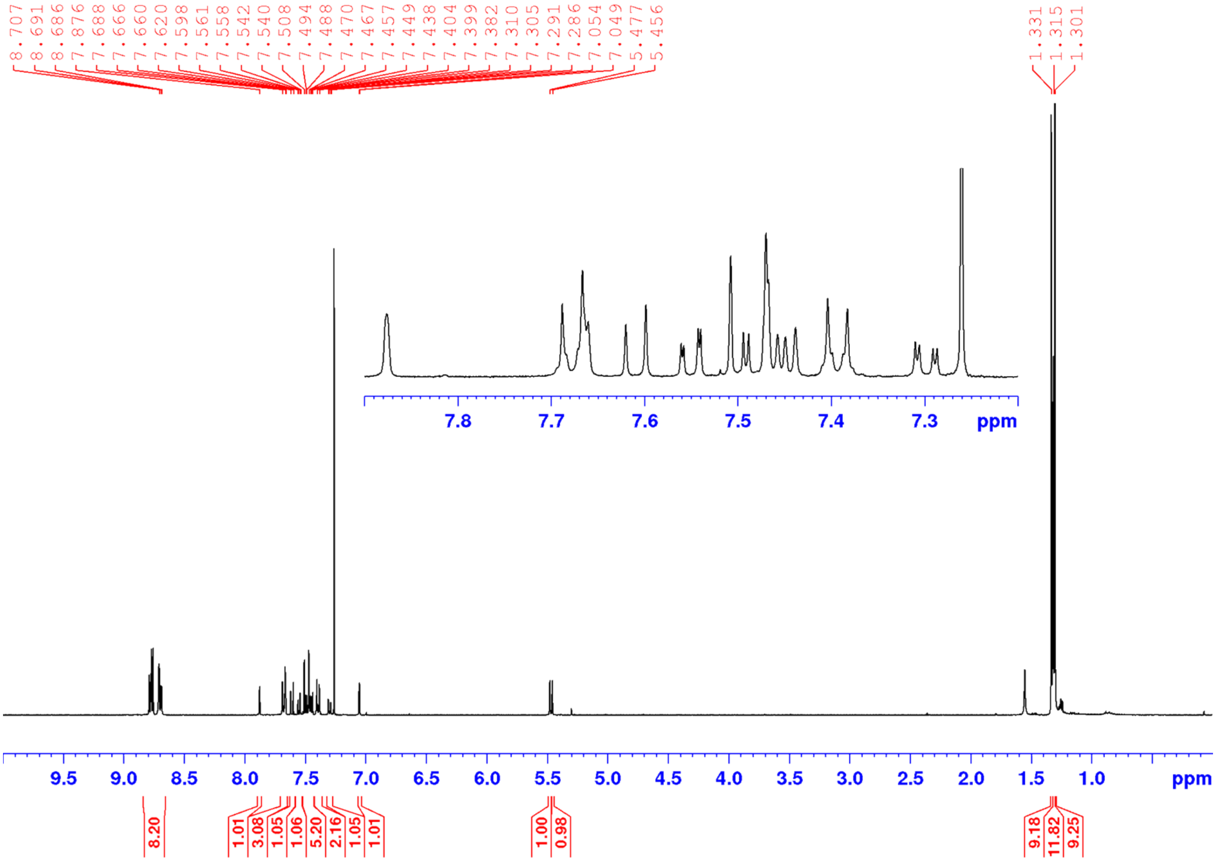

Fig S23: ^{1}H-NMR: Bpin-TTC(Cl)$_2$-PDI (CDCl$_3$, 400.1 MHz).

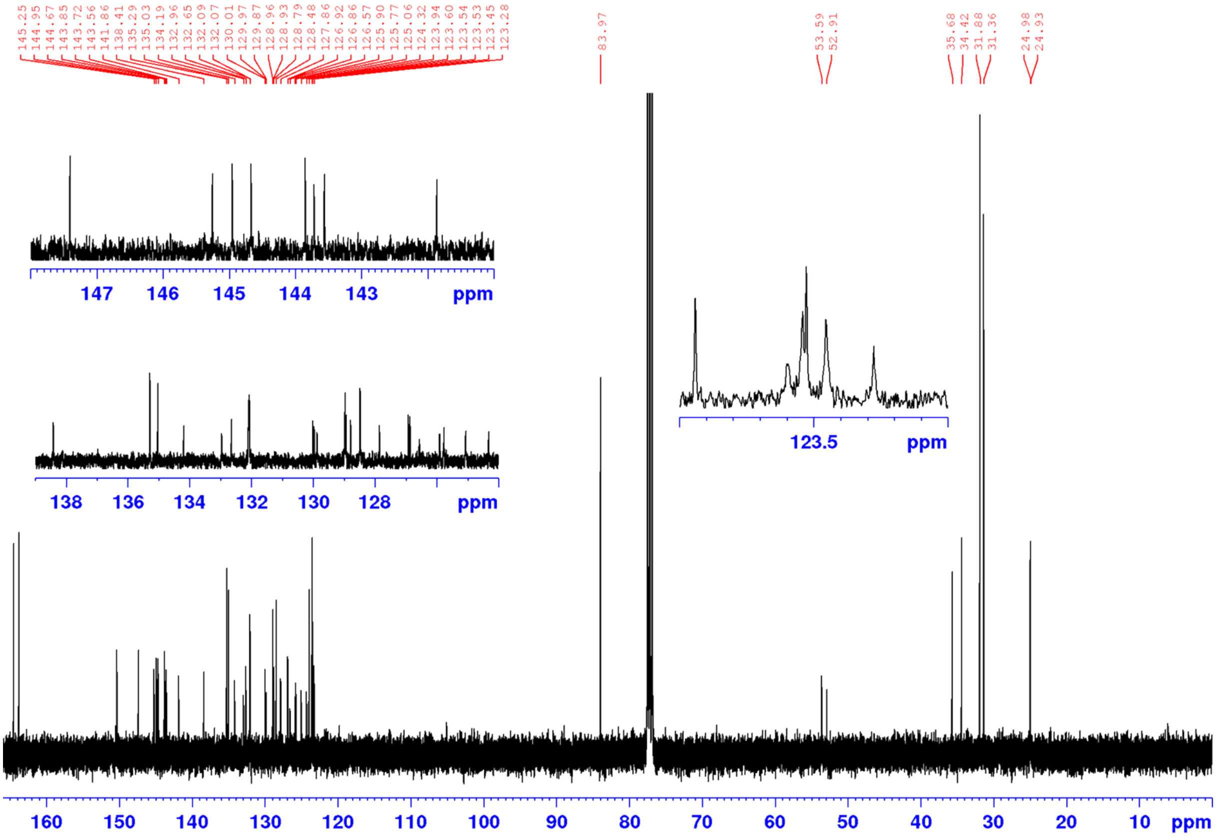

Fig S24: ^{13}C-NMR: Bpin-TTC(Cl)$_2$-PDI (CDCl$_3$, 100.6 MHz).

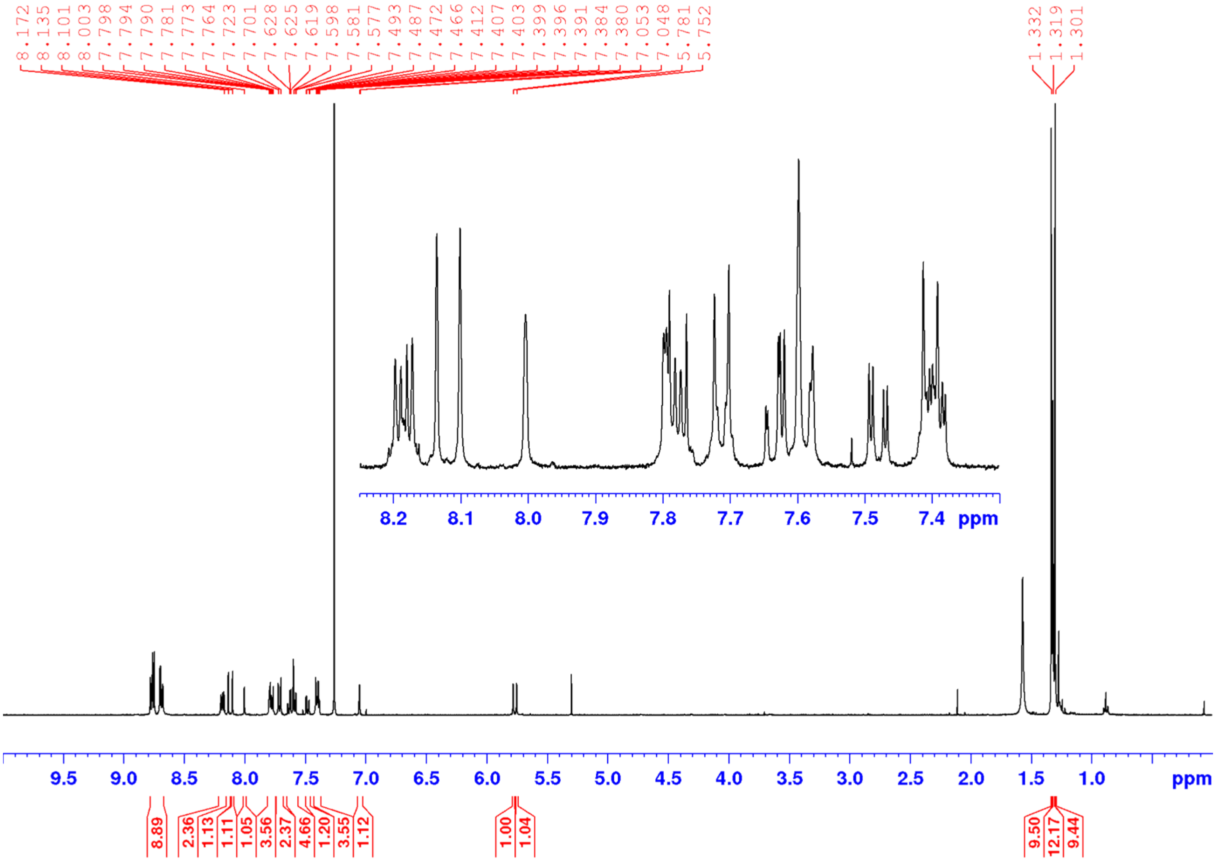

Fig S25: ^{1}H-NMR: Bpin-TTC(PAZ)-PDI ($CDCl_3$, 400.1 MHz).

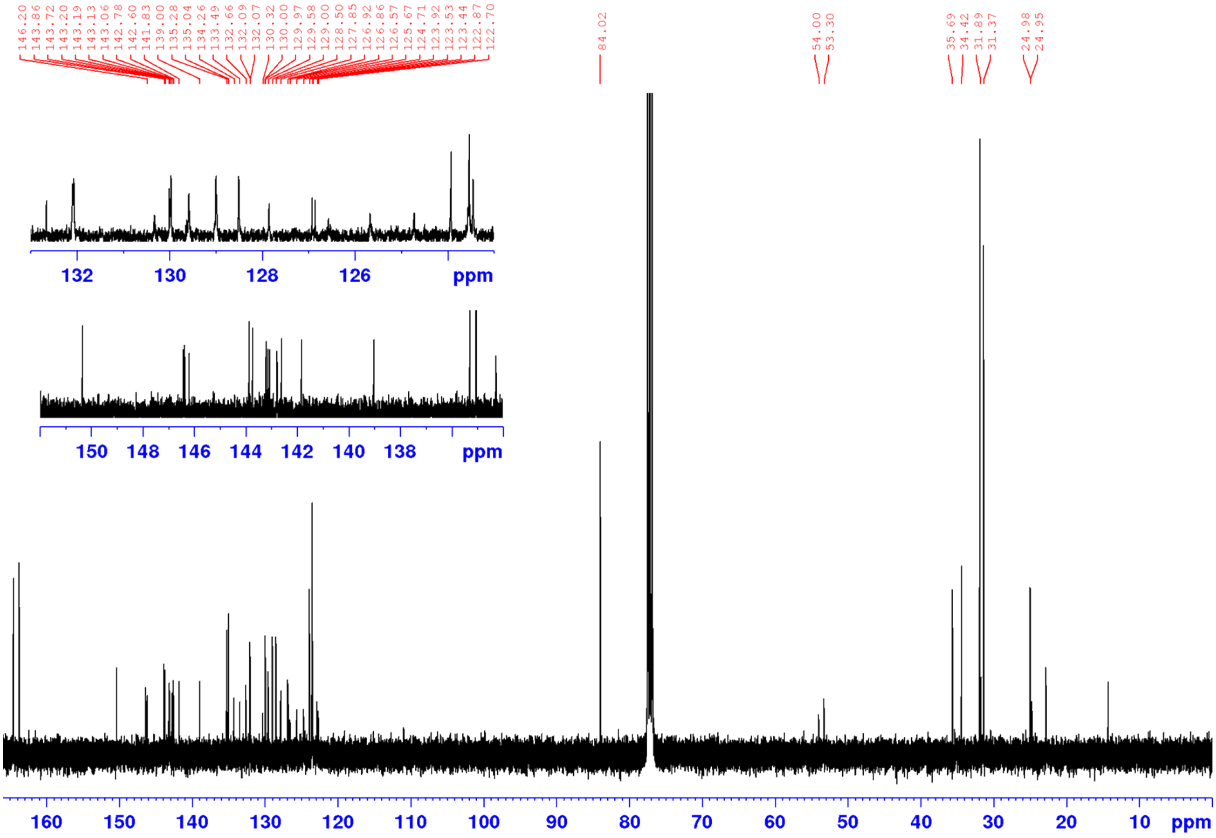

Fig S26: ^{13}C-NMR: Bpin-TTC(PAZ)-PDI ($CDCl_3$, 100.6 MHz).

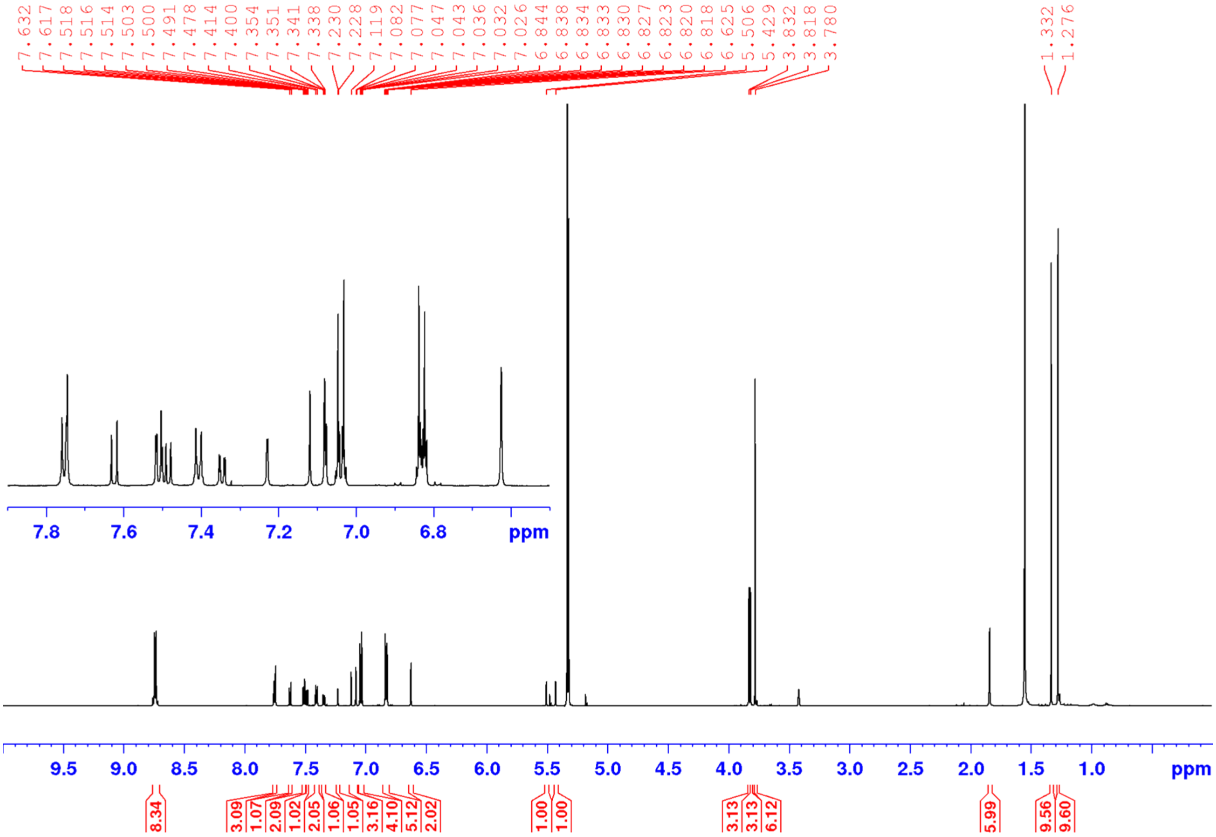

Fig S27: ^{1}H-NMR: TAA-TTC(OMe)$_2$-PDI (CD$_2$Cl$_2$, 600.1 MHz).

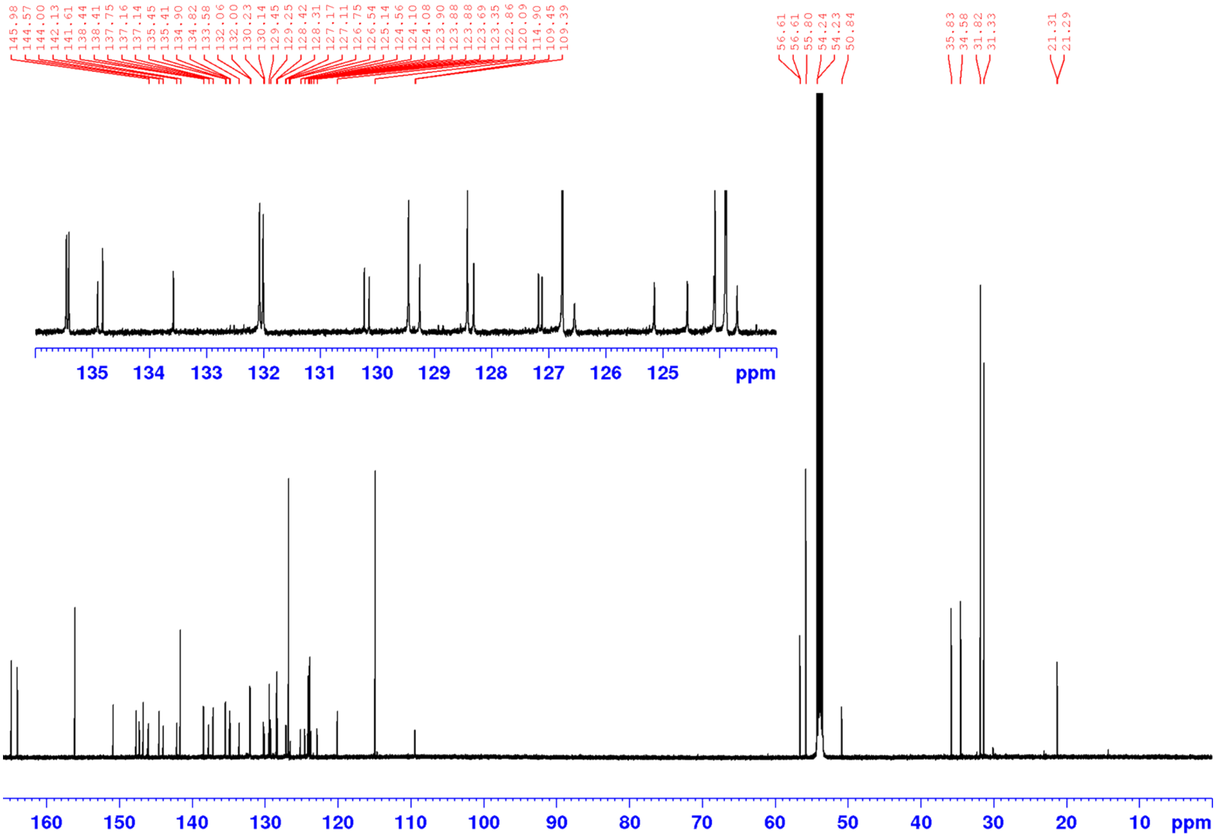

Fig S28: ^{13}C-NMR: TAA-TTC(OMe)$_2$-PDI (CD$_2$Cl$_2$, 150.9 MHz).

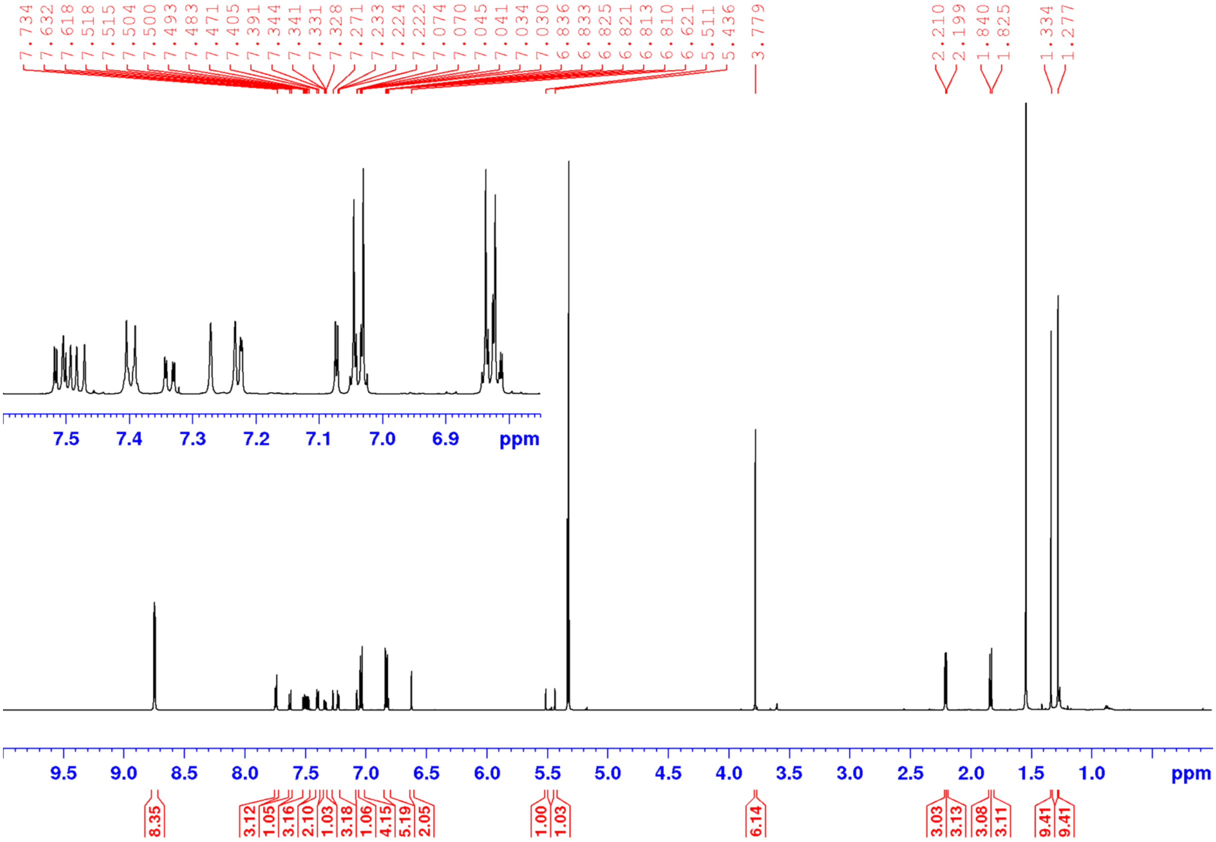

Fig S29: **^{1}H-NMR:** TAA-TTC(Me)$_2$-PDI (CD$_2$Cl$_2$, 600.1 MHz).

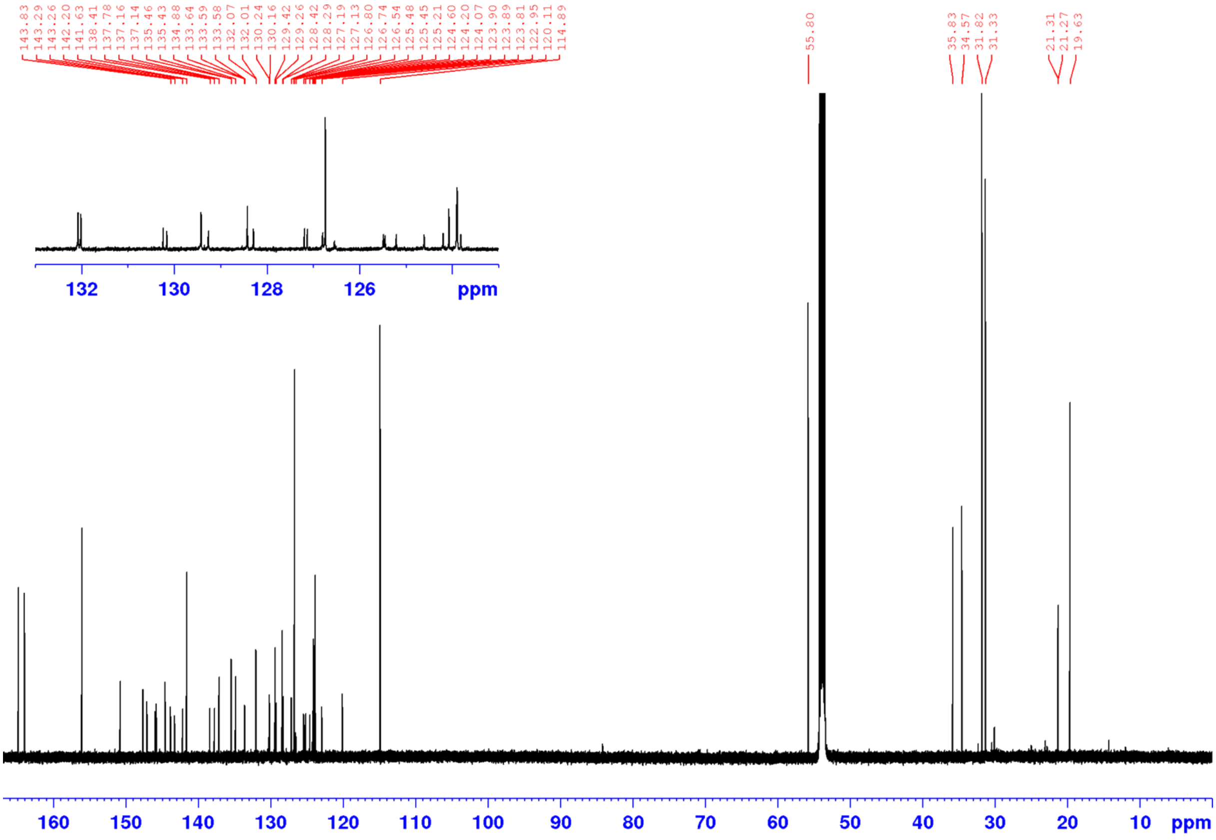

Fig S30: **^{13}C-NMR:** TAA-TTC(Me)$_2$-PDI (CD$_2$Cl$_2$, 150.9 MHz).

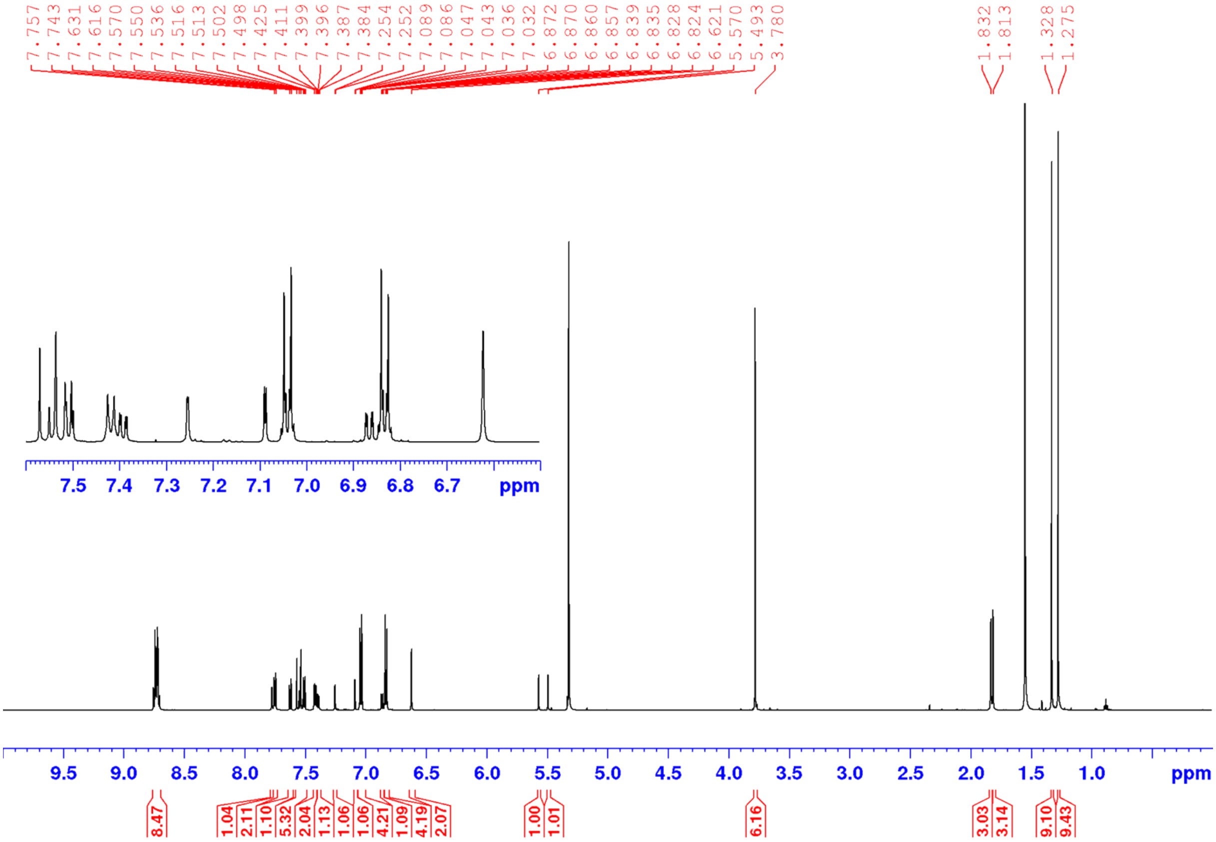

Fig S31: ^{1}**H-NMR:** TAA-TTC(Cl)$_2$-PDI (CD$_2$Cl$_2$, 600.1 MHz).

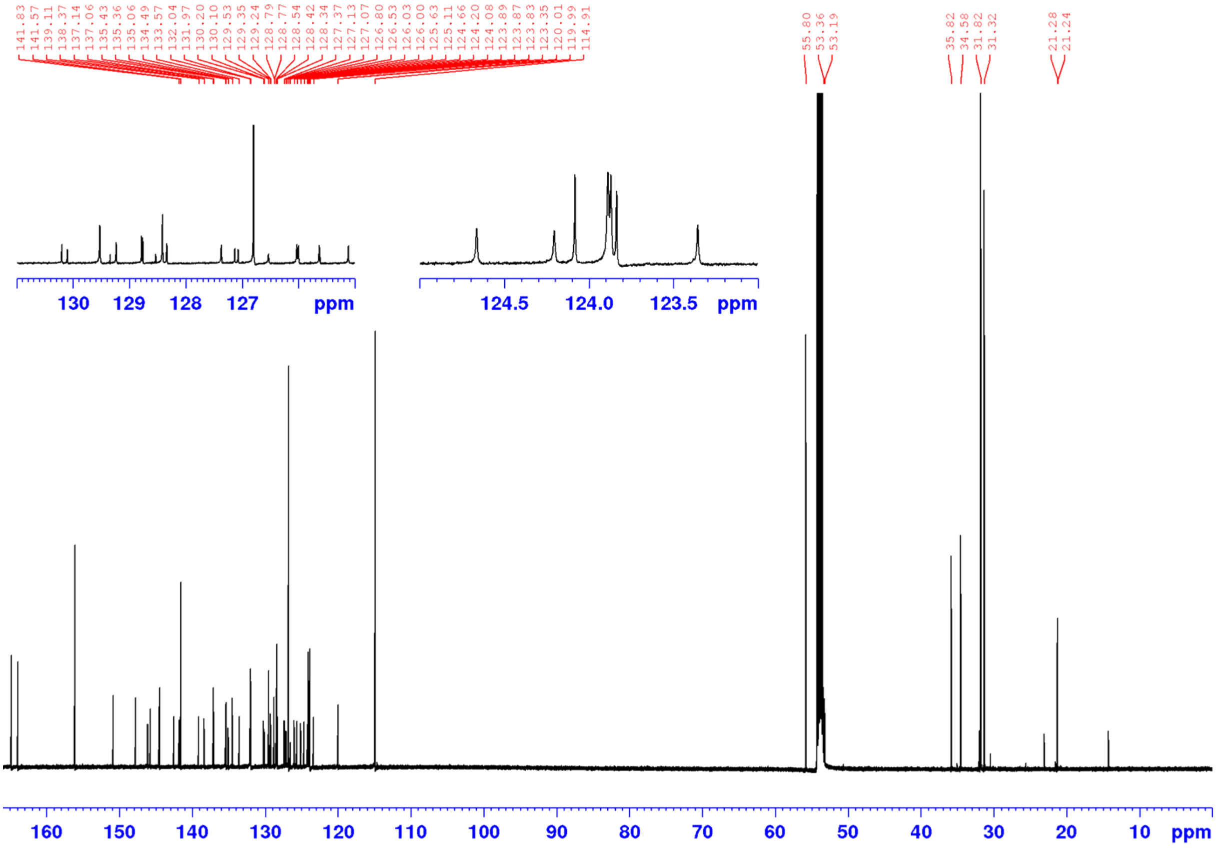

Fig S32: ^{13}**C-NMR:** TAA-TTC(Cl)$_2$-PDI (CD$_2$Cl$_2$, 150.9 MHz).

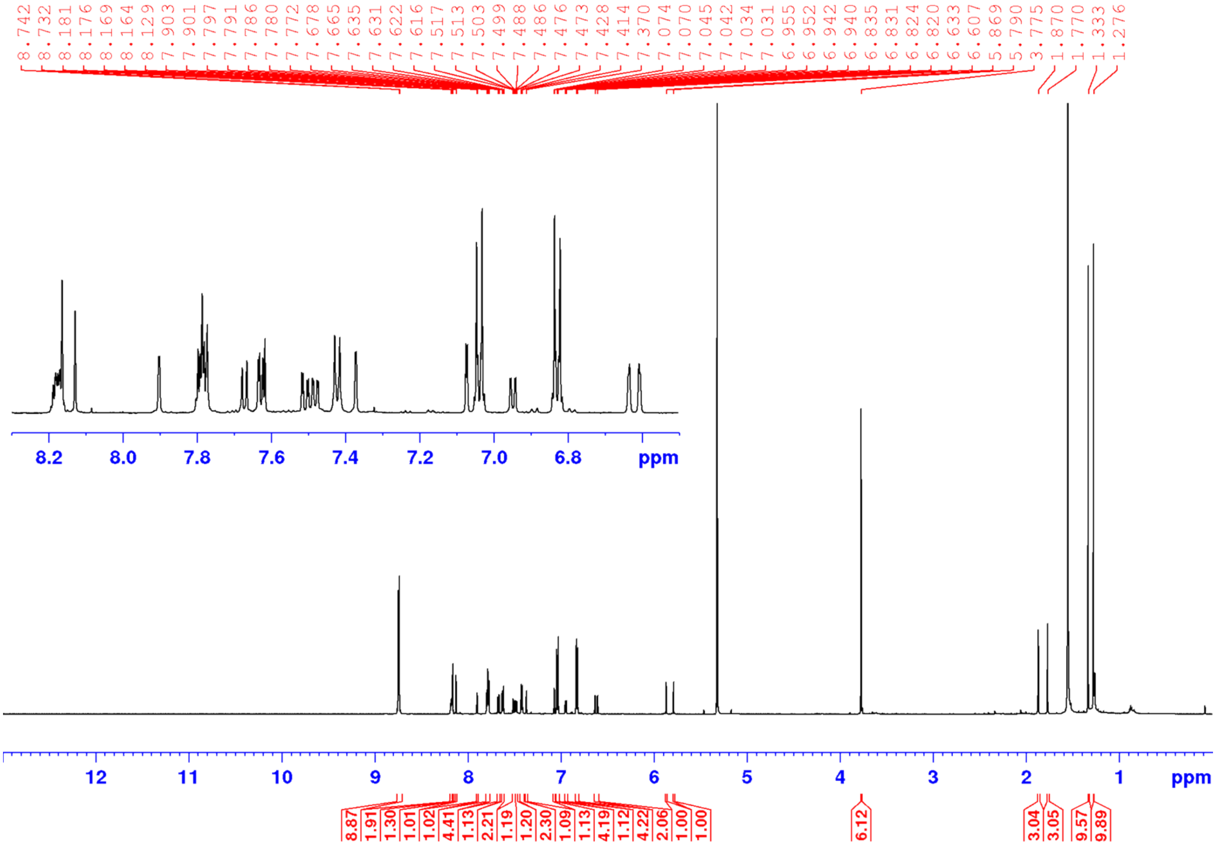

Fig S33: ^{1}H-NMR: TAA-TTC(PAZ)-PDI (CD_2Cl_2, 600.1 MHz).

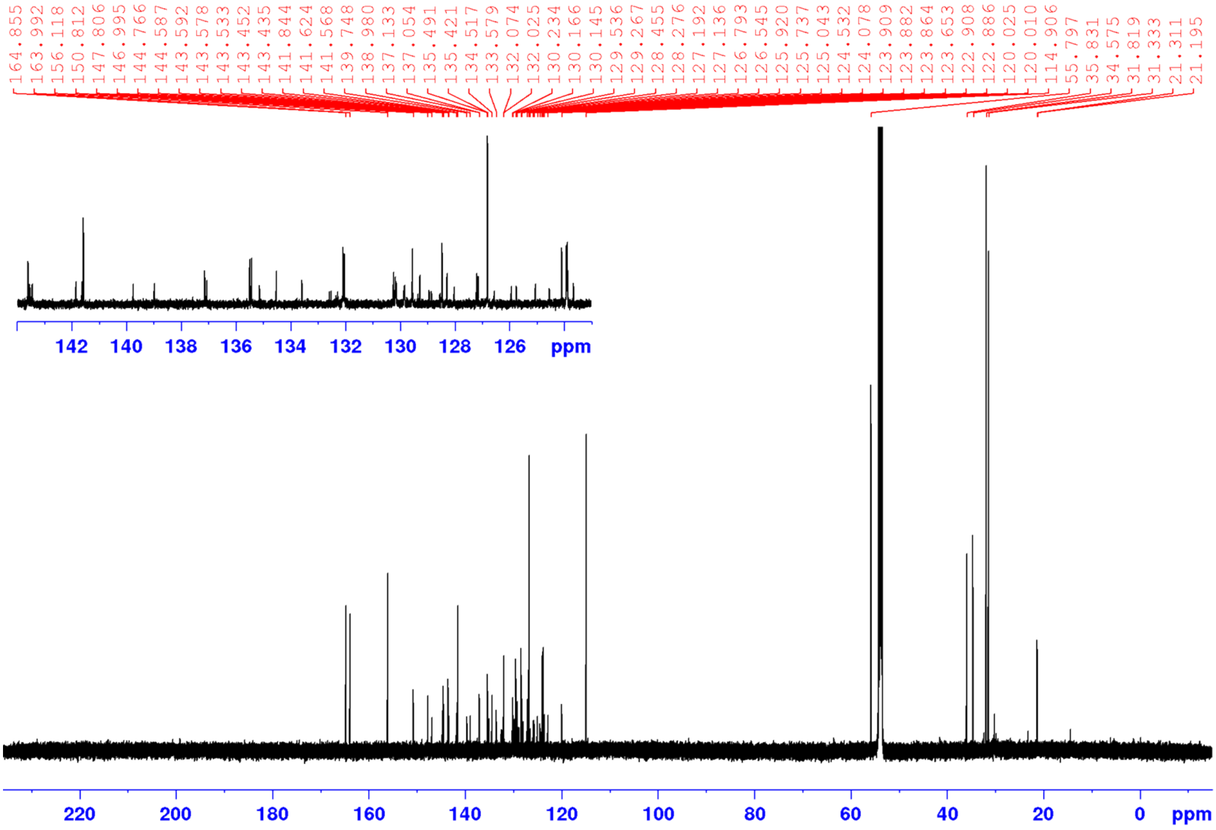

Fig S34: ^{13}C-NMR: TAA-TTC(PAZ)-PDI (CD_2Cl_2, 150.9 MHz).

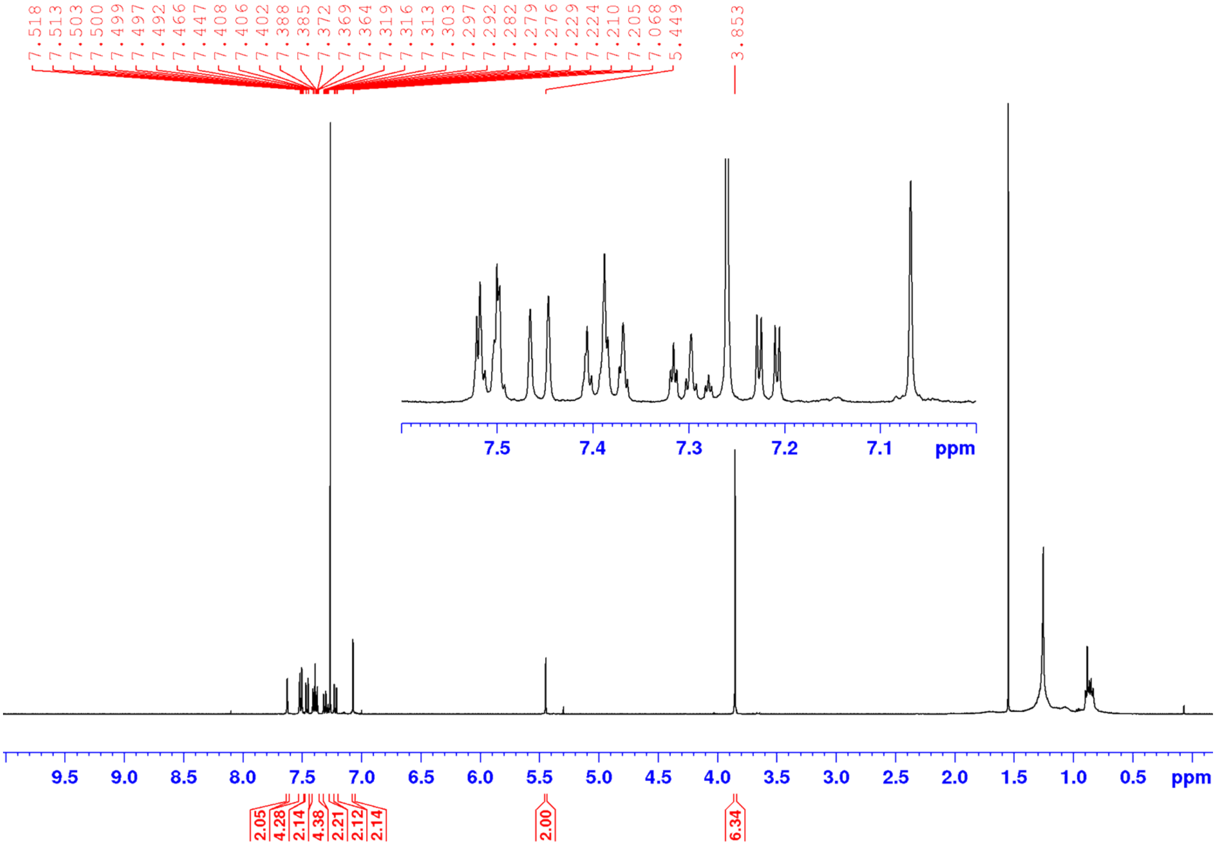

Fig S35: ^{1}H-NMR: TTC(OMe)$_2$-Ph$_2$ (CDCl$_3$, 400.1 MHz). (0.5 - 1.5 ppm = hexanes).

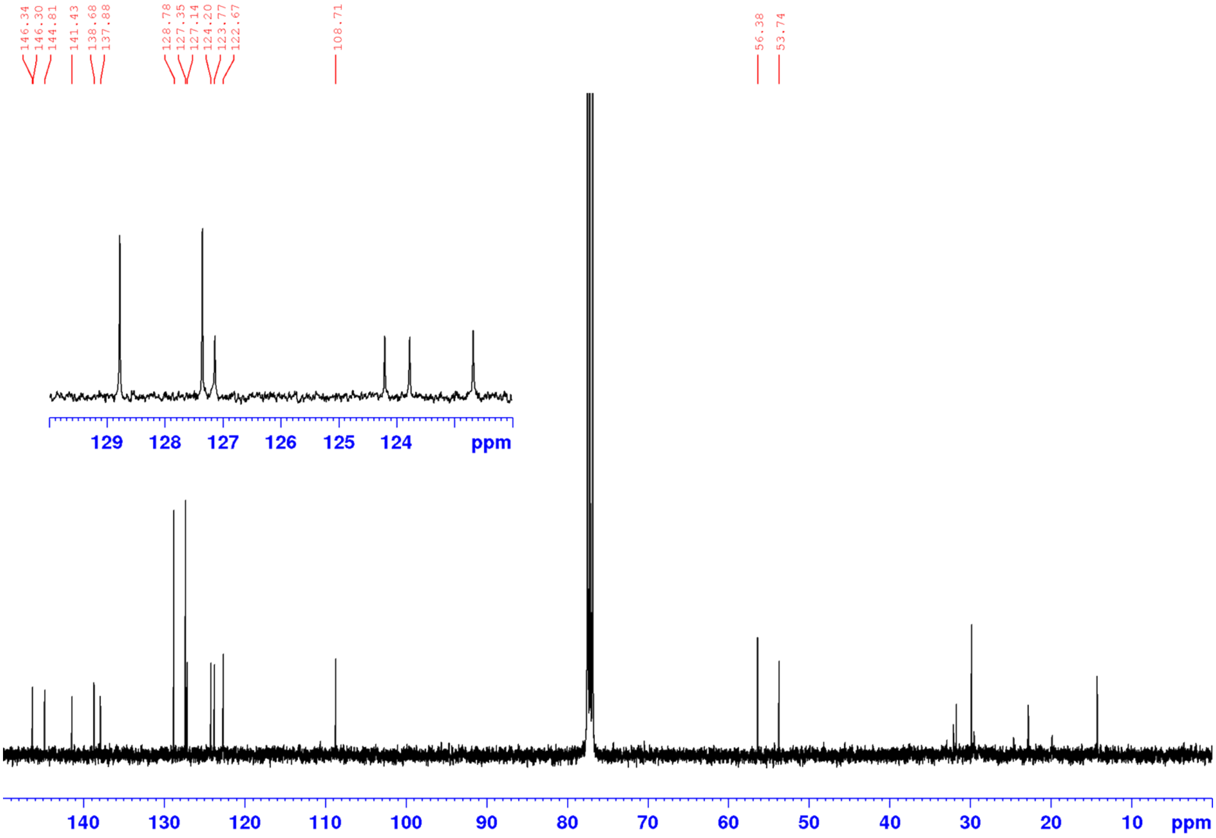

Fig S36: ^{13}C-NMR: TTC(OMe)$_2$-Ph$_2$ (CDCl$_3$, 100.6 MHz). (below 40 ppm = hexanes).

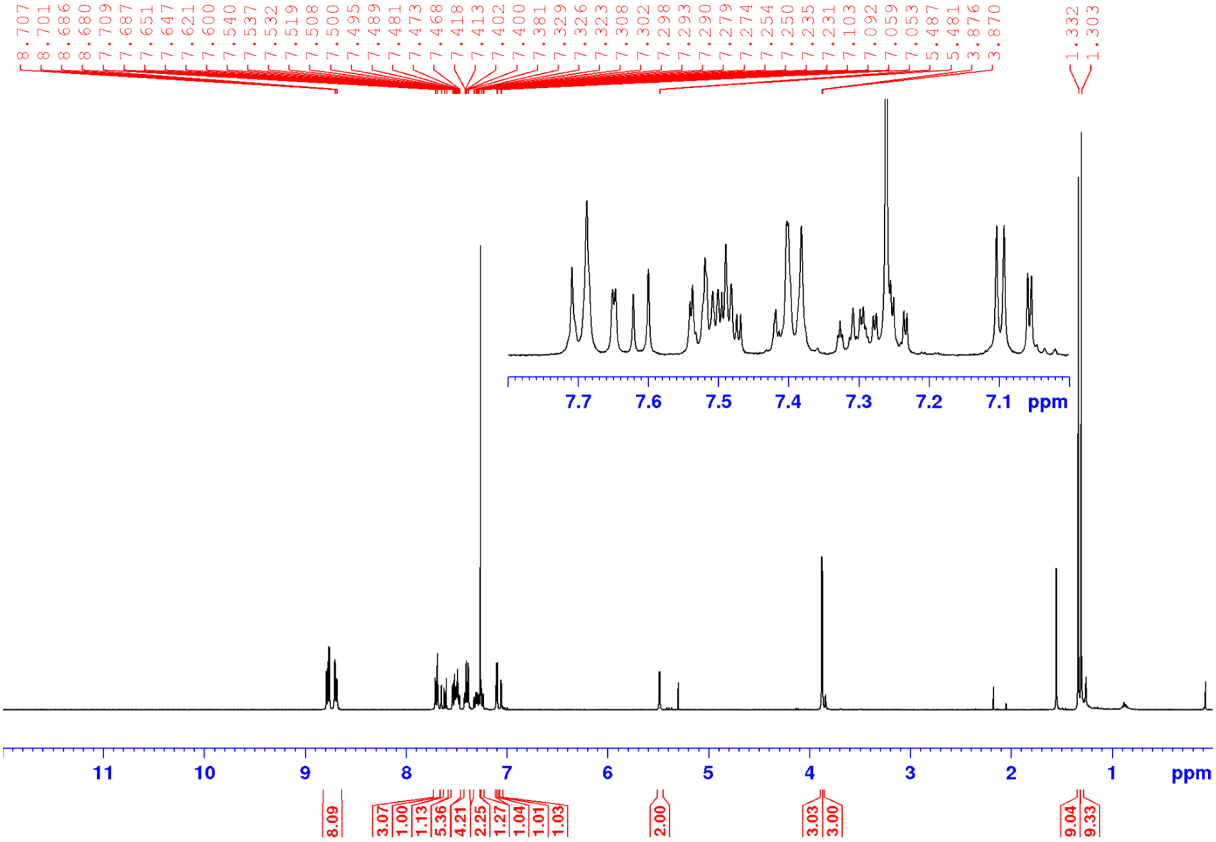

Fig S37: ^{1}H-NMR: Ph-TTC(OMe)$_2$-PDI (CDCl$_3$, 400.1 MHz).

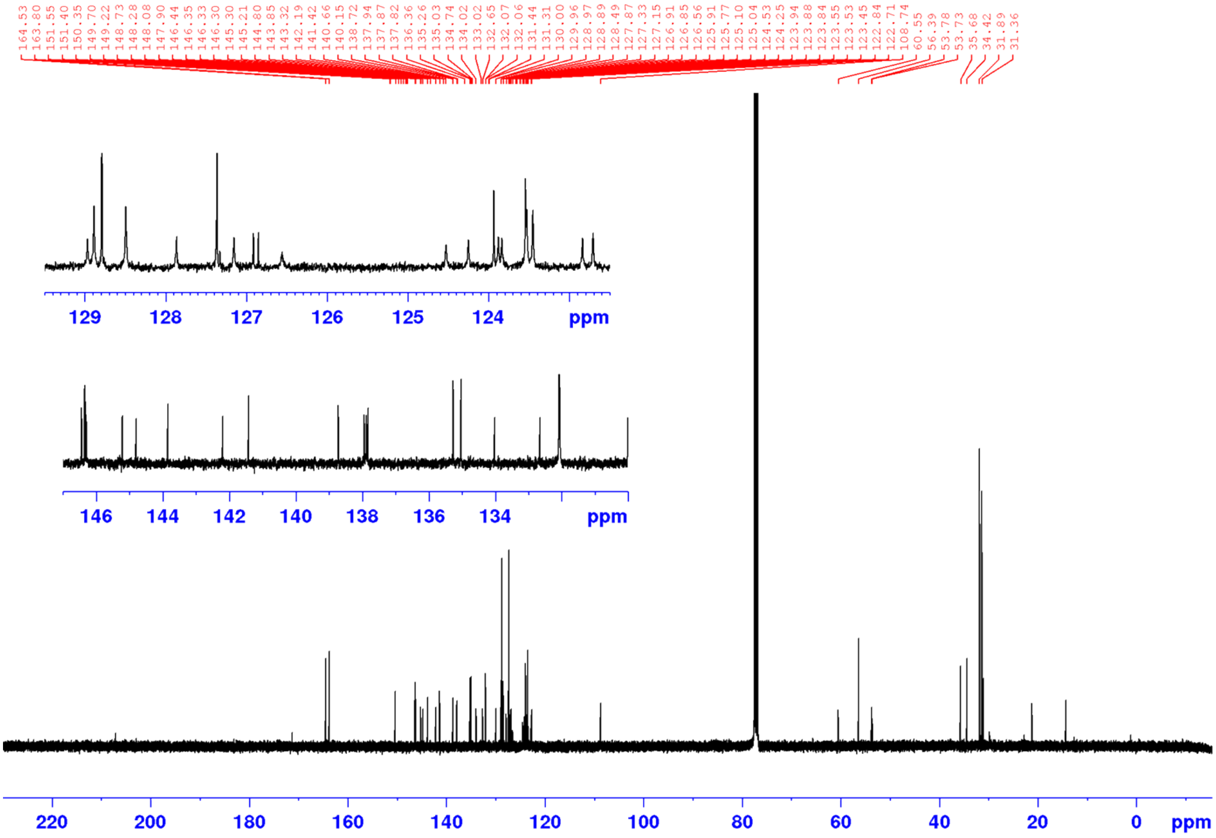

Fig S38: ^{13}C-NMR: Ph-TTC(OMe)$_2$-PDI (CDCl$_3$, 100.6 MHz).

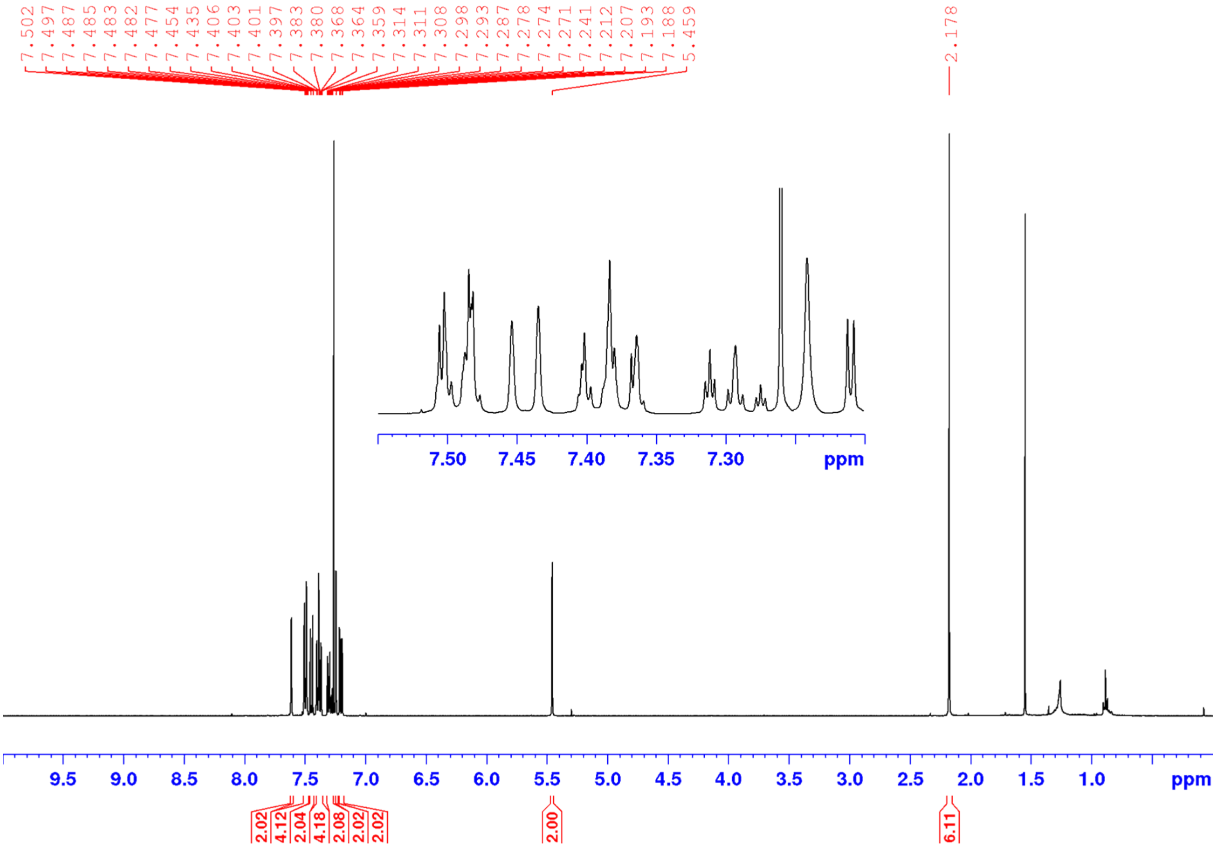

Fig S39: ^{1}H-NMR: TTC(Me)$_2$-Ph$_2$ (CDCl$_3$, 400.1 MHz). (0.5 - 1.5 ppm = hexanes).

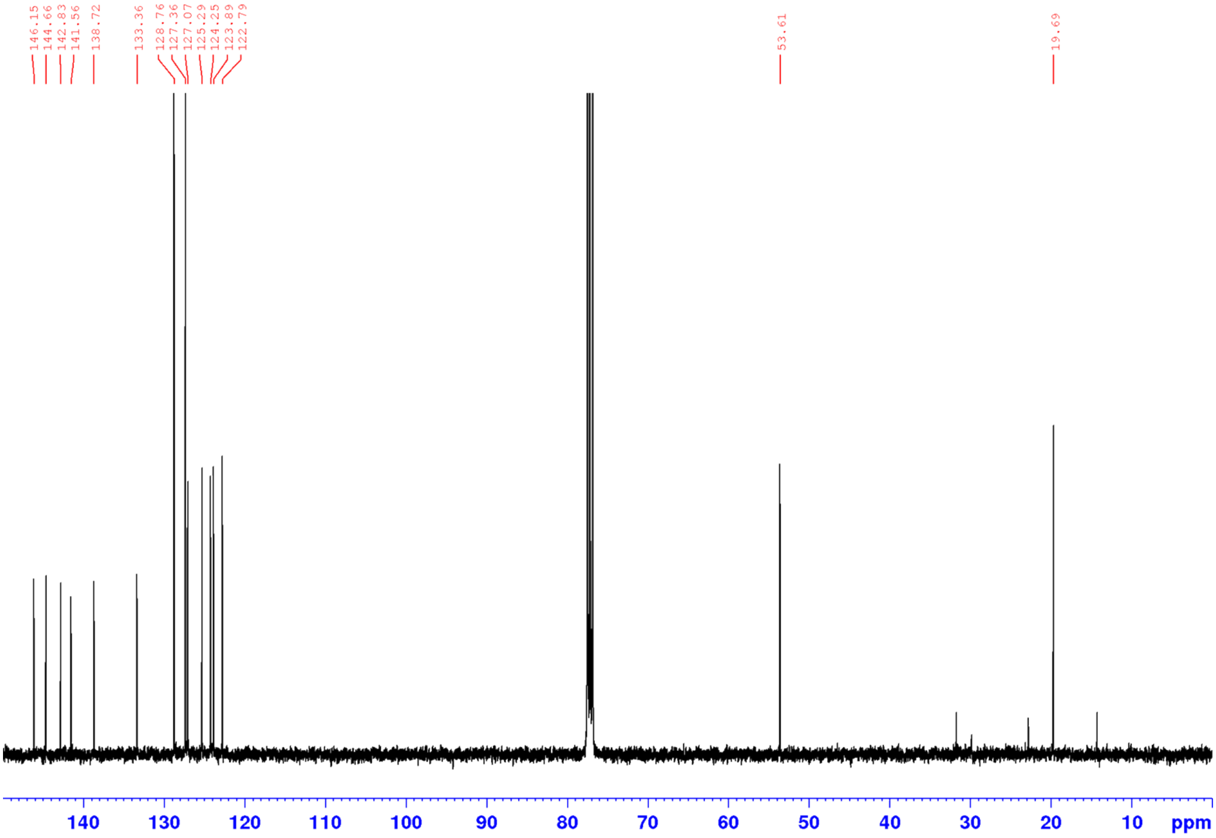

Fig S40: ^{13}C-NMR: TTC(Me)$_2$-Ph$_2$ (CDCl$_3$, 100.6 MHz). (small peaks <40 ppm = hexanes).

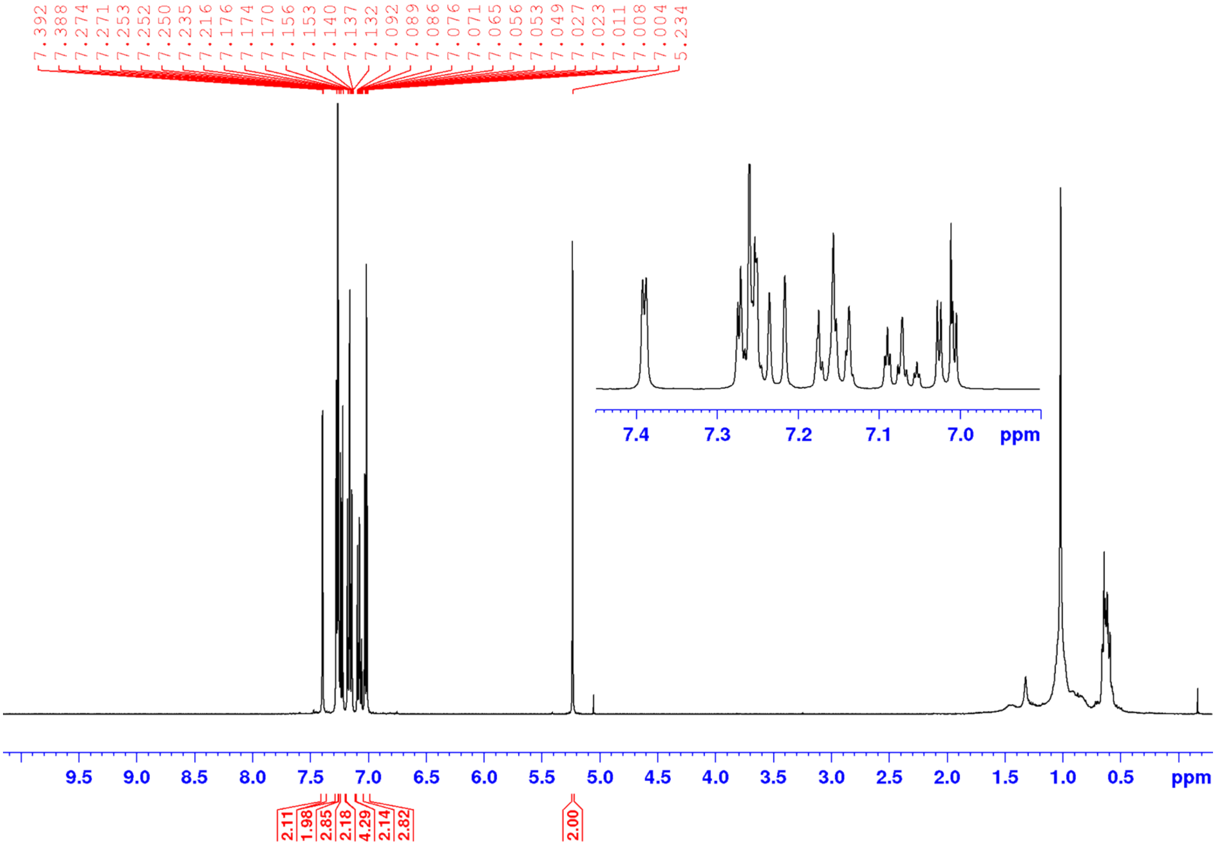

Fig S41: ^{1}**H-NMR:** TTC(Cl)$_2$-Ph$_2$ (CDCl$_3$, 400.1 MHz). (0.5 - 1.5 ppm = hexanes).

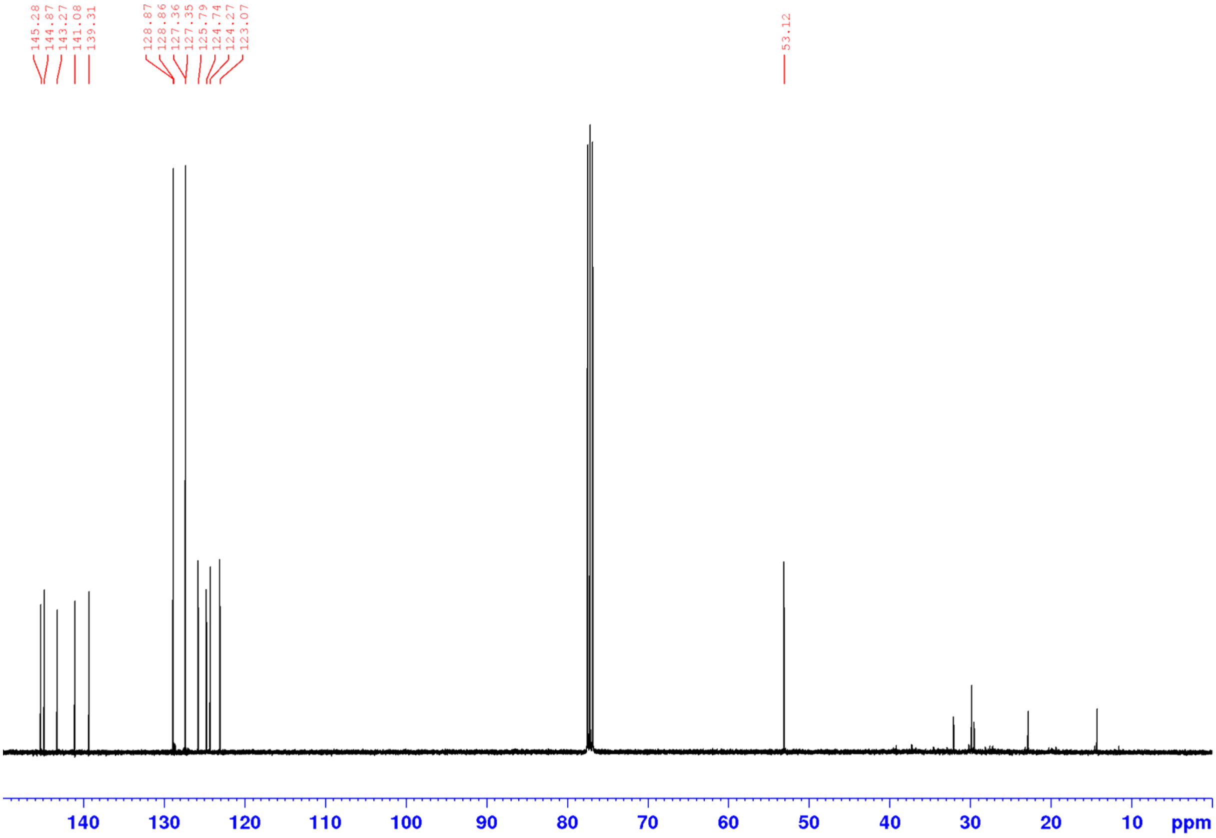

Fig S42: ^{13}**C-NMR:** TTC(Cl)$_2$-Ph$_2$ (CDCl$_3$, 100.6 MHz). (small peaks <40 ppm = hexanes).

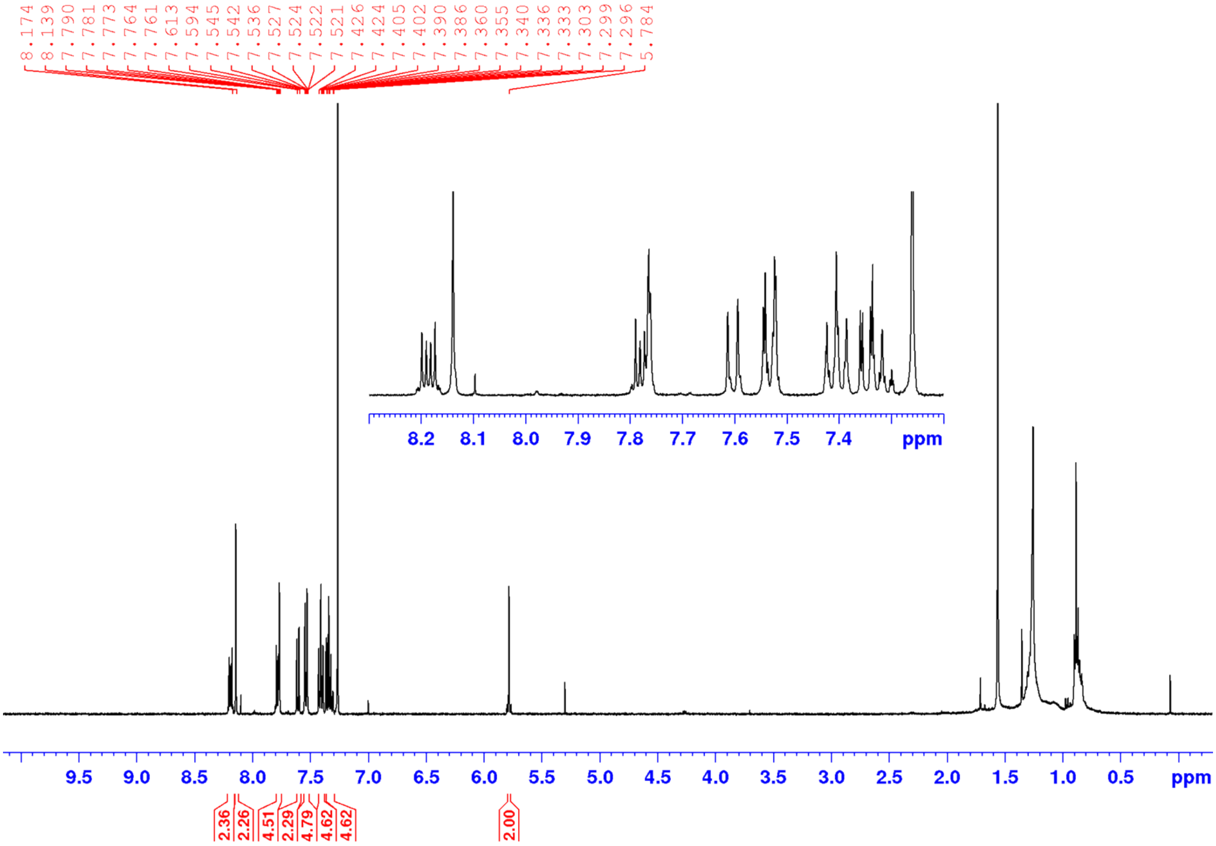

Fig S43: ^{1}H-NMR: TTC(PAZ)-Ph$_2$ (CDCl$_3$, 400.1 MHz). (0.5 - 1.5 ppm = hexanes).

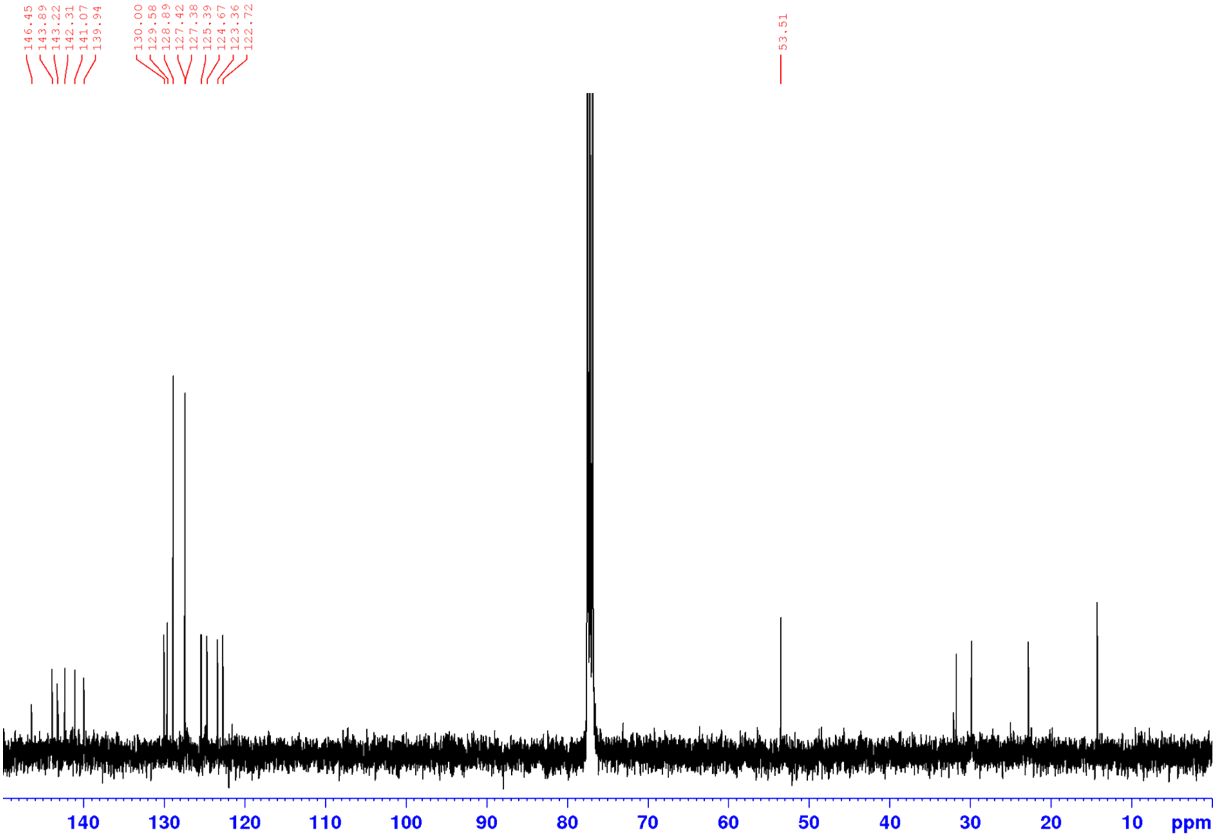

Fig S44: ^{13}C-NMR: TTC(PAZ)-Ph$_2$ (CDCl$_3$, 100.6 MHz). (peaks <40 ppm = hexanes).

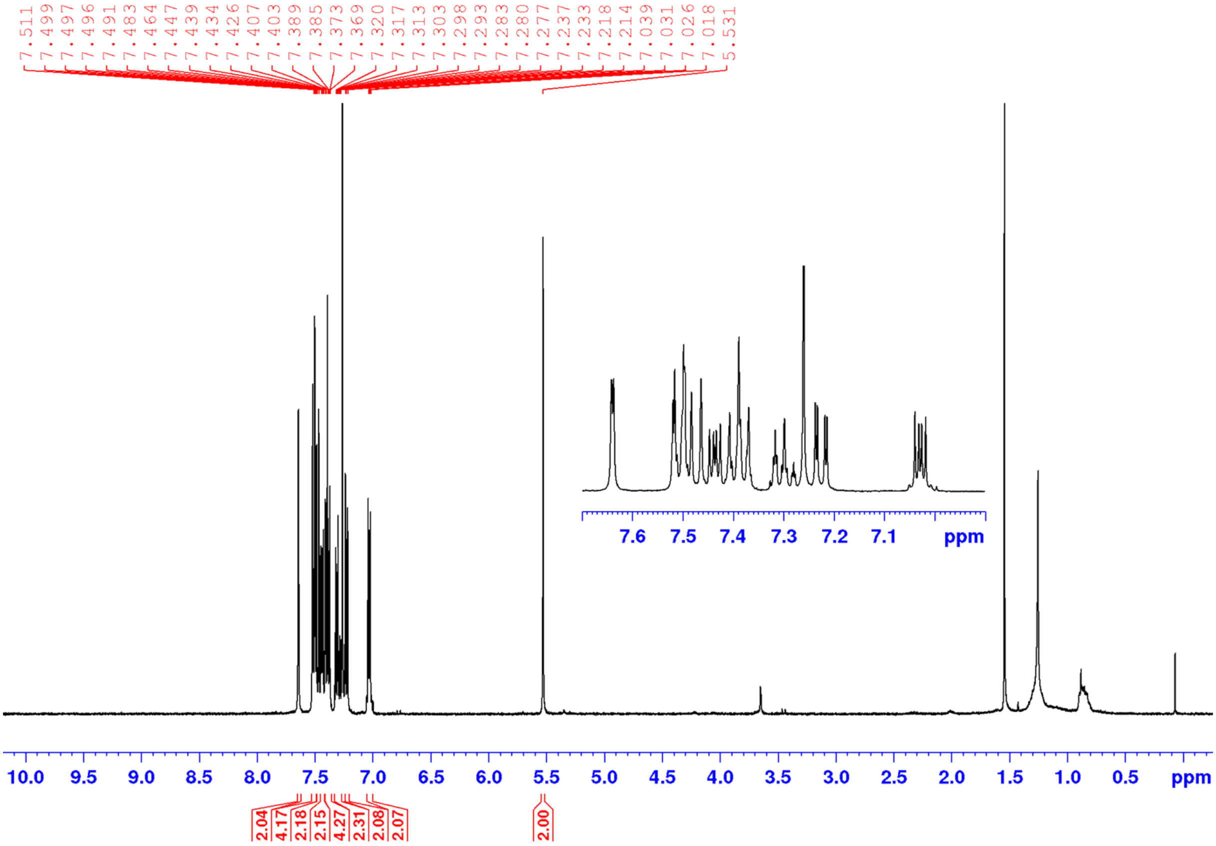

Fig S45: ^{1}H-NMR: TTC(H)$_2$-Ph$_2$ (CDCl$_3$, 400.1 MHz). (0.5 - 1.5 ppm = hexanes).

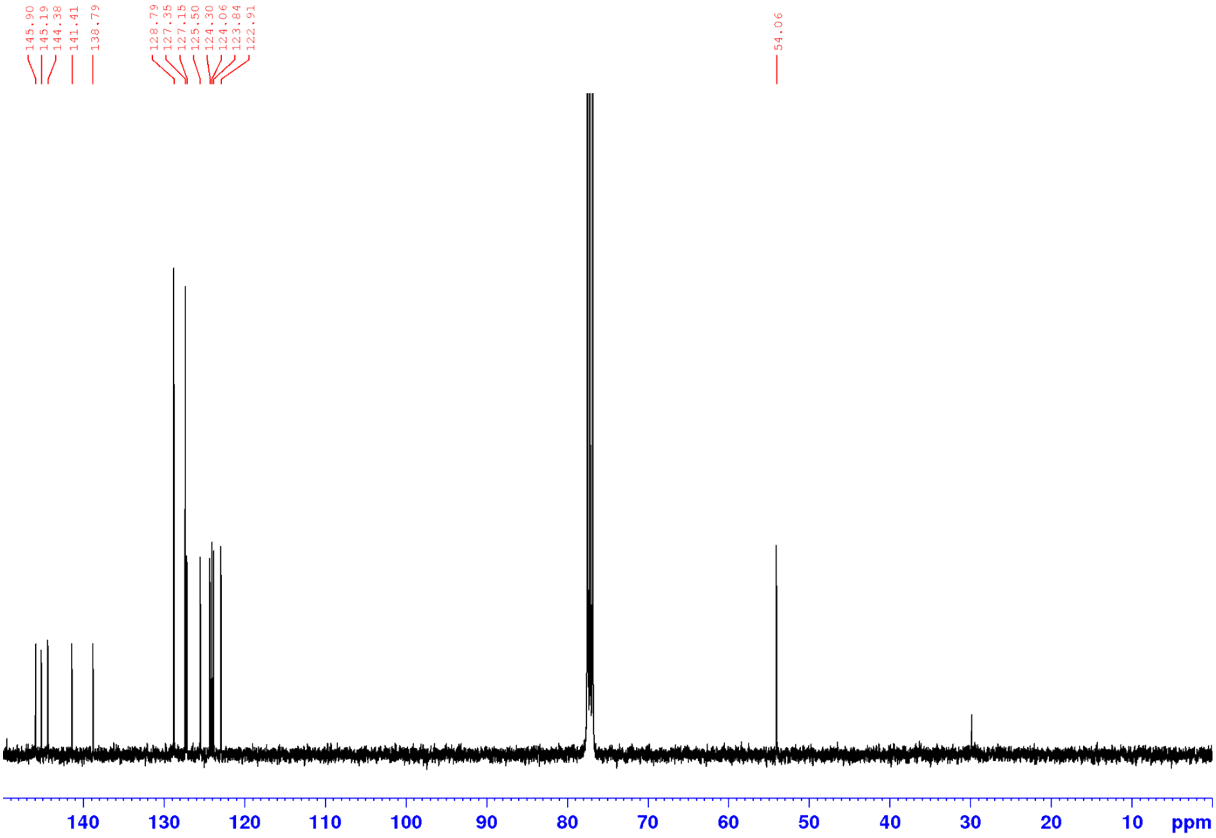

Fig S46: ^{13}C-NMR: TTC(H)$_2$-Ph$_2$ (CDCl$_3$, 100.6 MHz). (peaks <40 ppm = hexanes).

2. Cyclic voltammetry

All cyclic voltammograms were measured in DCM with 0.2 M TBAHFP as a supporting electrolyte under argon atmosphere at 298 K. The electrochemical measurements used a Gamry Instruments Reference 600 Potentiostat/Galvanostat/ZRA (v. 6.2.2) with a conventional three electrode setup (platinum disc working electrode Ø = 1 mm, Ag/AgCl 'LEAK FREE' reference electrode, platinum wire as counter electrode). All measurements were referenced against the ferrocene/ferrocenium (Fc/Fc^+) redox couple and were measured with a scan rate of 100 mV s^{-1} The chemical reversibility of each redox-process was tested using multicycle thin layer experiments.

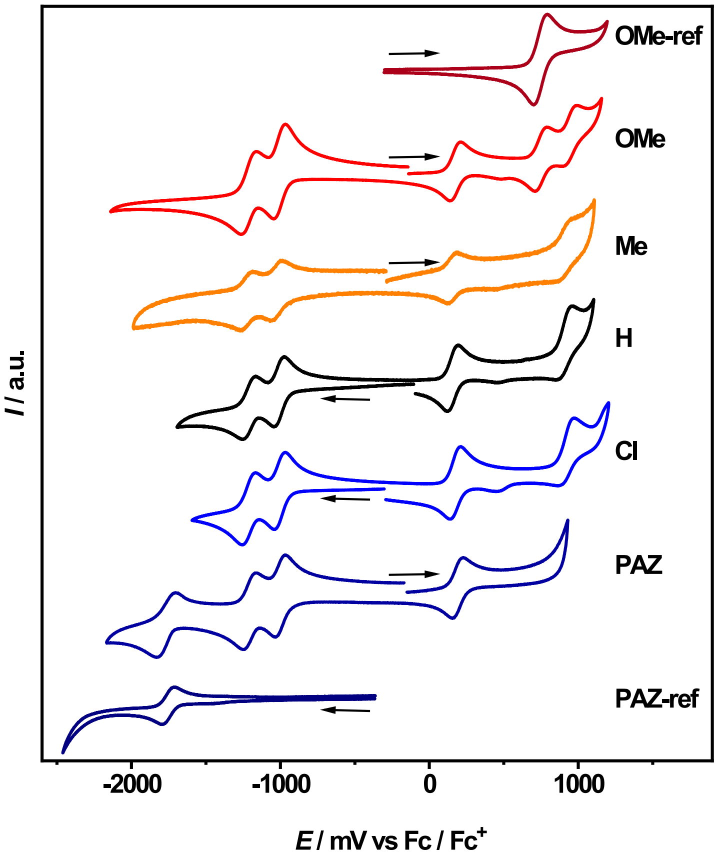

Fig S47: Cyclic voltammograms of all four triads in DCM containing 0.2 M TBAHF and referenced against Fc/Fc^+.

Table S1: Redox potentials of the triads measured with 0.2 M TBAHFP in DCM at 298 K. All voltammograms are measured with a scan rate of 100 mV s^{-1} and referenced against Fc/Fc^{+}.

	***E*$_{1/2}$ / mV**					
	ox$_1$	**ox$_2$**	**ox$_3$**	**red$_1$**	**red$_2$**	**red$_3$**
TAA-TTC(OMe)$_2$-PDI	178^{b}	749^{c}	955^{a,b}	-1001^{d}	-1218^{d}	
TAA-TTC(Me$_2$)-PDI	156	909^{a,b}	-	-1020^{d}	-1222^{d}	-
TAA-TTC(H)$_2$-PDI	164^{b}	909^{a,b}	-	-1015^{d}	-1224^{d}	-
TAA-TTC(Cl)$_2$-PDI	179^{b}	924^{a,b}	-	-999^{d}	-1207	-
TAA-TTC(PAZ)-PDI	160^{b}	-	-	-1004^{d}	-1214^{d}	-1768^{c}

^{a} irreversible. ^{b} TAA. ^{c} bridge. ^{d} PDI.

3. Weller-Approach and DFT computations

$$\Delta G_{1_{CS}}^{0} = \frac{N_A}{1000} Ze\big(E_{Ox}(D/D^{+}) - E_{red}(A/A^{-})\big) -$$

$$\frac{N_A e^2}{1000 \times 4\pi\varepsilon_0}\left[\left(\frac{1}{2r_D} + \frac{1}{2r_A}\right)\left(\frac{1}{\varepsilon_r} + \frac{1}{\varepsilon_s}\right) + \frac{1}{\varepsilon_s d_{DA}}\right]$$

(1)

The redox potential difference of the donor and the acceptor (in Volt) corresponds to the energy gap of the final charge separated state and the ground state. Their potentials were determined by cyclic voltammetry and are given in Table S1. In eqn 1 the separated charges are extra stabilized by Coulomb attraction, which is taken into account by a Coulomb term. In this term the radii of the donor (r_D) and acceptor (r_A) were calculated from the corresponding Connolly Molecular Surfaces of the subunits optimization with Chem3D Ultra[6] and the centre to centre distance between them (in Meter). The donor-acceptor distances r_{DA} were determined using Gaussian09 at a B3LYP/6-31G* level of theory.[7] N_A is Avogadro's constant, *e* the elementary charge, *z* the number of transferred charges. ε_0 is the vacuum permittivity, ε_r is the permittivity of the solvent used for cyclic voltammetry and ε_s is that for the solvent used in the photophysical experiment.

Internal reorganisation energies λ_i for CR (CS → S_0) were estimated from DFT calculations at B3LYP/6-31G* level of theory via the NICG (neutral in cation geometry) method [8-9] and outer reorganization energies λ_o were calculated based on the Born model.[10-11]

The same methodology was applied to estimate the inner and solvent reorganization energy of the virtual CS' bridge states by using model dyads Ph-TTC-PDI and Ph-TTC-TAA, see Table S2.

Table S2: Energies and reorganisation energies of the model bridge-PDI dyads (for the D-B-^{1}A* → D-B$^+$-A$^-$ process) and model bridge-TAA dyads (for the D$^+$-B-A$^-$ → D-B$^+$-A$^-$ process) in toluene

	$E_{DB^+A^-}$ / eV	$\lambda_{B1} = \lambda_v + \lambda_o$ / eV		$\lambda_{B2} = \lambda_v + \lambda_o$ / eV
Ph-TTC(OMe)$_2$-PDI	2.29	0.37	**Ph-TTC(OMe)$_2$-TAA**	0.36
Ph-TTC(Me)$_2$-PDI	2.79	0.29	**Ph-TTC(Me)$_2$-TAA**	0.27
Ph-TTC(H)$_2$-PDI	3.01	0.28	**Ph-TTC(H)$_2$-TAA**	0.26
Ph-TTC(Cl)$_2$-PDI	3.22	0.29	**Ph-TTC(Cl)$_2$-TAA**	0.27
Ph-TTC(PAZ)-PDI	3.29	0.26	**Ph-TTC(PAZ)-TAA**	0.24

In cyclovoltammetric experiments, an oxidation peak was only observable in case of the triad with the TTC(MeO)$_2$ bridge, from which a value of 2.29 eV was obtained for the free energy of formation of the bridge state D-B$^+$-A$^-$ by the Weller method, see above. For the less electron rich derivatives, the oxidation potential of the bridge falls outside the accessible electrochemical window. To assess the energies of the bridge states in these other cases, we estimated this quantity for all bridges by calculating the energy difference between the Kohn-Sham HOMO energy of TTC and the corresponding LUMO energy of PDI. These values falling between 6.04 eV (TTC(OMe)$_2$) and 7.04 eV (TTC(PAZ)) should give a reasonable estimate for the *relative* bridge state energies. Because the DFT energy differences calculated in that way do neither include Coulomb stabilization nor solvation effects in the CS' state, we added a constant shift value of 3.75 eV, defined in such a way as to yield the experimental value of 2.29 eV for the TTC(OMe)$_2$ bridge. The resulting adiabatic bridge energies for the ^{1,3}[D-B$^+$-A$^-$] states are collected in Tabel S2 together with the total bridge reorganization energy

The vertical bridge energies $\Delta E_v(^1A*B)$ and $\Delta E_v(CSB)$ as defined in Fig. 5 and collected in Table 3 were obtained by the following equations with data from Table S2 and E_{DB1A^*} = 2.33 eV and E_{D+BA-} = 1.85 eV:

$$\Delta E_v(^1A*B) = E_{DB^+A^-} + \lambda_{B1} - E_{DB1A^*}$$

$$\Delta E_v(CSB) = E_{DB^+A^-} + \lambda_{B2} - E_{D^+BA^-}$$

The frontier orbitals and their energies of the bridge moieties were calculated at B3LYP/6-311G**, see Table S3.

Table S3: HOMO and LUMO plots and their energies in eV of the bridge moieties and of TAA and PDI.

B3LYP / 6-311+G**	HOMO	LUMO
$(OMe)_2$	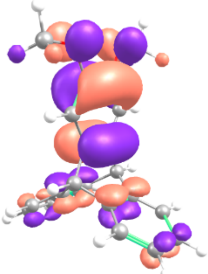 -5.44 eV	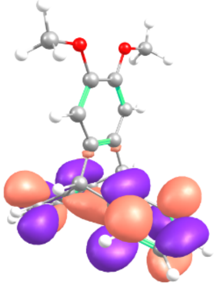 -0.58 eV
$(Me)_2$	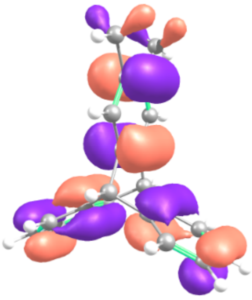 -5.94 eV	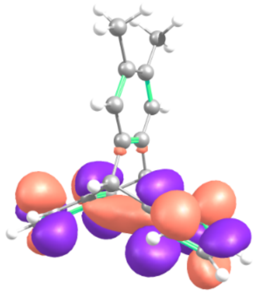 -0.58 eV
$(H)_2$	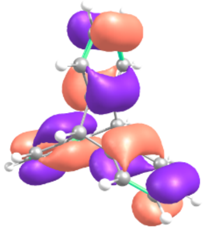 -6.16 eV	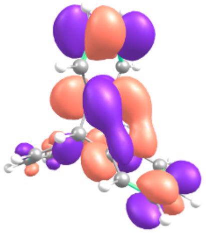 -0.64 eV

$(Cl)_2$	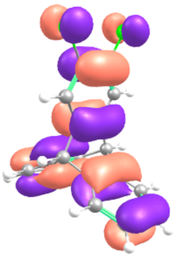 -6.37 eV	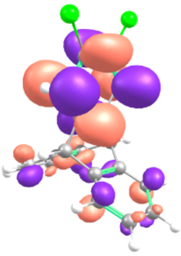 -1.12 eV
(PAZ)	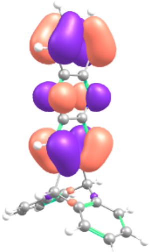 -6.29 eV	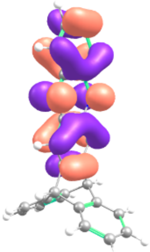 -2.62 eV
	HOMO-1 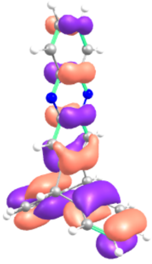 -6.44 eV	
TAA	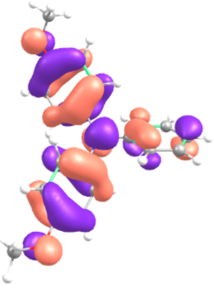 -8.82 eV	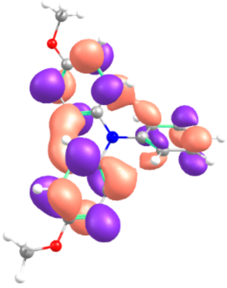 -4.39 eV
PDI	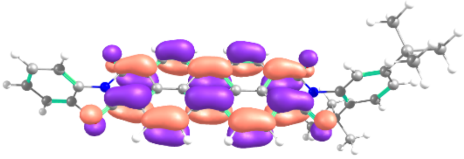 -1.79 eV	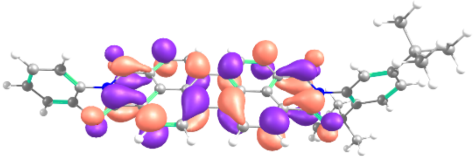 0.60 eV

4. Steady-state absorption spectroscopy

A JASCO V-670 UV/Vis/NIR spectrometer was used to measure the absorption spectra. Here, spectroscopic grade solvents from Sigma Aldrich and Acros Organics in 10 × 10 mm quartz-cuvettes from Starna were used and a cuvette with pure solvent was used as reference. In the examined concentration range of 10^{-7} – 10^{-5} M no concentration dependent effects were observed.

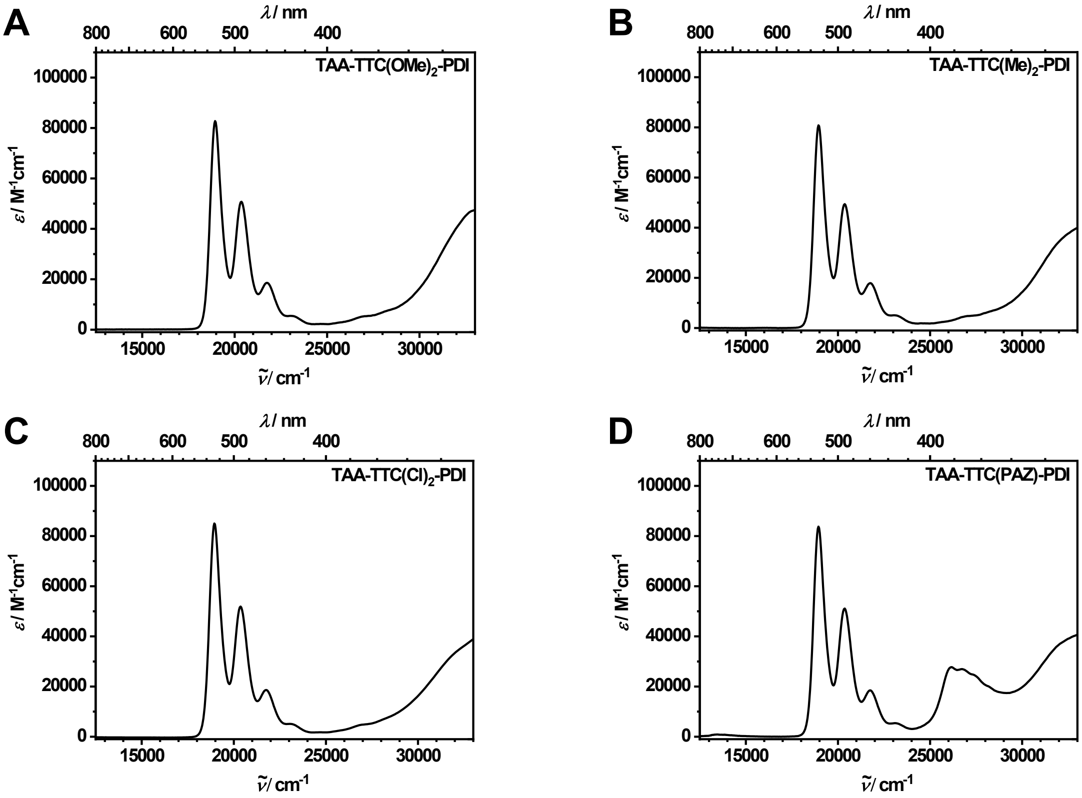

Fig S48: Absorption spectra of the traids in toluene at 298 K. Absorption spectrum from **TAA-TTC(H)$_2$-PDI** in reference.[1]

Table S4: Absorption data of the triads in toluene at 298 K.

	$\tilde{\nu}_{\mathrm{maxPDI}}$ / cm^{-1} ($\lambda_{\mathrm{maxPDI}}$ / nm)	$\varepsilon_{\mathrm{maxPDI}}$ / M^{-1}cm^{-1}
TAA-TTC(OMe)$_2$-PDI	18900 (528)	82300
TAA-TTC(Me)$_2$-PDI	18900 (528)	81000
TAA-TTC(H)$_2$-PDI	18900 (528)	84400
TAA-TTC(Cl)$_2$-PDI	18900 (528)	85000
TAA-TTC(PAZ)-PDI	18900 (528)	83800

5. Steady-state emission spectroscopy

An Edinburgh Instruments FLS980 fluorescence lifetime spectrometer equipped with a 450 W Xenon lamp and a single photon counting photomultiplier R928P was used for the emission spectroscopy measurements. The measurements were done at r.t. in 10 × 10 mm quartz-cuvettes from Starna. All solvents were of spectroscopic grade (Sigma Aldrich, Acros Organics). The optical density of all samples was below 0.05 for the maximum absorption band of the PDI moiety.

Fluorescence quantum yields were determined using a calibrated integrating sphere and corrected for self-absorption.[12]

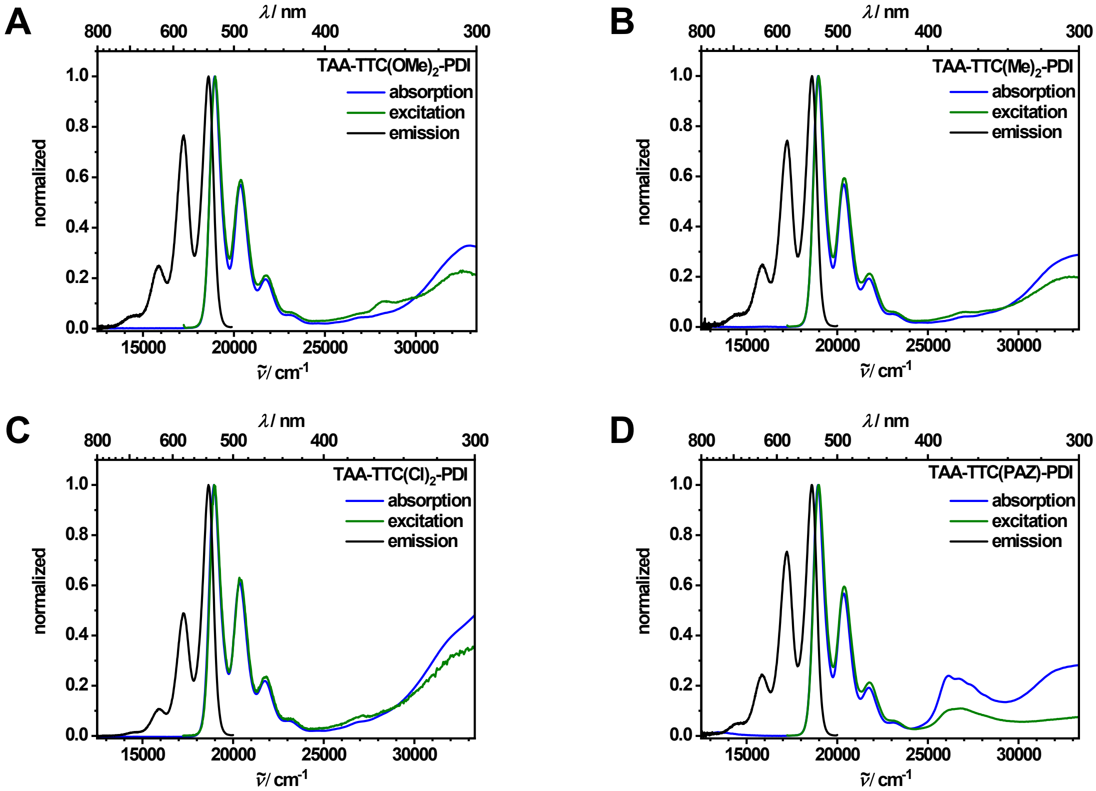

Fig S49: Normalised steady-state absorption (blue), excitation (green) and emission spectra (black) of the triads in toluene at 298 K. Emission spectra were recorded after excitation at 20400 cm^{-1} (490 nm, 0-1 absorption band of the **PDI**) and excitation spectra were recorded by probing at 16900 cm^{-1} (590 nm, 1-0 emission band of the **PDI**). Emission and excitation spectra were recorded at a concentration of $5\cdot10^{-6}$ mol l^{-1} and the absorption spectra at $1\cdot10^{-5}$ mol l^{-1}. Steady-state absorption, excitation and emission spectra from **TAA-TTC(H)$_2$-PDI** in reference.[1]

Table S5: Emission maxima and fluorescence quantum yields in toluene at 298 K.

	$\tilde{\nu}_{\mathrm{maxPDI}}{}^{a}$ / cm^{-1} (λ_{max} / nm)	ϕ_f
TAA-TTC(OMe)$_2$-PDI	18600 (537)	0.01
TAA-TTC(Me)$_2$-PDI	18600 (537)	0.03
TAA-TTC(H)$_2$-PDI	18600 (537)	0.04
TAA-TTC(Cl)$_2$-PDI	18600 (537)	0.08
TAA-TTC(PAZ)-PDI	18600 (537)	0.09

6. Transient absorption spectroscopy

6.1. fs-transient absorption spectroscopy

The Transient absorption setup (TAS) consists of a one-box femtosecond laser system "Solstice" from Newport Spectra Physics, a "HELIOS" transient absorption spectrometer (TASp) from Ultrafast Systems, a home-built NOPA, and a "TOPAS-C" from LightConversion. The fundamental wavelength from the Solstice is 12500 cm^{-1} (800 nm) with a pulse length of 100 fs and a repetition rate of 1 kHz. The HELIOS spectrometer is equipped with two channels, one used for measurement and one for reference. It is equipped with a fibre-coupled linear CMOS sensor with a sensitivity from 31700 cm^{-1} (315 nm) to 10800 cm^{-1} (925 nm) and an intrinsic spectral resolution of 1.5 nm. The white light continuum (WLC) is created by an oscillating 3 mm thick CaF$_2$ crystal. The latter was pumped by the TOPAS-C output at 10000 cm^{-1} (1000 nm) to obtain a gapless WLC from 29400 cm^{-1} (340 nm) to 10900 cm^{-1} (915 nm). A 25000 cm^{-1} (400 nm) long pass filter and a 11100 cm^{-1} (900 nm) short pass filter were used to to chop the probe wavelength range. The pump beam from the TOPAS-C for the WLC is guided over a linear stage which provides a time delay up to 7 ns. The step size for the first 4 ps is 20 fs and afterwards the steps increase in a logarithmic way up to 200 fs. The angle in space between both beams was 10° and the angle between the polarization directions between pump and probe was 54.7°. The pump beam for the sample was produced by a home-built NOPA at 18900 cm^{-1} (528 nm) and the pulse lengths were shorter than 40 fs in a Gaussian fit. The pulse shape was close to the bandwidth limitation. The instrument response function derived from the coherent artefact was approx. 100 fs. All samples were dissolved in toluene from Merck. The measurements were done in a cuvette with an optical path length of 0.2 mm, a window thickness of 0.1 mm and pumped with 30 nJ.

GLOTARAN (v. 1.2) was used to analyse the recorded time resolved spectra by a global deconvolution using a sequential model to yield evolution associated difference spectra (EADS).[13] The white light dispersion (chirp) was corrected by fitting a third order polynomial to the cross-phase modulation signal of the pure solvent.

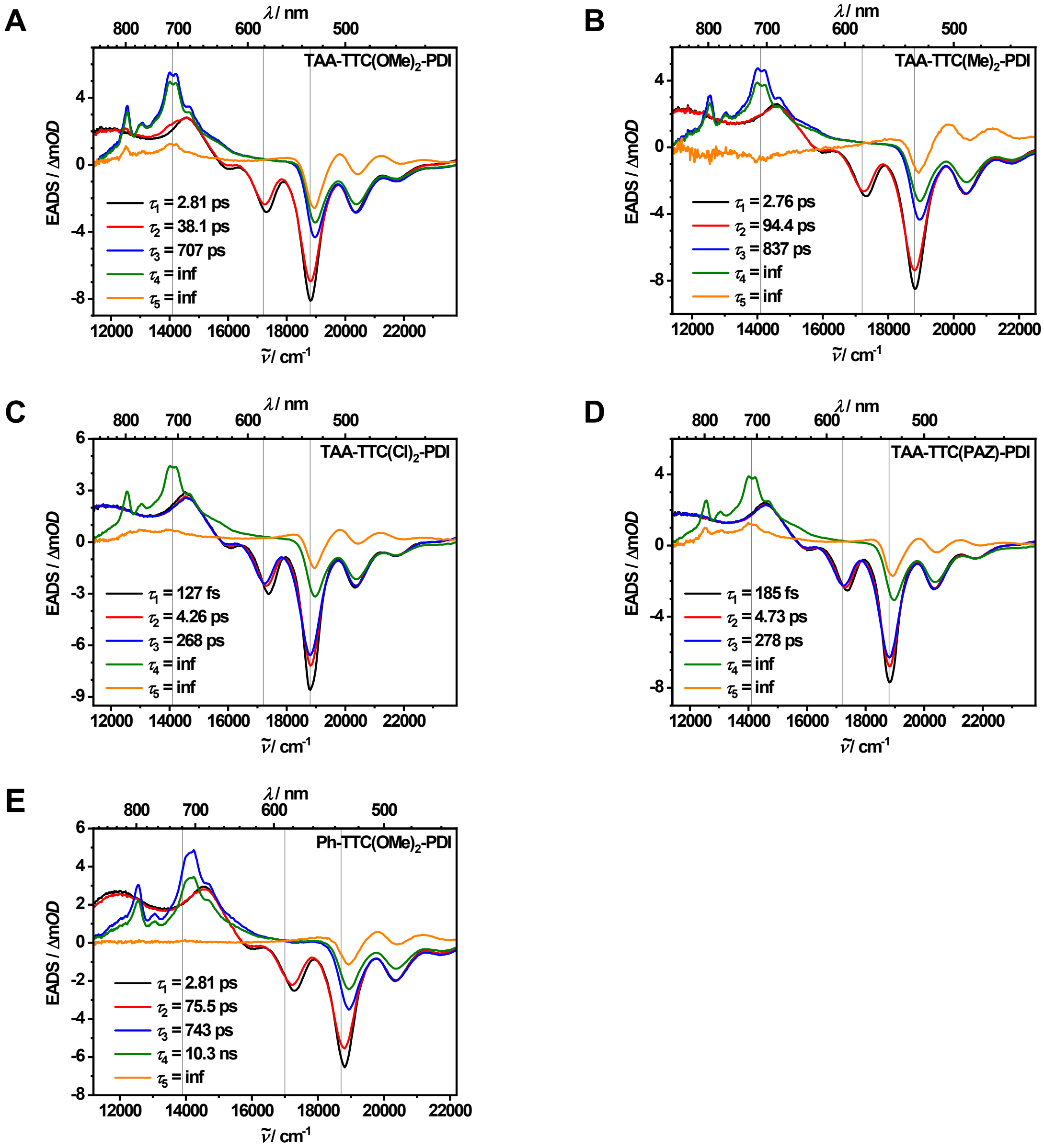

Fig S50: *Evolution associated difference spectra* (EADS) in toluene at 298 K after pumping at 18900 cm^{-1} (528 nm) and probing with continuous withe light between 11500 cm^{-1} (870 nm) and 23800 cm^{-1} (420 nm). The EADS of **TAA-TTC(H)$_2$-PDI** can be found in reference.[1]

6.2. Target fits

A target fit of the transient map was performed under the assumption that that at 20400 cm^{-1} (490 nm) the EADS of excited PDI and the PDI radical anion only show GSB and no superimposed ESA or SA. For the triplet PDI, however, this is not true as this shows a strong ESA in this spectra region. Therefore, species associated difference spectra (SADS) of the singlet PDI and the CS state should possess the same (but unknown) extinction coefficient at 20400 cm^{-1} (490 nm). Therefore, we adjusted the efficiencies of depopulation channels of all pertinent states in a way, that this criterion concerning the extinction coefficient was met, using a global target fit. In this way, the rate constant for depopulation of a specific state changed during the global fit. In comparison, in the evolution associated difference spectra, where a sequential model was assumed, all efficiencies are unity. The quotient of the efficiency of the charge separation channel and the lifetime of the excited PDI state then gives the rate constants for the charge separation channel.

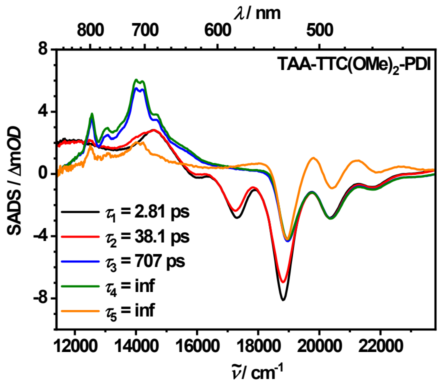

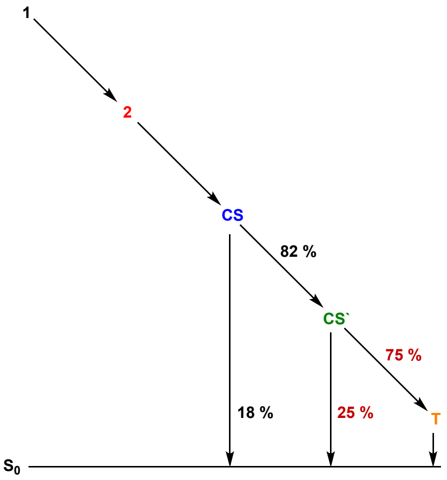

k_{CS} = 2.6·10^{10} s^{-1}

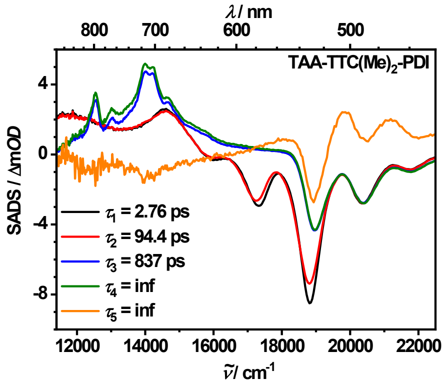

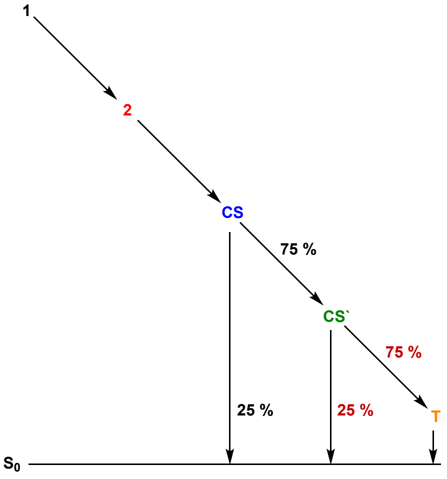

k_{CS} = 1.1·10^{10} s^{-1}

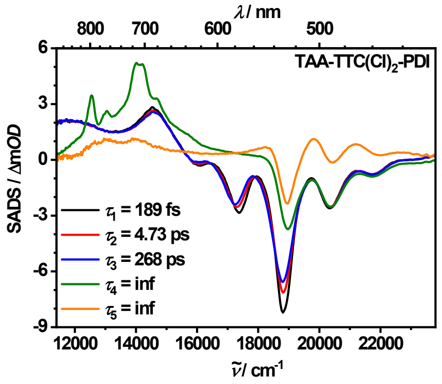

$k_{CS} = 3.7 \cdot 10^9\ s^{-1}$

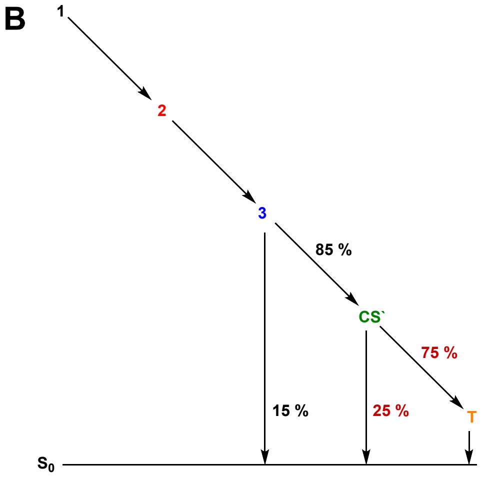

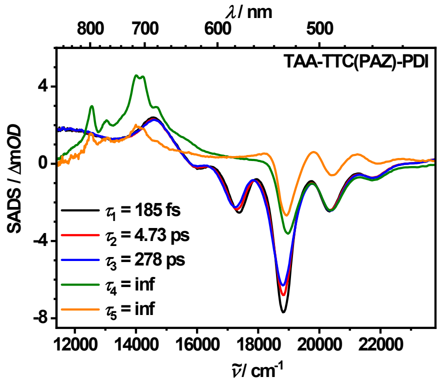

$k_{CS} = 3.1 \cdot 10^9\ s^{-1}$

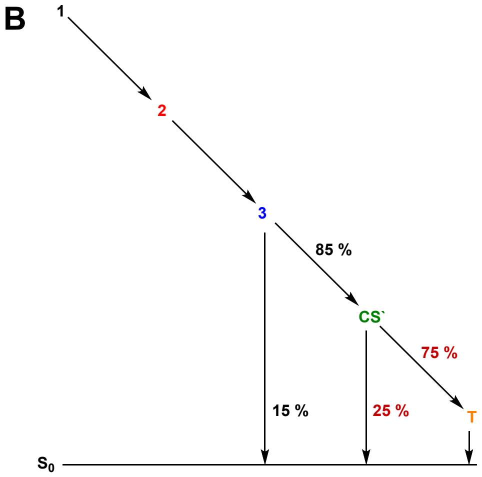

Fig S51: Target fits of the transient maps under the assumption that all SADS spectra match at ca. 20400 cm^{-1} (490 nm). Target fit of **TAA-TTC(H)$_2$-PDI** can be found in reference.[1]

6.3. ns-transient absorption spectroscopy

The ns-transient absorption spectroscopy measurements were done using an Edinburgh LP 920 laser flash spectrometer using an EKSPLA NT340 Nd:YAG laser with integrated optical parametric oscillator. The white light was generated by a 450 W Xe arc flash lamp in which the white light and the pump light beams were perpendicular to each other. The used solvent was of spectroscopic grade from thermoScientific, which was degassed by at least 7 freeze pump thaw cycles. Sample preparation was carried out in a nitrogen filled glovebox in 10 x 10 mm quartz-cuvettes equipped with a *Young's* valve. In a concentration range of 10^{-6} to 10^{-5} M no bimolecular processes were observed. All samples were excited with approx. 5 ns laser pulses (ca. 1.2 mJ pulse energy) with a 10 Hz repetition rate at the maximum ground state absorption of the respective PDI moiety at 18900 cm^{-1} (528 nm). The transient maps were obtained by measuring temporal decay profiles in 4 nm steps between 25000 cm^{-1} (400 nm) and 12500 cm^{-1} (800 nm). The decay profiles were corrected for fluorescence. The decay curves were deconvoluted with the instrumental response function using the spectrometer L900 software.

The magnetic field dependent measurements were performed using a GMW Associates C-frame electromagnet 5403 (pole diameter = 76 mm, pole face = 38 mm, axial hole in poles 6.35 mm, pole gap = 13 mm) implemented in the aforementioned laser set-up. The magnetic field strength was controlled using a Teslameter (Projekt Elektronik GmbH Berlin) where the sensor was embedded in a neutral cuvette and placed at the side of the pole face. The stability of all samples was checked by repeatedly testing selected magnetic fields as well as comparing steady-state absorption spectra that were recorded at the beginning and the end of all measurements.

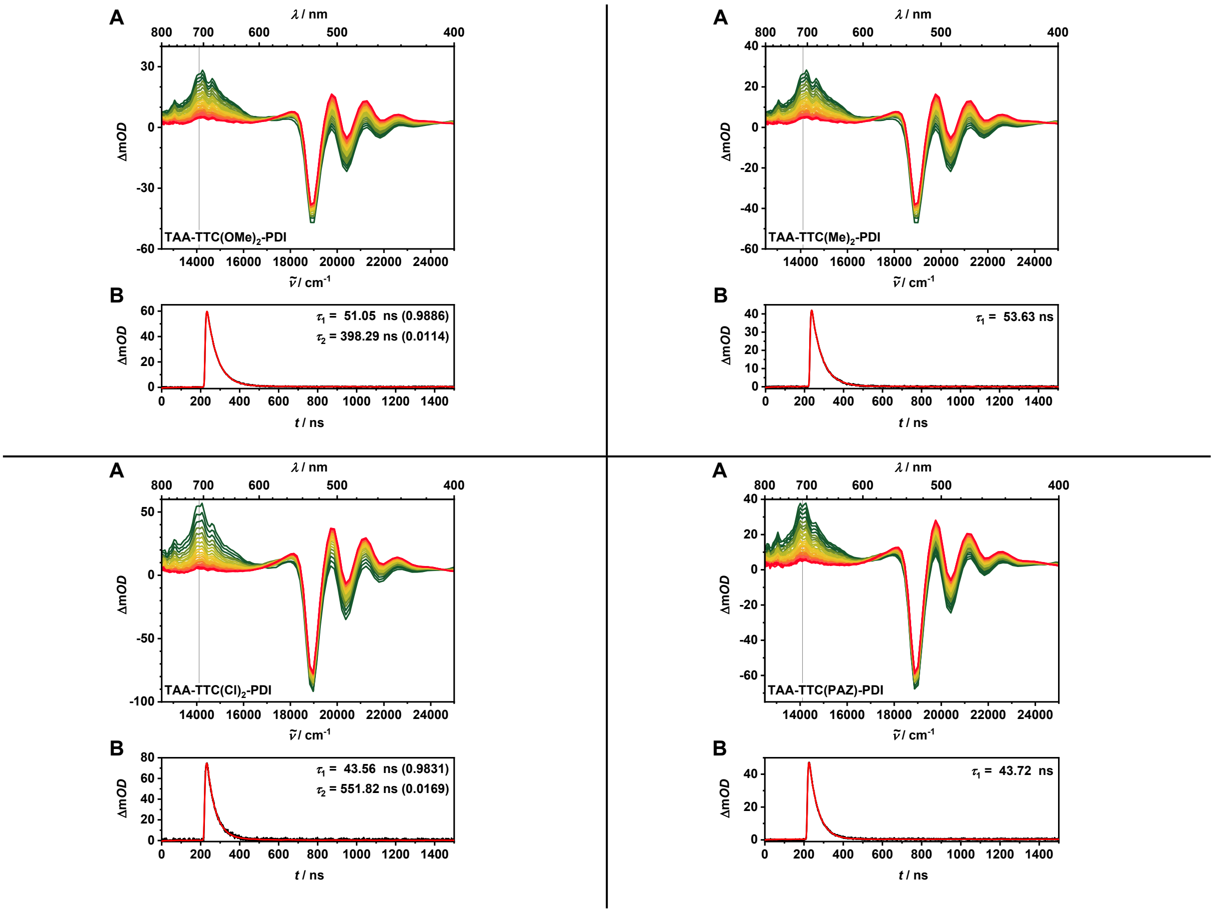

Fig S52: A: ns-transient maps in toluene at 298 K after excitation at 18900 cm^{-1} (528 nm) and probing with continuous withe light between 12500 cm^{-1} (800 nm) and 25000 cm^{-1} (400 nm). The displayed spectra are at 7 ns steps with early times shown in dark green and later times in red. **B:** CSS decay curve (black) with the corresponding deconvolution fit (red) at 14100 cm^{-1} (grey line in **A**). Transient map of **TAA-TTC(H)$_2$-PDI** can be found in reference.[1]

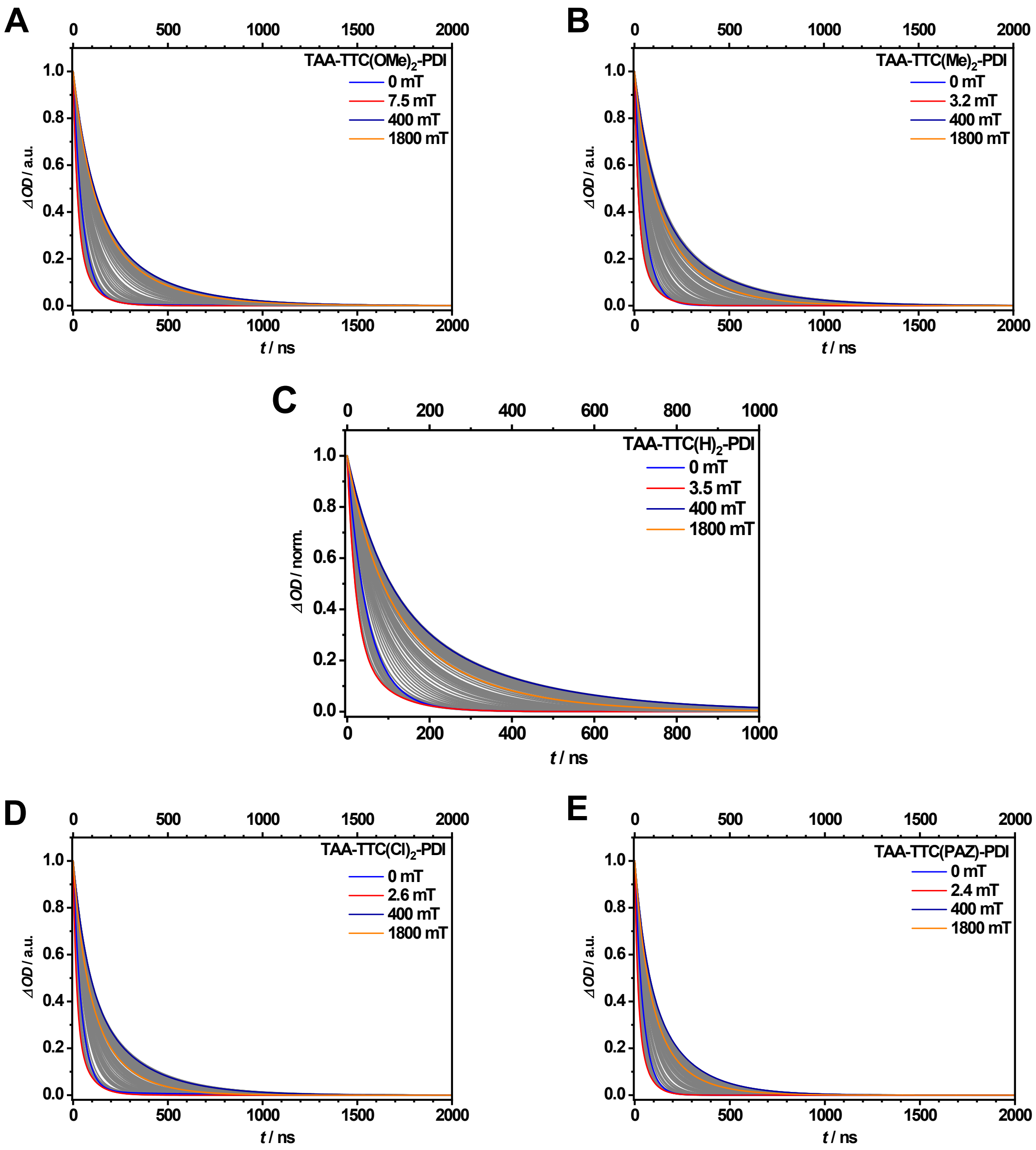

Fig S53: Multiexponential fit functions of the transient absorption decay profiles at selected magnetic fields for all triads in toluene at 298 K after pumping at 18900 cm^{-1} (528 nm) and probing at 14100 cm^{-1} (710 nm).

Table 6: Selected CSS lifetimes τ and the corresponding amplitudes *a* of the triads in toluene obtained by using a deconvolution fit on the ns-TA decay curves. The magnetic fields given correspond to the highlighted curves in Fig S53.

	external magnetic field	τ_1 **/ ns**	a_1	τ_2 **/ ns**	a_2
TAA-TTC(OMe)$_2$-PDI	0 mT	51.05	0.9886	398.29	0.0114
	7.5 mT	20.90	0.6771	79.11.	0.3229
	400 mT	98.62	0.5278	313.85	0.4722
	1800 mT	93.20	0.5263	285.65	0.4737
TAA-TTC(Me)$_2$-PDI	0 mT	53.63	1.0000		
	3.2 mT	18.50	0.6765	75.42	0.3235
	400 mT	95.48	0.4923	324.02	0.5077
	1800 mT	70.30	0.3651	227.57	0.6349
TAA-TTC(H)$_2$-PDI	0 mT	46.34	0.8750	94.59	0.1250
	3.5 mT	20.09	0.7105	79.53	0.2895
	400 mT	84.64	0.4737	284.49	0.5263
	1800 mT	65.72	0.3919	198.63	0.6081
TAA-TTC(Cl)$_2$-PDI	0 mT	43.56	0.9831	551.82	0.0169
	2.6 mT	16.98	0.6887	69.65	0.3113
	400 mT	75.54	0.4941	268.21	0.5059
	1800 mT	58.71	0.4355	180.44	0.5645
TAA-TTC(PAZ)-PDI	0 mT	43.72	1.0000		
	2.4 mT	14.46	0.6129	52.11	0.3871
	400 mT	61.86	0.4426	208.25	0.5574
	1800 mT	64.26	0.5323	176.12	0.4677

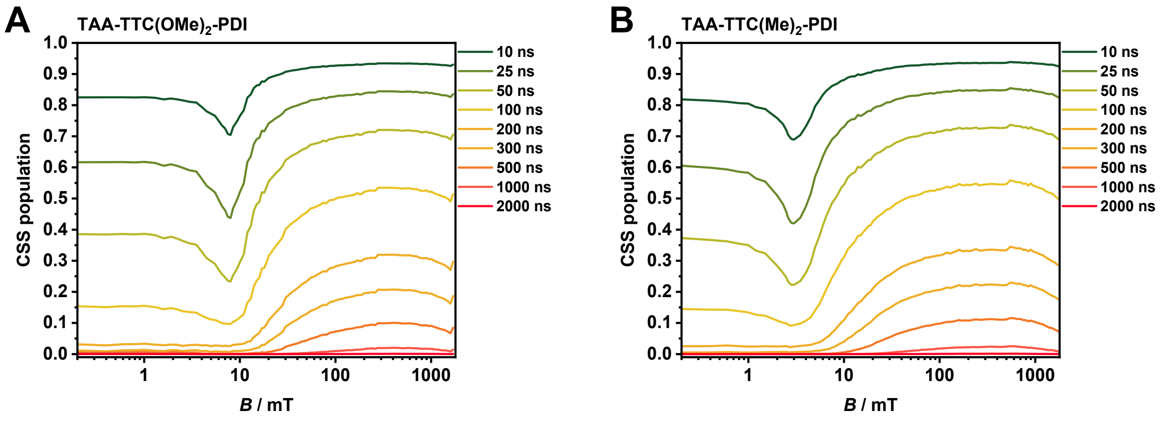

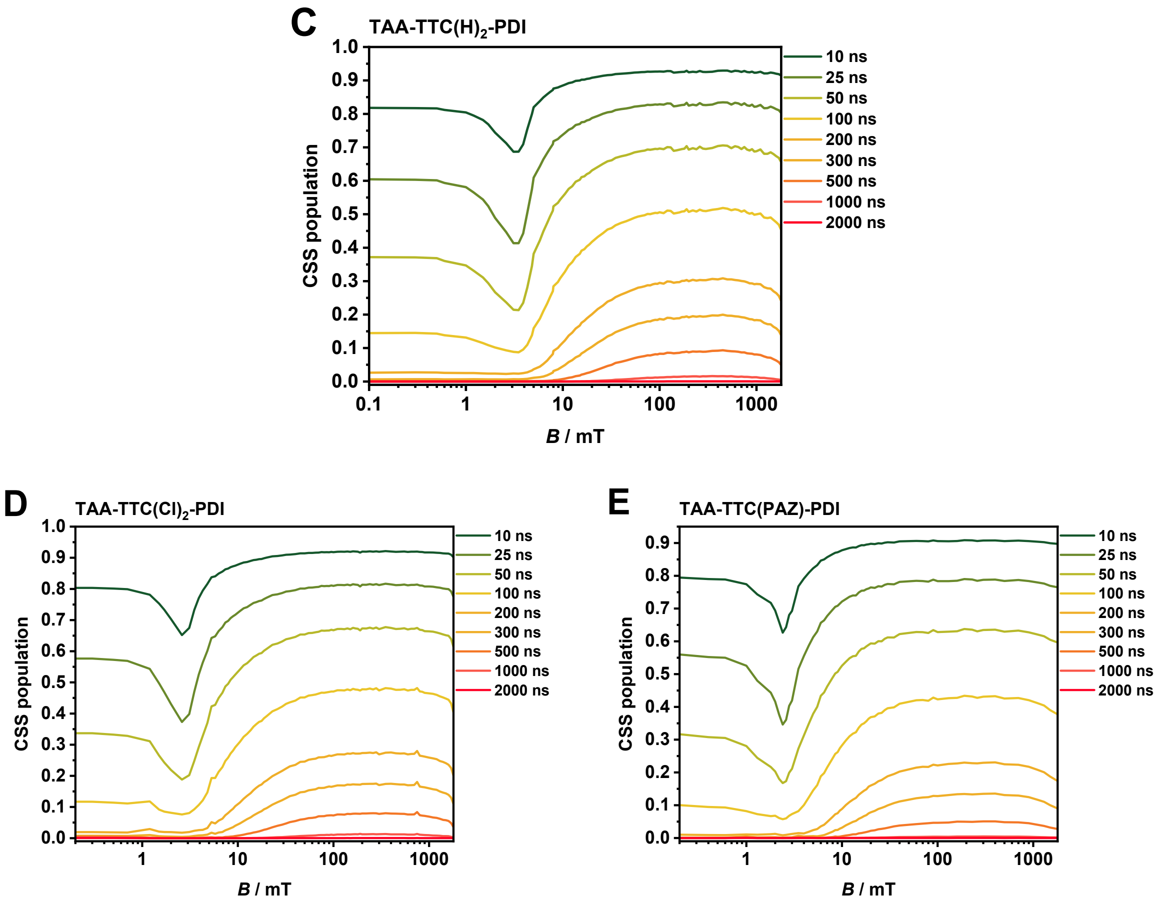

Fig S54: MARY plots in toluene at 298 K.

7. Error limits for k_S

As shown in the plot in Fig. S55. the maximum values of k_S are 1.7 × 10^5 s^{-1} for **TAA-TTC(H)$_2$-PDI** and 1 ×10^6 s^{-1} for **TAA-TTC(OMe)$_2$-PDI** and **TAA-TTC(PAZ)-PDI** for $T_{long} = \infty$. Decreasing T_{long} to the limiting values shown on the vertical axis and setting k_S to zero yields the same $k(B)$ curve in the quantum simulation. Thus, for the pertinent derivatives, possible values of k_S range in the intervals defined by the maximum value and zero. On the other hand, if one allows for an average deviation of 5% in the $k(B)$ fit, this would allow for $k_S = 6*10^5$ in the cases of **TAA-TTC(H)$_2$-PDI**, **TAA-TTC(Me)$_2$-PDI**, and **TAA-TTC(Cl)$_2$-PDI**. Therefore, this value was taken as an upper limit of k_S in these cases.

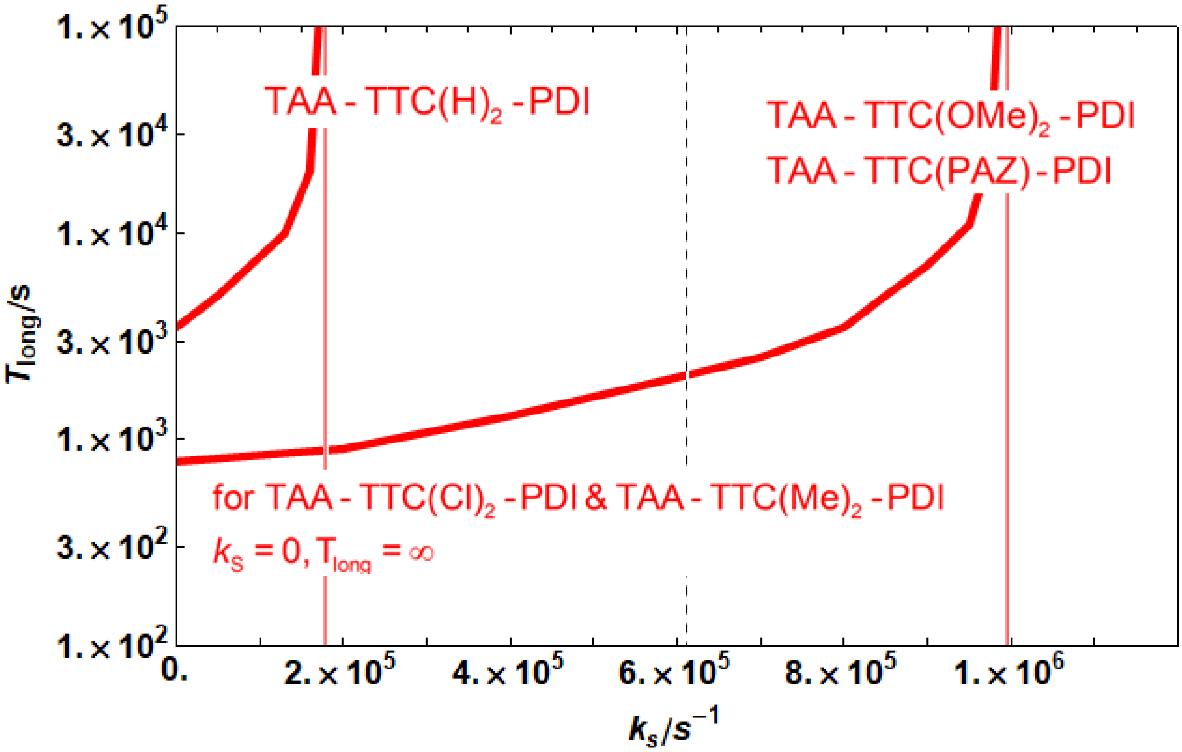

Fig. S55 T_{long} vs k_S as related to each other by the condition of producing equivalent simulations of $k(B)$. The dashed vertical line indicates the k_s value for an 5% error in $k(B)$ in the cases of **TAA-TTC(H)$_2$-PDI**, **TAA-TTC(Me)$_2$-PDI**, and **TAA-TTC(Cl)$_2$-PDI**.

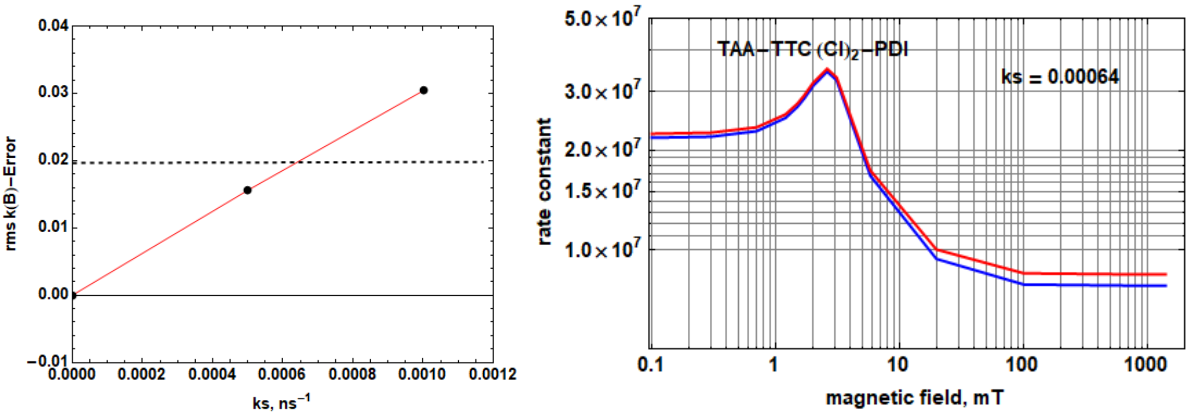

Fig. S56 Left: dependence of rms error of Log($k(B)$) on value of k_S. A value of 0.2 correspond to an average error of 5% for $k(B)$. Right: standard fit curve (blue) and deviation (red) for k_S = 0.00064 ns^{-1}.

8. Necessity to adapt the effective hyperfine coupling constant

In the following figures, simulations of the $k(B)$ spectrum for the case of **TAA-TTC(OMe)$_2$-PDI** are shown. The parameters $k_d = 0.15$, $\tau_c = 0.6$, $T_{long} = \infty$, $\Delta a_N = 1.51$ mT were kept fixed (time units ns). As shown in Fig. S57b, changing only the value of J, cannot account for the differences in the k(B) spectra in the present series of triads, because a mere change of J would lead to a strong effect on the value k(B) at zero field. (cf. also Section 9)

Increasing k_T compensates for the change of $k(0)$, but it also leads to a broadening of the resonance line to the extent that it disappears completely ($k_T = 3$). This effect follows from the lifetime broadening of the triplet level. The 2J value corresponds to a frequency of 1.34. The k_T value of 3 is twice as large. For the experimental curve, the ratio of $k(B)$ values between zero field and the maximum amounts to a value of 1.60. This ratio is also approximately obtained for $k_T = 1.0$, in which case the ratio of zero-field and high-field values is 2.94. The theoretical curve in Fig. S57 d) just corresponds to the experimental one, except for the absolute values which are too small by a factor of 1.5. From Figs. S57a-h it follows that the situation represented by Fig.S57d is the best that can be achieved in terms of similarity of experimental and theoretical curves. A mere vertical shift of the curve can be only achieved if the effective hyperfine coupling is increased. Such attempts with changes of the isotropic hyperfine coupling constant a_N, the isotropic hyperfine coupling constant of the TAA-nitrogen, are shown in the diagrams S57i-k, wherein the effective value of a_N is increased

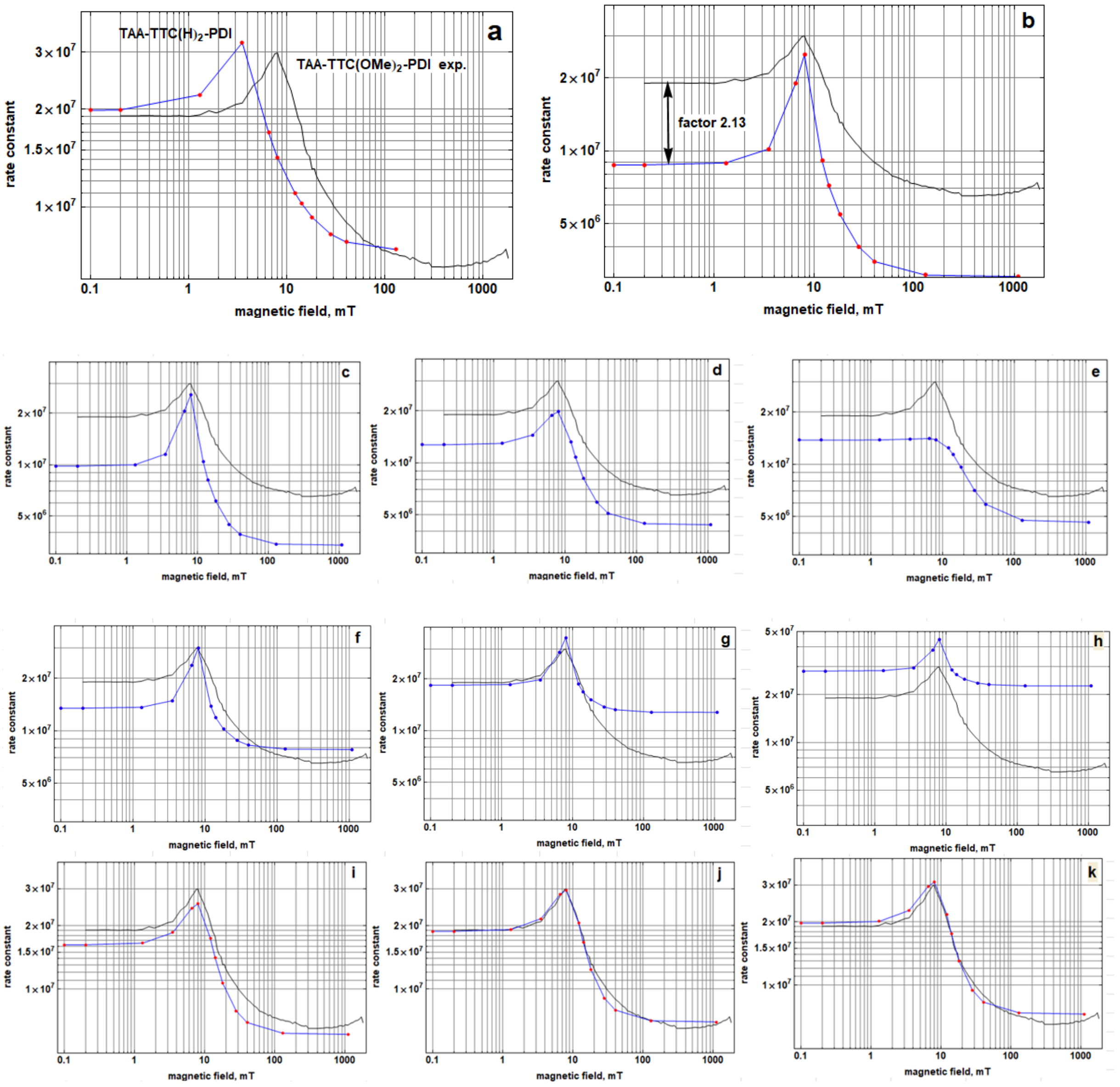

Fig. S57. a) Comparison of $k(B)$ spectra of **TAA-TTC(H)$_2$-PDI** with **TAA-TTC(OMe)$_2$-PDI**. For **TAA-TTC(H)$_2$-PDI** the best theoretical fit is shown with k_S = 0.0002 ns^{-1}, k_T = 0.15 ns^{-1}, J = 1.55 mT, a_N = 0.926 mT. The spectra appear to be only horizontally displaced. The B_{max} value rises from 3.4 mT to 7.9 mT. b) Simulation (red data points): apart from the J-value of 3.8 mT all other parameters for **TAA-TTC(H)$_2$-PDI** were kept as in a). c)-e) Variation of k_T through the values 0.15 (c), 1.0 (d), 3.0 (e), other parameter values as in (b). Increasing k_T by a factor of 10 causes only a relatively little increase of $k(B)$ by a factor of 1.6. This demonstrates that the rate constant $k(B)$ is mainly determined by the ISC-process. The same conclusion follows from the fact that $k(B)$ in high field is reduced to about 1/3 of the $k(B)$-value at zero field (cf. also Section 9); f – h) Variation of k_S through the values 0.005 (f), 0.01 (g), 0.02 (h), other parameter values as in (b). As long as k_S is small compared to k_T , there are no significant changes. An

Caption to Fig. S57 continued

increase by a factor of 25 (cf. Fig S57 b and f) causes *k*(0) to grow just by a factor of 1.5. At higher values of k_S , the effect on *k*(0) becomes stronger. Important observation: the greater k_S, the closer the *k*(*B*) values at low-field and high-field approach each other. Since their experimental ratio is close to 3, k_S must definitely range far below k_T. i-k): Variation of effective hfc a_N. (1.1 mT (i), 1.25 mT (j). 1.3 mT (k)). Other parameter values as in (b). A value of a_N =1.25 mT seems to be the optimum.

9. Pure *J*-effect on *k*(*B*) *spectra*

We consider the isolated role of exchange interaction *J* on the recombination kinetics of CSS, when created in the singlet state and recombining through the triplet state. A standard set of kinetic parameters is kept constant while varying the magnetic field for different values of *J* (Fig. S58). The *k*(*B*) spectra exhibit the characteristic 2*J*-resonances. For *J* smaller than several times a_N, the resonance maxima appear at fields somewhat larger than 2*J,* because of the finite hyperfine splitting. In Fig. S58 it is important to observe, that after an initial decrease the maximum value of the *k*(*B*) resonance approaches a limiting value for high values of *J*. On the other hand, the low-field and high-field values decrease much faster than the maximum value, such that the 2*J*-resonance appears sharper and sharper, as *J* increases.

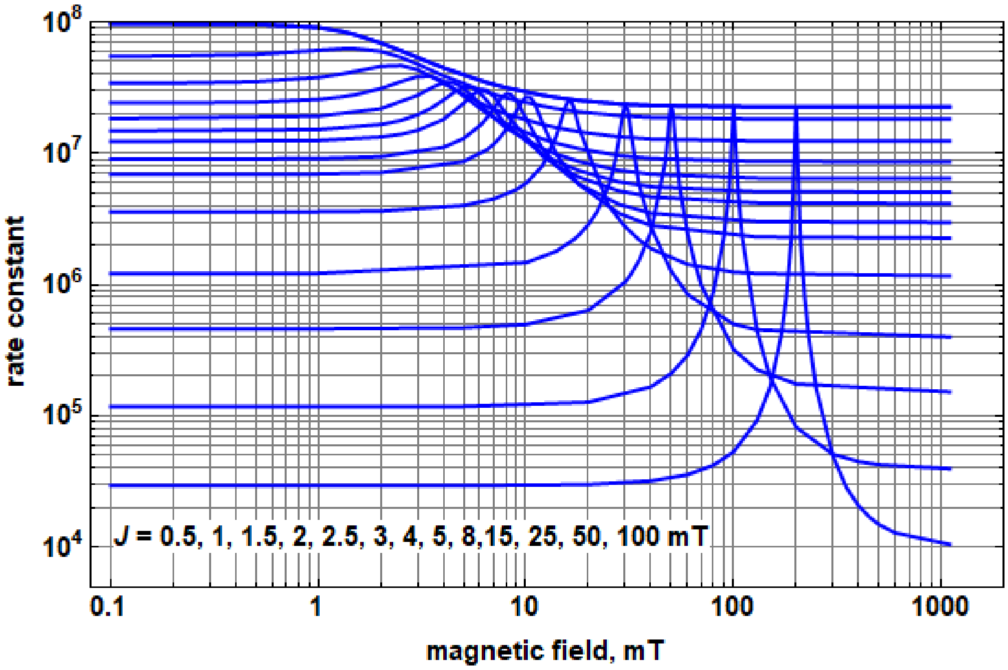

Fig. S58 Variation of *k*(*B*) spectra with exchange energy *J*. The following parameters are kept constant: k_T = 0.3 ns^{-1}, k_S = 0 ns^{-1}, k_{STD} = 0.1 ns^{-1},T_{long} = infinity, τ = 0.6 ns, a_N = 1.0 mT.

10 Discussion of dephasing rate constant k_{STD}

Table 4 from Ref. [1] Results of dynamical angular distribution.

	Π	Δ	Δ / Π	J /mT	ΔJ /mT	τ_J / ps	$k_{STD,th}$ / ns^{-1}	k_{STD} / ns^{-1}
Me23	0.0017	0.0042	2.48	0.25	0.62	3.3	0.00015	: 0
Me2	0.012	0.020	1.51	1.55	2.34[a]	4.1	0.0030	0.15
Me3	0.010	0.018	1.72	1.85	3.19	4.2	0.0053	0.21
Me0	0.070	0.066	0.94	6.5	6.12	4.5	0.021	1.3

[a] a typo ("2.43") in Ref. [1] was corrected

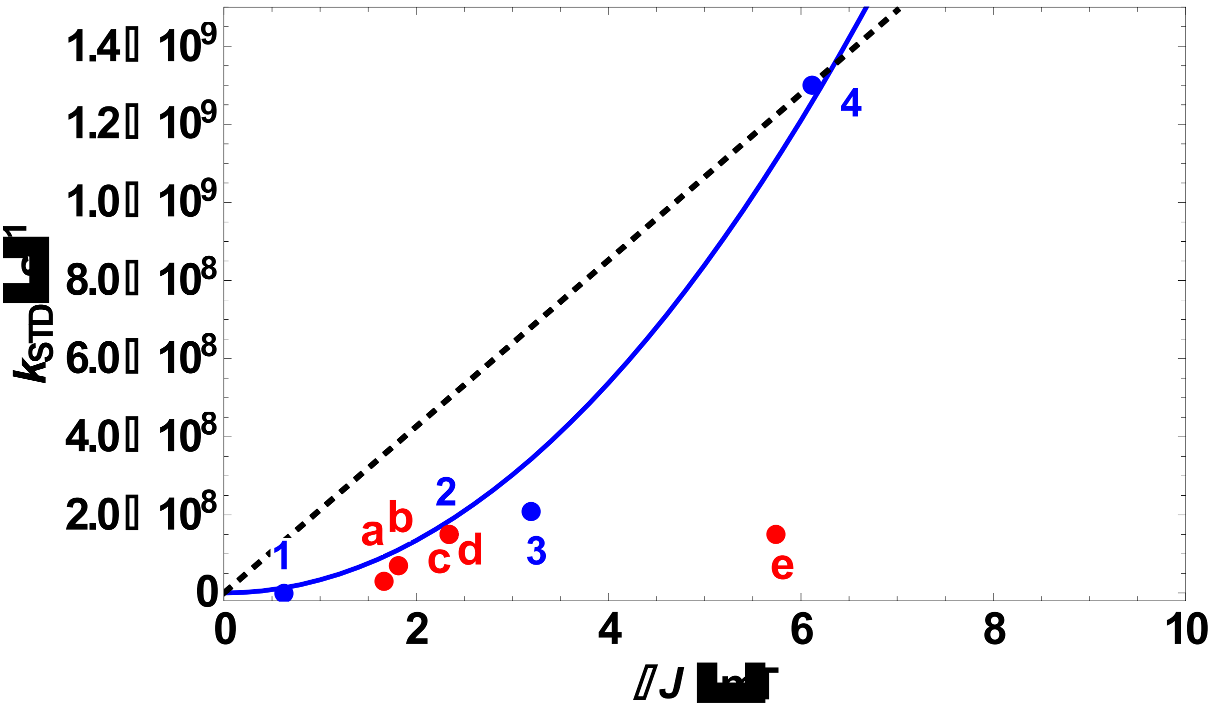

Fig. S59 Rate constant of singlet/triplet dephasing versus standard deviation of J under dynamic internal rotational motions of triad backbone. The data points in blue refer to the results of the previous paper,[1] the numbers indicating the triads **Me23** (1), **Me2** (2), **Me3** (3), and **Me0** (4). The data points in red refer to the triads from the present paper , viz. **TAA-TTC(PAZ)-PDI** (a)., **TAA-TTC(Cl)$_2$-PDI** (b), **TAA-TTC(H)$_2$-PDI** (c), **TAA-TTC(Me)$_2$-PDI** (d), and **TAA-TTC(OMe)$_2$-PDI** (e). Triads 2 and c are identical. Therefore, their data points overlap each other perfectly. Triad d has the same values, accidentally.

In Ref. [1], the diagram shown in Fig. S59 with the data points in blue was presented for the triads with no modified TTC bridge, but with partial blockings of internal backbone rotations by Me substituent. For those triads, the ΔJ values were estimated by scaling the standard deviation of the cosine square products along the four backbone angles with a factor that matches the average of the cosine square products to the experimentally observed J value. If we assume that this scaling factor resulting from the backbone dynamics is not changed by the TTC substituents, we can use the factor 1.55/1.51 determined for **Me2** in ref.[1] (cf. Table 4), also for the present triads, since it has the same two Me blocking elements as the latter. Thus, we can obtain their ΔJ values from their experimental J values. The resulting data points for the previous and the present triads can be compared in Fig. S59. While the data points a -d reasonably fall within the series of the previous triads, corresponding to a square relation between k_{STD} and ΔJ, the data point with the highest ΔJ does not show correspondingly enhanced k_{STD}, which means that ΔJ is overestimated for **TAA-TTC(OMe)$_2$-PDI** (e). From our previous investigations it is quite unlikely, that the discrepancy should be due to a variation of the autocorrelation time τ_J. On the other hand a special behaviour of ΔJ in compound (e) goes along with another peculiar behaviour of the latter triad: it seems strange that the strong increase of ΔJ does not cause a decrease in the singlet/triplet conversion rate at zero field, as discussed in sections **S8** and **S9.**

[1] C. Roger, A. Schmiedel, M. Holzapfel, N. N. Lukzen, U. E. Steiner, C. Lambert, *Phys. Chem. Chem. Phys.* **2024**.

[2] J. C. C. Atherton, S. Jones, *Tetrahedron* **2003**, *59*, 9039-9057.

[3] L. Friedman, F. M. Logullo, *J. Am. Chem. Soc.* **1963**, *85*, 1549-1549.

[4] N. Miyaura, A. Suzuki, *J. Chem. Soc., Chem. Commun.* **1979**, 866-867.

[5] K. Baumgärtner, M. Hoffmann, F. Rominger, S. M. Elbert, A. Dreuw, M. Mastalerz, *J. Org. Chem.* **2020**, *85*, 15256-15272.

[6] PerkinElmer, *Chem3D Ultra, Version 20.0.0.41,*, PerkinElmer Informatics, Inc.

[7] M. J. M. J. Frisch, G. W. G. W. Trucks, H. B. Schlegel, G. E. Scuseria, M. A. Robb, J. R. Cheeseman, G. Scalmani, V. Barone, B. Mennucci, G. A. Petersson, H. Nakatsuji, M. Caricato, X. Li, H. P. Hratchian, A. F. Izmaylov, J. Bloino, G. Zheng, J. L. Sonnenberg, M. Hada, M. Ehara, K. Toyota, R. Fukuda, J. Hasegawa, M. Ishida, T. Nakajima, Y. Honda, O. Kitao, H. Nakai, T. Vreven, J. Montgomery, J. E. P. J. A., F. Ogliaro, M. Bearpark, J. J. Heyd, E. Brothers, K. N. Kudin, V. N. Staroverov, R. Kobayashi, J. Normand, K. Raghavachari, A. Rendell, J. C. Burant, S. S. Iyengar, J. Tomasi, M. Cossi, N. Rega, N. J. Millam, M. Klene, J. E. Knox, J. B. Cross, V. Bakken, C. Adamo, J. Jaramillo, R. Gomperts, R. E. Stratmann, O. Yazyev, A. J. Austin, R. Cammi, C. Pomelli, J. W. Ochterski, R. L. Martin, K. Morokuma, V. G. Zakrzewski, G. A. Voth, P. Salvador, J. J. Dannenberg, S. Dapprich, A. D. Daniels, Ö. Farkas, J. B. Foresman, J. V. Ortiz, J. Cioslowski, D. J. Fox, Gaussian, Inc., Wallingford CT, **2009**.

[8] S. F. Nelson, S. C. Blackstock, Y. Kim, *J. Am. Chem. Soc.* **1987**, *109*, 677-682.

[9] S. F. Nelson, H. Chang, J. J. Wolff, J. J. Adamus, *J. Am. Chem. Soc.* **1993**, *115*, 12276.

[10] J. H. Klein, T. L. Sunderland, C. Kaufmann, M. Holzapfel, A. Schmiedel, C. Lambert, *Physical Chemistry Chemical Physics* **2013**, *15*, 16024-16030.

[11] C. Kaiser, A. Schmiedel, M. Holzapfel, C. Lambert, *J. Pys. Chem. C.* **2012**, *116*, 15265-15280.

[12] C. Würth, M. Grabolle, J. Pauli, M. Spieles, U. Resch-Genger, *Nat. Protoc.* **2013**, *8*, 1535-1550.

[13] J. K. Hurley, N. Sinai, H. Linschitz, *Photochem. Photobiol.* **1983**, *38*, 9-14.